





Two Late Cretaceous sauropods reveal titanosaurian dispersal across South America

E. Martín Hechenleitner ^{1,2✉}, Léa Leuzinger^{1,3}, Agustín G. Martinelli ⁴, Sebastián Rocher ⁵, Lucas E. Fiorelli ¹, Jeremías R. A. Taborda⁶ & Leonardo Salgado⁷

South American titanosaurians have been central to the study of the evolution of Cretaceous sauropod dinosaurs. Despite their remarkable diversity, the fragmentary condition of several taxa and the scarcity of records outside Patagonia and southwestern Brazil have hindered the study of continental-scale paleobiogeographic relationships. We describe two new Late Cretaceous titanosaurians from Quebrada de Santo Domingo (La Rioja, Argentina), which help to fill a gap between these main areas of the continent. Our phylogenetic analysis recovers both new species, and several Brazilian taxa, within Rinconsauria. The data suggest that, towards the end of the Cretaceous, this clade spread throughout southern South America. At the same locality, we discovered numerous accumulations of titanosaurian eggs, likely related to the new taxa. With eggs distributed in three levels along three kilometres, the new site is one of the largest ever found and provides further evidence of nesting site philopatry among Titanosauria.

¹Centro Regional de Investigaciones Científicas y Transferencia Tecnológica de La Rioja (CRILAR), Provincia de La Rioja, UNLaR, SEGEMAR, UNCa, CONICET, Entre Ríos y Mendoza s/n (5301), Anillaco, La Rioja, Argentina. ²Instituto de Biología de la Conservación y Paleobiología (IBICOPA), DACEFyN-UNLaR, 5300 La Rioja, Argentina. ³Laboratorio de Paleontología de Vertebrados, Departamento de Ciencias Geológicas, Facultad de Ciencias Exactas y Naturales, Pabellón II, Universidad de Buenos Aires, Intendente Güiraldes 2160, Ciudad Universitaria (C1428EGA), Buenos Aires, Argentina. ⁴CONICET-Sección Paleontología de Vertebrados, Museo Argentino de Ciencias Naturales “Bernardino Rivadavia”, Av. Ángel Gallardo 470, C1405 DJR Buenos Aires, Argentina. ⁵Instituto de Geología y Recursos Naturales, Centro de Investigación e Innovación Tecnológica, Universidad Nacional de La Rioja (INGeReN-CENIIT-UNLaR), Av. Gob. Vernet y Apóstol Felipe, 5300 La Rioja, Argentina. ⁶Centro de Investigaciones en Ciencias de la Tierra (CICTERRA), Universidad Nacional de Córdoba, CONICET, FCEfYn, Vélez Sarsfield 1611, Ciudad Universitaria, X5016GCA Córdoba, Argentina. ⁷Instituto de Investigación en Paleobiología y Geología, Universidad Nacional de Río Negro-CONICET, Av. Presidente Julio A. Roca 1242, 8332 General Roca, Río Negro, Argentina. ✉email: emhechenleitner@gmail.com

Titanosaurian sauropods are a group of large, long-necked, herbivorous dinosaurs with a complex evolutionary history^{1–6}. During the Late Cretaceous, they underwent an extensive evolutionary radiation worldwide. Most of their record in South America is restricted to Argentine Patagonia (e.g., Neuquén, Golfo San Jorge and Austral basins) and the Bauru Basin of SW Brazil^{7–9} (Fig. 1a). Some studies have attempted to establish paleobiogeographic links between these regions^{10,11}, although there are remarkable faunistic differences between Patagonian and Brazilian titanosaurs^{12–15}. Similarly, other contemporaneous tetrapods, such as pleurodiran turtles and notosuchian mesoeucrocodylians, also show heterogeneous distributions^{16,17}.

By the Late Cretaceous, vast regions of South America remained flooded by epicontinental seas¹⁸, and although there are high-rank taxonomic similarities, the evidence of eventual connections between northern and southern terrestrial faunas are still scarce. The ubiquity of the clade Titanosauria in a geographically intermediate area is validated by the occurrence of the saltasaurids *Yamansaurus* from Ecuador¹⁹ and *Saltasaurus*²⁰—plus a putative record of *Neuquensaurus*²¹—from NW Argentina (Fig. 1a), along with fragmentary accounts of sauropod dinosaurs in the latter region. However, saltasaurids have not been documented so far in the Bauru Basin nor other units in Brazil^{11,22}, and the non-saltasaurid specimens in NW Argentina are too

fragmentary²³ to allow determination of paleobiogeographic relationships. In addition to saltasaurids, the other high-level clade amongst titanosaurs is the Colossosauria, recently stem-based defined as the most inclusive clade containing *Mendozasaurus* but not *Saltasaurus*, nor *Epachthosaurus*⁹. It includes the subclades Rinconsauria and Lognkosauria (plus a few related taxa), whose taxonomic composition has fluctuated over the years^{2–4}. The fossil record of colossosaurians has, so far, a disparate distribution, with most of its members reported in Patagonia and SW Brazil.

Herein, we report the discovery of new dinosaurs from the Upper Cretaceous red beds of the Quebrada de Santo Domingo locality (QSD) in the Andes of La Rioja, NW Argentina (Fig. 1b). We recovered three partial skeletons that belong to two new derived titanosaurian dinosaur species (Fig. 1c, d) in different stratigraphic positions of the Ciénaga del Río Huaco Formation. Moreover, we found titanosaurian egg clutches and eggshells in an intermediate stratigraphic position, distributed in three levels. With an overwhelming abundance of eggs, QSD is one of the largest nesting sites documented worldwide. The results of our phylogenetic analysis incorporating the two new taxa suggest that they have Patagonian and Brazilian affinities, reinforcing the hypothesis of a close relationship between the titanosaurian sauropod faunas from northern and southern South America during the Late Cretaceous.

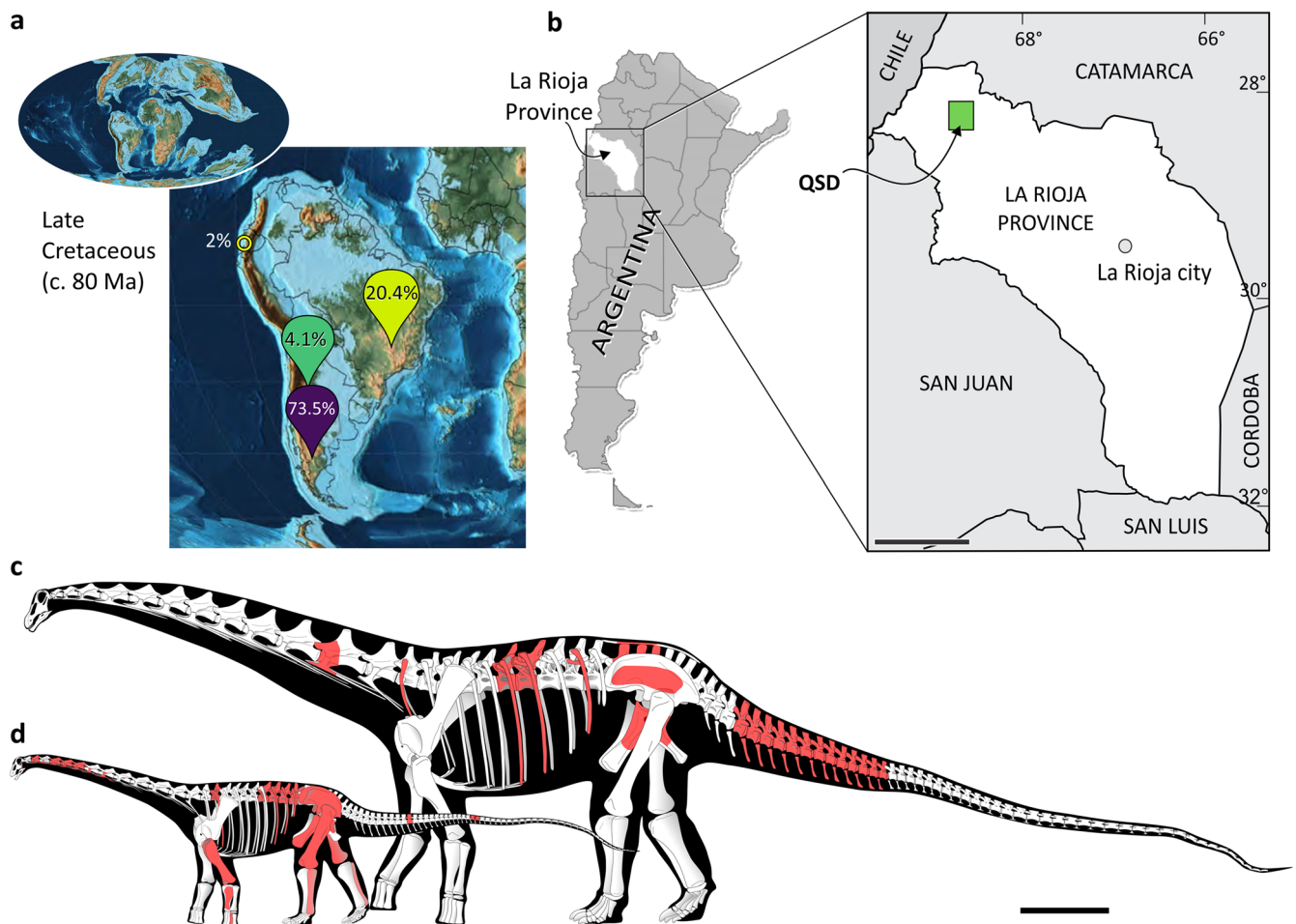


Fig. 1 Titanosaurian record in South America, map of the study area and skeletal reconstructions of the new titanosaurian species. **a** Percentage diversity of Cretaceous titanosaurian sauropods in three main regions of South America: Patagonia (purple), NW Argentina (green), and SW Brazil (yellow) (Supplementary Table 3). The yellow ring corresponds to the record of the saltasaurid titanosaurian *Yamansaurus* in Ecuador. Map modified from Scotese¹⁷. **b** Location of the discoveries. **c** *Punatitan coughlini* gen. et sp. nov. **d** *Bravasaurus arrierosorum* gen. et sp. nov. Preserved elements are coloured in red in **c**, **d**. Scale bar: 100 km in **b**, and 1 m in **c**, **d**.

Results

Systematic palaeontology.

Sauropoda Marsh, 1878

Titanosauria Bonaparte and Coria, 1993

Colossosauria González Riga et al., 2019

Punatitan coughlini gen. et sp. nov.

Etymology. ‘Puna’ is the local name that distinguishes the oxygen-depleted atmosphere typical of the high Andes, and ‘coughlini’ refers to the geologist Tim Coughlin, who reported the first dinosaur fossils in the area.

Holotype. CRILAR-Pv 614 (Paleovertebrate Collection of Centro Regional de Investigaciones Científicas y Transferencia Tecnológica de La Rioja, Argentina), partial skeleton composed of the anterior portion of posterior cervical vertebra (likely C12), two middle dorsal vertebrae (likely D6–D7), partial sacrum, 13 articulated caudal vertebrae (some with articulated haemal arches), right pubis, left ischium, and several dorsal ribs.

Horizon and type locality. Sandstone levels 170 m above the base of the Ciénaga del Río Huaco Formation (Campanian-Maastrichtian) at QSD, La Rioja, NW Argentina (Geological Setting in Supplementary Information).

Diagnosis. A medium-sized titanosaurian sauropod characterised by the following combination of features (autapomorphies marked with an asterisk): (1) middle dorsal vertebrae (likely D6–D7) with anterior and posterior spinodiapophyseal laminae (spdl) forming wide and flat surface, between aliform and transverse processes*; (2) accessory posterior centrodiaepophyseal lamina (apcdl) crossed over by the posterior centroparapophyseal (pcpl) lamina, forming a X-shaped intersection in D6–D7; (3) pcpl reaches the bottom of posterior centrodiaepophyseal lamina (pcdl) in D6–D7*; (4) extra-depression ventrally to intersection of pcpl and apcdl in D6–D7*; (5) deep postzygodiaepophyseal centrodiaepophyseal fossa (pocdf) in D6–D7; (6) neural spine of D6 tapering dorsally, forming an inverted-“V” profile in anterior/posterior view; (7) caudal transverse processes persist beyond Ca15; (8) slightly anteriorly inclined neural spines in anterior-middle caudal vertebrae (Ca5–6 to Ca10); and (9) distally expanded prezygapophyses in anterior-middle caudal vertebrae.

Description and comparisons of *Punatitan*. Most diagnostic features are in the axial skeleton of *Punatitan* (Fig. 2), allowing us to distinguish the new taxon from other titanosaurians. The holotype CRILAR-Pv 614 represents a medium-sized individual, larger than the holotypes of *Overosaurus*²⁴, *Saltasaurus*²⁵, *Neuquensaurus*^{26,27}, and *Trigonosaurus*²⁸, about the same size as the holotype of *Uberabatitan*²⁹, and smaller than *Aeolosaurus*³⁰, ‘*Aeolosaurus*’¹¹, *Mendozasaurus*³ and giant taxa (e.g., *Argentinosaurus*, *Patagotitan*).

A cranial portion of a posterior cervical vertebra is only available (Fig. 2a, b). It may correspond to C12, based on *Overosaurus* and *Trigonosaurus* (MCT 1499-R²⁸). The centrum is shorter dorsoventrally than it is wide transversely, with its anterior surface strongly convex. The base of the right parapophysis is level with the ventral border of the centrum and ventrally delimits the deeply concave lateral surface of the centrum. The prezygapophyses are anterolaterally projected and well separated from each other. Their anterior edge is placed slightly anterior to the level of the articular surface. Both are medially connected by a sharp interprezygapophyseal lamina (tprl) that forms an opened U-shaped edge in dorsal view. The right base of a rounded dorsomedially projected spinoprezygapophyseal lamina (sprl) is preserved. Although the

neural arch is incomplete, the position and development of the prezygapophyses, together with the position, orientation, and robustness of the sprl, suggest a wide and concave spinoprezygapophyseal fossa (sprf). Overall, the cervical vertebra of *Punatitan* is similar to that of most titanosaurians. The robust sprl is more similar to that of *Malawisaurus*³¹, *Mendozasaurus*³, *Futalognkosaurus*³², and *Dreadnoughtus*³³ than to *Overosaurus*²⁴, in which the lamina is weakly developed, and the floor of the sprf is reduced. In *Trigonosaurus*²⁸ the sprl is also conspicuous but relatively short, thus defining a small sprf.

Two dorsal vertebrae are known for *Punatitan*, interpreted as D6 (Fig. 2c, d) and D7 (Fig. 2e), based on comparisons with *Overosaurus*²⁴ and *Trigonosaurus*²⁸ (e.g., the relative position of parapophysis and diapophysis, orientation of neural spine). The centra are opisthocelous, almost as high as wide. Laterally, they show deep and partitioned pleurocoels that have tapering, acute caudal margins. They are located dorsally, near the neurocentral junction. The neural arches are fused to the centra, without a sign of suture.

The diapophyses are robust and well projected laterally, while the parapophyses are more anteriorly and slightly ventrally positioned, as occurs in middle dorsal vertebrae (e.g., D5–D7 of *Overosaurus*²⁴). Below these processes, the neural arches are notably intricate, showing a broad, deeply excavated fossa (Fig. 2c) with a conspicuous asymmetry in both lateral sides, as seen in other sauropods (e.g., *Trigonosaurus*²⁸, *Lirainosaurus*³⁴).

The pcpl and its anterior projection, the apcdl, plus the well-developed pcpl are the most conspicuous traits in the lateral aspects of these vertebrae (Fig. 2c), as seen in several titanosaurians, such as *Malawisaurus*³¹, *Elaltitan*³⁵, *Overosaurus*²⁴, *Trigonosaurus*²⁸, and *Dreadnoughtus*³³. The pcpl projects posteriorly to reach the posterodorsal border of the centrum. The apcdl projects anteriorly from the dorsal edge of this lamina, contacting the anterodorsal border of the centrum. The accessory lamina is crossed over by the pcpl, forming an X-shaped intersection that is evident on the right side of D6 and D7 (on left sides of both, the pcpl finishes when contacting the apcdl, forming a Y-shaped pattern). The pattern observed in D6–D7 of *Punatitan* is roughly observed in D7 of *Overosaurus*²⁴ (other dorsal vertebrae have no clear X-pattern) and *Petrobrasaurus*³⁶, but not in other titanosaurians such as *Malawisaurus*³¹, *Elaltitan*³⁵, *Trigonosaurus*²⁸, *Lirainosaurus*³⁴, and *Dreadnoughtus*³³. Conspicuously, these laminae define deep fossae in *Punatitan*. The deep, subtriangular fossa, dorsally delimited by the pcpl and apcdl is identified as posterior centrodiaepophyseal fossa (pcdl-f)³³. It is deeper in *Punatitan* than in *Overosaurus*²⁴, *Trigonosaurus*²⁸, *Muyelensaurus*³⁷, and *Dreadnoughtus*³³.

The anterior centroparapophyseal lamina (acpl) and pcpl project ventrally and posteroventrally, respectively, from the parapophysis. The pcpl is truncated on the left side of D6–D7 when touching the apcdl; consequently, on this side, the pcdl-f is much larger than on the right side. In both dorsal vertebrae, the acpl and pcpl also define a deep but small fossa.

The oval-shaped prezygapophyses are connected medially by transversely short tprl (Fig. 2e). They are detached from the diapophyseal body by a marked step that dorsally elevates their articular surface. In anterior view, the centroprezygapophyseal lamina (cprl) has a sharp border, and it widens dorsally. This lamina and the acpl define a deep fossa that faces anterolaterally. The sprl in these dorsal vertebrae are present as blunt structures that are poorly preserved. They connect the prespinal lamina (prsl) medially, without obstructing its path. A similar condition was inferred for *Barrosasaurus*³⁸, and a posterior dorsal vertebra referred as to *Trigonosaurus*³⁹, but they can correspond to accessory laminae rather than to the true sprl, which is usually seen in more anterior vertebrae⁴⁰.

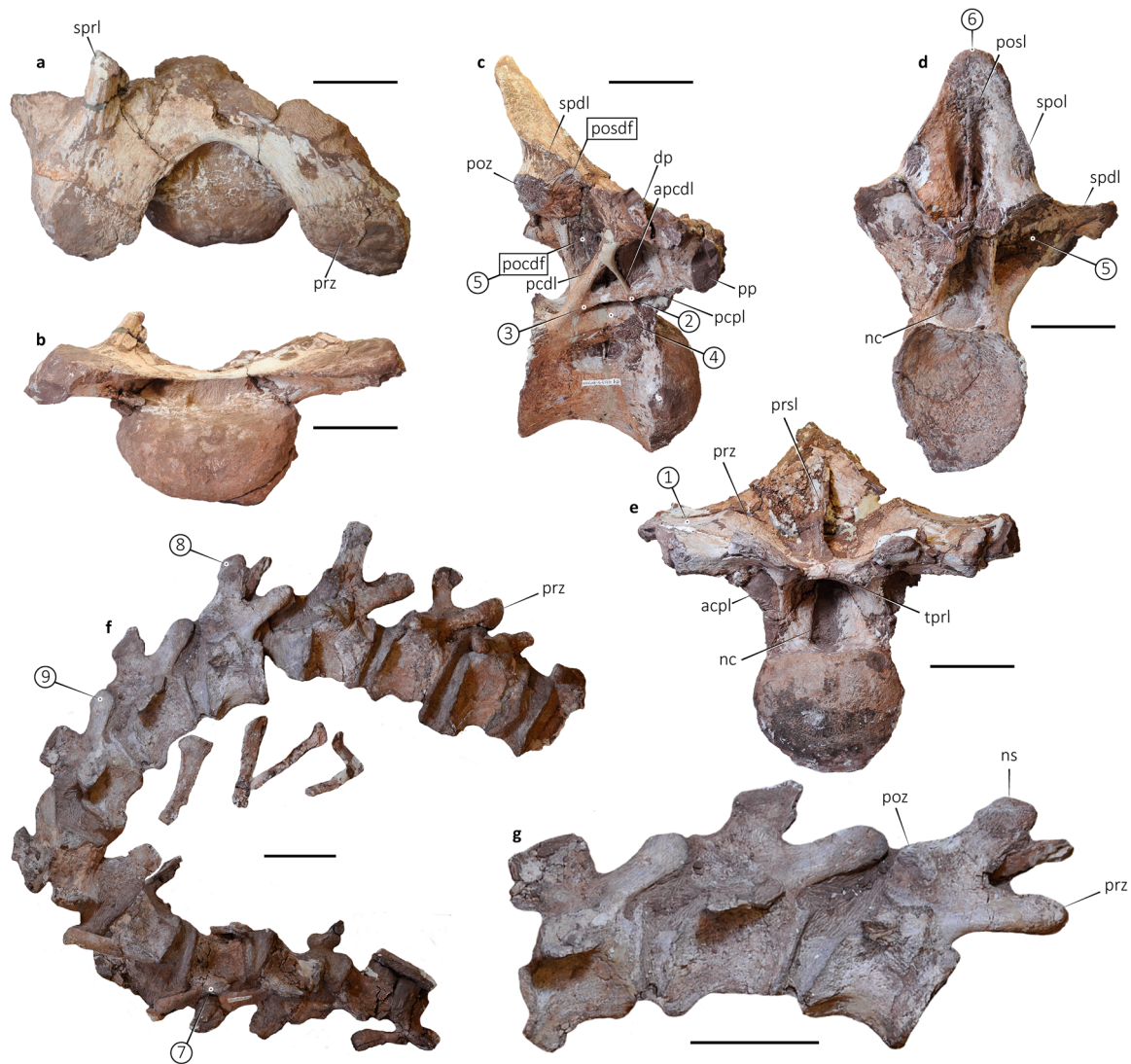


Fig. 2 *Punatitan coughlini* gen. et sp. nov. (CRILAR-Pv 614). **a, b** Cervical vertebra (C12) in dorsal **a** and anterior **b** views. **c, d** Dorsal vertebra (D6) in right lateral **c** and posterior **d** views. **e** Dorsal vertebra (D7) in anterior view. **f** Articulated series of caudal vertebrae (Ca5–Ca17). **g** Detail of Ca8–Ca12. acpl anterior centroparapophyseal lamina, apcdl accessory posterior centrodiapophyseal lamina, dp diapophysis, nc neural canal, ns neural spine, pcdl posterior centrodiapophyseal lamina, pcpl posterior centroparapophyseal lamina, pocdf postzygapophyseal centrodiapophyseal fossa, posdf postzygapophyseal spinodiapophyseal lamina, posl postspinal lamina, poz postzygapophysis, pp parapophysis, prsl prespinal lamina, prz prezygapophysis, spd spinodiapophyseal lamina, spol spinopostzygapophyseal lamina, sprl spinoprezygapophyseal lamina, tpri interprezygapophyseal lamina. Circled numbers correspond to apomorphies numbered in the text. Measurements in Supplementary Table 1. Scale bars: 100 mm.

The postzygapophyses are higher than the lateral tip of the diapophysis in D6–D7, and there is no direct contact between the postzygapophyses and the diapophyses. Instead, there is a lamina that starts at the postzygapophysis and projects anterodorsally to connect to the spd, closer to the base of the spine than to the base of the diapophysis. The homology of this lamina is debated^{40,41}; it is here interpreted as the podl. This lamina is similar to the podl observed in dorsal vertebrae of *Malawisaurus*³¹, *Choconsaurus* (D6?⁴²) and *Dreadnoughtus* (D6?³³), and its unusual connection with the spd may be related to changes of the neural spine inclination and the relative position of the postzygapophyses and diapophyses in middle dorsal vertebrae⁴¹. At this point, this short podl delimits ventrally a very small postzygapophyseal spinodiapophyseal fossa (posdf), which faces laterally (Fig. 2c). A similar small fossa is present in the anteriormost dorsal of *Rapetosaurus*⁴³ and the mid-posterior dorsal of *Bonitasaura*⁴⁴. It differs from the condition seen in *Lirainosaurus* and *Neuquensaurus*, in which the posdf is well developed and faces more posteriorly. The

postzygapophyses in D6 slope dorsally to the neural spine without a spinopostzygapophyseal lamina (spol), differing from the condition of *Dreadnoughtus*³³, *Mendozasaurus*³ and *Elaltitan*³⁵, which have a sharp lamina. The centropostzygapophyseal lamina is also well developed, contacting the pcdl near the level of the neural canal. Both laminae define a large and deep pocdf.

The neural spine is complete in D6 of *Punatitan*. It is somewhat inclined posteriorly, with the tip extending as far posteriorly as the posterior border of the centrum (Fig. 2c). It is anteroposteriorly narrow and tapers dorsally. In anterior view, the contour of the tip is rounded, without any expansion, forming an inverted V-shaped profile, with a slightly sigmoid outline owing to the presence of aliform processes. The neural spine bears a prsl and a postspinal lamina (posl). The prsl is sharp in the basal half of the spine, separating two deep, wide fossae, laterally delimited by the prominent spd. The posl is also sharp and expands over almost all the neural spine, delimiting two deep, narrow fossae, laterally bordered by the postzygapophyses, and

the aliform processes (Fig. 2d). The neural spine of D6 in *Punatitan* differs from that of most titanosaurs, which have expanded (e.g., *Dreadnoughtus*³³) or squared (e.g., *Choconsaurus*⁴², *Overosaurus*²⁴, *Trigonsaurus*²⁸) neural spines.

The still unprepared sacrum of *Punatitan* is incomplete and will be described elsewhere. However, it was possible to observe an ossified supraspinous rod placed over the preserved neural spines (two or more). This structure is known for *Epachthosaurus*, *Malawisaurus*, and basal titanosauriforms⁴⁵.

The holotype of *Punatitan* also preserves 13 articulated caudal vertebrae as well as several haemal arches (Fig. 2f). The first preserved caudal possibly represents Ca5. As in most titanosaurs, these caudal vertebrae have strongly procoelous centra¹. The centra are dorsoventrally tall, differing from the depressed centra of saltasaurines^{25,46}. Their anterodorsal border is anteriorly displaced from the anterodorsal one, resulting in an oblique profile in lateral view. They have slightly concave lateral surfaces, with transversely thin ventrolateral ridges that delimit a deeply concave ventral surface that is devoid of fossae. The internal tissue of the caudal centra is spongy, and the neural arches are pneumatic.

In the anterior caudal vertebrae, a suture is present above the base of the transverse processes (Fig. 2g). It forms a conspicuous ridge, which is not evident in related taxa, although it resembles the dorsal tuberosity described for *Baurutitan*⁴⁷, and also CRILAR-Pv 518c from Los Llanos, east La Rioja²³. The neural arch of each caudal vertebra is situated over the anterior two-thirds of the centrum, and each is relatively tall with well-developed prezygapophyses and neural spines. The transverse processes are sub-triangular to laminar and gradually change from laterally to posterolaterally projected along the vertebral column. The prezygapophyses are long and project anterodorsally. The postzygapophyses contact the neural spine via a short spool and are located almost at the midline of the centra. This condition differs from the much more anteriorly placed postzygapophyses of the Patagonian *Aeolosaurus*³⁰. The neural spine is rectangular in cross-section and anteroposteriorly longer than transversely wide (including prsl and posl). The spines are tall in the anterior caudal vertebrae and become shorter and square in the posterior ones. They also project slightly anteriorly, especially in Ca8–Ca10 (Fig. 2g). Some degree of anterior inclination of the neural spines is also reported for *Trigonsaurus*²⁸ and *Aeolosaurus*³⁰, contrasting with the most common condition amongst titanosaurs, i.e., vertical or posteriorly oriented neural spines (e.g., *Baurutitan*⁴⁷, *Dreadnoughtus*³³, *Saltasaurus*²⁵). The available haemal arches are opened Y-shaped, with no expanded pedicels, as are those reported for other derived titanosaurs⁴⁸.

Bravasaurus arrierosorum gen. et sp. nov.

Etymology. *Bravasaurus*, referred to the Laguna Brava, a lake that gives name to the Laguna Brava Provincial Park, and *arrierosorum*, refers to the people who crossed the Andes carrying cattle during the 19th century.

Holotype. CRILAR-Pv 612, right quadrate and quadratojugal, four cervical, five dorsal, and three caudal vertebrae, few dorsal ribs, three haemal arches, left humerus, fragmentary ulna, metacarpal IV, partial left ilium with sacral ribs, right pubis, partial ischium, left femur, and both fibulae.

Paratype. CRILAR-Pv 613, isolated tooth, right ilium, right femur, and dorsal ribs.

Horizon and type locality. Sandstone levels 34 m above the base of the Ciénaga del Río Huaco Formation (Campanian-Maastrichtian) at QSD, La Rioja, NW Argentina (Geological Setting in Supplementary Information).

Diagnosis. A small-sized titanosaurian sauropod characterised by the following association of features (autapomorphies marked with an asterisk): (1) quadrate with articular surface entirely divided by medial sulcus*; (2) sprl forms conspicuous step between neural spine and prezygapophyses, in middle cervical vertebrae*; (3) strongly depressed centra (up to twice as wide as tall) in posterior dorsal vertebrae; (4) robust dorsal edge of pneumatic foramen in dorsal centra, forming prominent shelf that extends laterally, beyond the level of the ventral margin of the centum*; (5) posterior dorsal vertebrae with a rough posl, ventrally interrupted by middle spinopostzygapophyseal laminae (m.spol) that contact the postzygapophyses; (6) posterior dorsal vertebrae with small ventral spinopostzygapophyseal fossa (v.spof) delimited dorsally by the m.spol and ventrally by the interpostzygapophyseal lamina (tpol); (7) humerus with narrow midshaft, with midshaft/proximal width ratio of 0.36; (8) deltopectoral crest of the humerus expanded distally; (9) slender fibula (Robustness Index [RI]⁴⁹ = 0.15); (10) distal condyle of the fibula transversely expanded, more than twice the midshaft breadth.

Description and comparisons of *Bravasaurus*. The holotype of *Bravasaurus* (Figs. 3 and 4), as well as the referred specimen, indicates a small-sized titanosaurian, much smaller than *Punatitan* (Fig. 1c, d) and other medium-sized sauropods, such as *Trigonsaurus*, *Overosaurus*, and *Bonitasaura*. Considering that both specimens could be adults (see below), they would be similar to *Neuquensaurus* or *Magyarosaurus*⁵⁰. Cranial elements include partial right quadrate and quadratojugal (Fig. 3a, b). The quadrate is anteroventrally directed and bears part of the quadrate fossa. The articular surface for the mandible is transversely elongated. It shows two condyles that separate from each other by a longitudinal sulcus (Fig. 3b). The medial condyle is round, whereas the lateral is anteroposteriorly elongated. *Diplodocus*⁵¹ also has a sulcus but restricted to the posterior region of the articular surface. Among titanosaurs, the articular surface of the quadrate has a kidney shape in *Nemegtosaurus* and *Quaesitosaurus*⁵², with the sulcus restricted to its anterior portion. In *Bonitasaura*⁵³ and *Rapetosaurus*⁵⁴, the articular surface is not divided. The anterior process of the quadratojugal projects ventrally, whereas the posterolateral process barely extends ventrally, similar to *Nemegtosaurus*⁵², and much less developed than in *Tapuiasaurus*⁵⁵ and *Sarmientosaurus*⁴. Unlike in these latter taxa, the posterolateral process reaches the articular condyle of the quadrate, which can only be seen behind (and not below) the quadratojugal in lateral view (Fig. 3a).

The holotype of *Bravasaurus* preserves cervical, dorsal, and caudal vertebrae. The neural arches of all elements are completely fused to their respective centra, which may indicate that it had reached somatic maturity before death^{56–58}.

We recovered four anterior-middle cervical vertebrae less than half a meter away from the cranial material. Three of them are articulated and associated with ribs. They are opisthocelous, with sub-cylindrical and relatively elongated centra (Fig. 3c). The neural arches have low neural spines, as observed in *Rinconosaurus*⁵⁹ and *Uberabatitan*²⁹. The diapophyses have posterior extensions, and the prezygapophyses are placed beyond the articular condyle of the centrum, as seen in the latter taxa. In *Bravasaurus* the postzygodiapophyseal lamina (podl) splits into a diapophyseal and a zygapophyseal segment, which become parallel with each other. Previous studies identified this feature as exclusive of *Uberabatitan*^{13,29}. In derived titanosaurs, the neural spines contact the prezygapophyses via the sprl, which is straight or slightly curved ventrally in lateral view. In the anterior cervical vertebrae of few titanosaurs (e.g. *Saltasaurus*²⁵ and

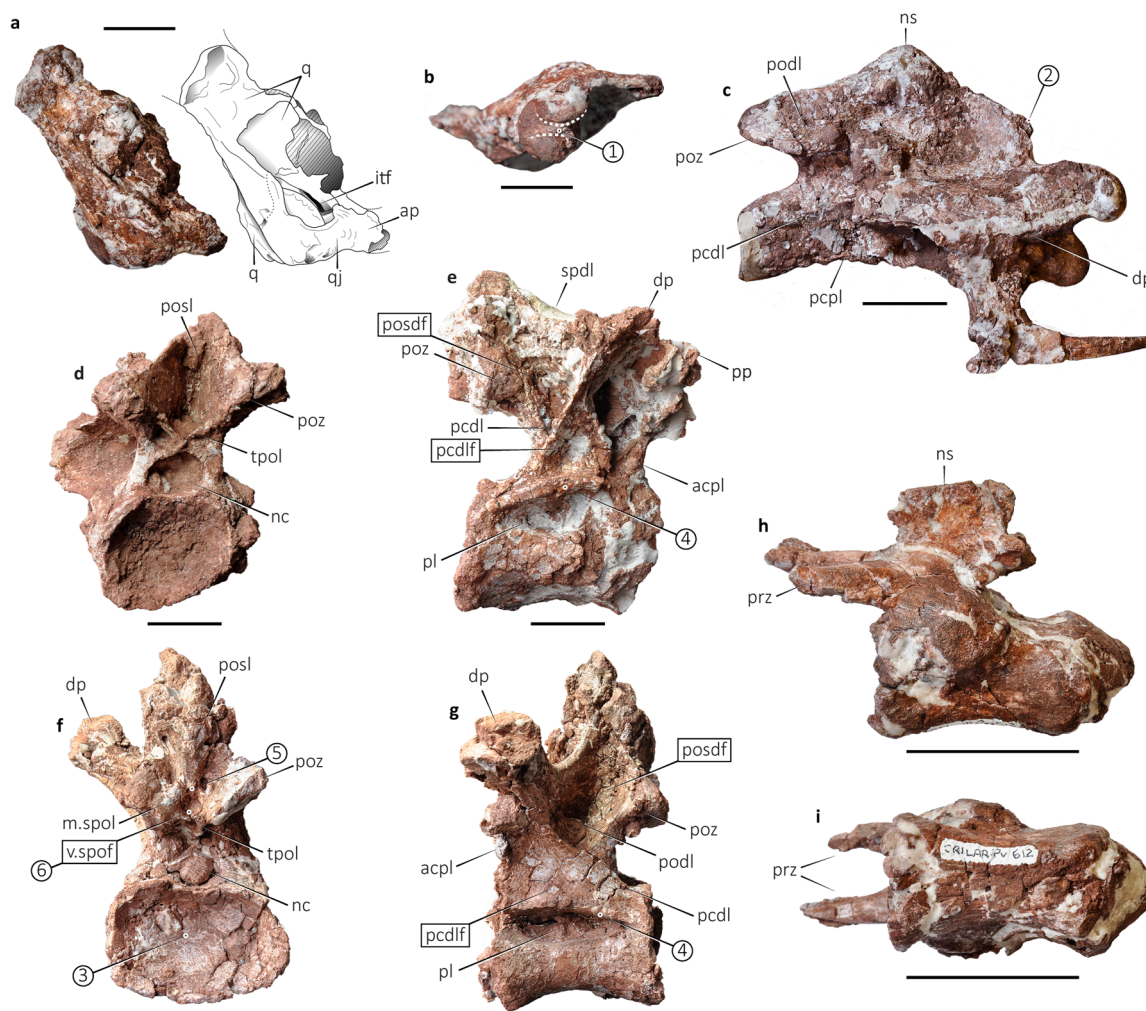


Fig. 3 Axial elements of *Bravasaurus arrierosorum* gen. et sp. nov. (CRILAR-Pv 612). **a, b** Quadrate and quadratojugal with interpretative drawing in right lateral **a**, and ventral **b** views (anterior to the right). **c** Middle cervical vertebra in right lateral view. **d** Anterior dorsal vertebra (D2) in posterior view. **e** Middle dorsal vertebra (D7) in right lateral view. **f–g** Posterior dorsal vertebra (D8) in posterior **f** and left lateral **g** views. **h, i** Middle caudal vertebra in left lateral **h** and ventral **i** views (anterior towards left). acpl anterior centroparapophyseal lamina, ap anterior projection, dp diapophysis, itf infratemporal fenestra, m.spol middle spinopostzygapophyseal lamina, nc neural canal, ns neural spine, pcdl posterior centrodiaepophyseal lamina, pcdlf posterior centrodiaepophyseal fossa, pcpl posterior centroparapophyseal lamina, pl pleurocoel, podl postzygodiapophyseal lamina, posdf postzygapophyseal spinodiapophyseal fossa, posl postspinal lamina, poz postzygapophysis, pp parapophysis, prz prezygapophysis, q quadrate, qj quadratojugal, spdl spinodiapophyseal lamina, tpol interpostzygapophyseal lamina, and v.spof ventral spinopostzygapophyseal fossa. Circled numbers correspond to apomorphies numbered in the text. Measurements in Supplementary Table 2. Scale bars: 10 mm in **a, b**, and 50 mm in **c–i**.

*Rocasaurus*⁴⁷), the sprl curves dorsally, forming a step close to the prezygapophysis. This step disappears beyond the first cervical vertebrae but remains present in middle cervical vertebrae of *Bravasaurus* (C5?–C6?; Fig. 3c).

The dorsal vertebrae of *Bravasaurus* have relatively short, opisthocelous centra (Fig. 3d–g). The well-developed pleurocoels are located just below the dorsal margin of the centrum, which forms a shelf that extends laterally, beyond the limits of the centrum, in middle and posterior dorsal vertebrae. Except for D10, the preserved dorsal centra are strongly dorsoventrally depressed (Fig. 3d, f), as in *Opisthocoeleicaudia*⁶⁰, *Alamosaurus*⁶¹, *Trigonosaurus*²⁸, and the “Series A” from Brazil³⁰. The neural arches of the dorsal vertebrae are tall, but not as tall as in *Punatitan*, in which the pedicels are particularly long. The orientation of the preserved neural spines follows the same pattern as in other derived titanosaurians, i.e., vertical in anterior and posterior-most dorsal vertebrae, and inclined (as much as 40°) in middle dorsal vertebrae (e.g., *Trigonosaurus*²⁸). The prsl

and posl are robust along their entire length (especially in the posterior dorsal vertebrae).

The anterior dorsal (D2) shows a low, laterally expanded neural arch (Fig. 3d). Although poorly preserved anteriorly, this vertebra exhibits a broad prespinal fossa with a weak prsl. It has rounded, ventrolaterally inclined postzygapophyses that reach the diapophyses though long podl. Medially, the postzygapophyses join each other by small laminae (tpol?) that intersect at the height of the dorsal edge of the neural canal. The junction between these laminae and the dorsal edge of the neural canal forms two small fossae, as seen in the posterior cervical vertebrae of *Overosaurus*²⁴. The neural spine is relatively low, and the postspinal fossa is particularly deep compared with the other dorsal vertebrae. The posl is weak. On the lateral aspect, the pcdl and the apcdl are the most conspicuous laminae. The diapophysis is eroded, and the parapophysis is located on the centrum above the pleurocoel.

The middle dorsal (D7) shows a slightly higher neural arch than D2, and its neural spine is inclined posteriorly, beyond the



Fig. 4 Appendicular elements of *Bravasaurus arrierosorum* gen. et sp. nov. (CRILAR-Pv 612). **a** Left humerus in anterior view. **b** Right pubis in ventrolateral view. **c, d** Left femur in anterior **c** and posterior **d** views. **e, f** Right fibula in lateral **e** and medial **f** views. dc deltopectoral crest, fh femoral head, ft fourth trochanter, gt greater trochanter, lb lateral bulge, lt lateral tuberosity, and vc ventral crest. Circled numbers correspond to apomorphies numbered in the text. Measurements in Supplementary Table 2. Scale bars: 100 mm.

posterior articular surface of the centrum (Fig. 3e). The parapophysis is missing, but the orientation of acpl and pcpl suggests a position slightly below and anterior to the diapophysis. In D8 and D10, a pair of m.spol interrupts the path of the posl, ventrally limiting a single, small fossa, here interpreted as v.spof (Fig. 3f). Its ventral limit corresponds to the tpol. A similar structure is present in *Lirainosaurus*³⁴. The podl is present in all the posterior dorsal vertebrae (D8–D10).

The anterior and middle caudal vertebrae of *Bravasaurus* are procoelous. The centra are as tall dorsoventrally as they are wide transversely, without any concavities on their ventral surfaces (Fig. 3h, i). The anterior margin of the centra does not appear to be anteroventrally inclined, as occurs in *Punatitan*, *Overosaurus*²⁴, or *Aeolosaurus*³⁰. The neural arches are on the anterior portion of the centra, as in most titanosaurs, and some other titanosauriforms (e.g., *Wintonotitan*⁶²). The neural spines are laminar and vertically directed, while the prezygapophyses are short and anteriorly projected. Such morphology shows many similarities with *Rinconosaurus*⁵⁹ and *Muyelensaurus*³⁷, but even more so with the Brazilian *Trigonosaurus*²⁸ and *Uberabatitan*^{13,29}. As for the centra, *Bravasaurus* differs from saltasaurines, in which they are depressed, with a ventral longitudinal hollow (e.g., *Saltasaurus*²⁵). Nor do they possess the ventrolateral ridges (Fig. 3i) present in other titanosaurs such as *Aeolosaurus*³⁰, *Overosaurus*²⁴, and *Punatitan*. *Bravasaurus* also differs from the latter taxa by the orientation of the neural spine in the anterior caudal, which is vertical rather than anteriorly directed. None of the preserved caudal vertebrae shows signs of distal expansion in the prezygapophyses, as seen in *Punatitan*.

The morphology of the humerus is compatible with that of many colossosaurian titanosaurs. Its robustness is high (RI = 0.35), as in *Opisthocoelicaudia*⁶⁰, *Diamantinasaurus*⁶³, and *Savannasaurus*⁶⁴, much more than in *Rinconosaurus*⁵⁹ and *Muyelensaurus*³⁷. The deltopectoral crest is markedly expanded distally (Fig. 4a), as in *Saltasaurus*²⁵, *Neuquensaurus*²⁷, *Opisthocoelicaudia*⁶⁰, and *Dreadnoughtus*³³. All pelvic elements are represented in the holotype, although only the pubis (Fig. 4b)

allows comparisons. It is proximodistally elongate and less robust than in *Futalognkosaurus*³² or *Opisthocoelicaudia*⁶⁰. The distal end is markedly expanded, as in several derived forms (e.g., *Rapetosaurus*⁴³, *Bonitasaura*⁴⁴, *Muyelensaurus*³⁷). The ilium of the specimen CRILAR-Pv 613 resembles the ilium of other derived titanosaurs, such as *Rapetosaurus* and *Bonitatitan*⁶⁵. The femur is straight, with the fourth trochanter placed at the proximal third (Fig. 4c, d), as in *Uberabatitan*¹³, *Patagotitan*², *Bonitasaura*⁴⁴, and *Futalognkosaurus*³², whereas in *Rinconosaurus*⁵⁹, *Muyelensaurus*³⁷, and *Diamantinasaurus*⁶³ it is located in the middle third. The humerus-to-femur length ratio in *Bravasaurus* is 0.75, similar to *Opisthocoelicaudia*, higher than *Neuquensaurus* and *Saltasaurus*, but lower than *Patagotitan* and *Epachthosaurus*. The fibula (Fig. 4e, f) markedly contrasts with the rest of the appendicular elements, as it is particularly gracile. Its distal condyle is transversely expanded, as observed in *Epachthosaurus*⁶⁶.

The known specimens of *Bravasaurus* indicate a small adult size. We estimate a body mass of 2.89 tons (2.17–3.61 tons, considering 25% error), based on a calibrated equation⁶⁷ (see “Methods” section). Estimates of <10 tons are few among titanosaurs. The European *Magyarosaurus* (750 kg), is interpreted as a case of insular dwarfism^{50,68}. The mass of the European *Lirainosaurus* was less than two tons⁵⁰, whereas that of the Argentinean *Saltasaurus* and *Neuquensaurus* was five and six tons², respectively. Among colossosaurians, estimations for *Rinconosaurus* indicate just four tons² and at least some other genera (e.g., *Overosaurus*, *Trigonosaurus*, *Baurutitan*), lacking appendicular bones, are small-sized forms, slightly larger than *Bravasaurus*, based on their vertebral size.

Phylogenetic analysis. The result of our phylogenetic analysis nests *Punatitan* and *Bravasaurus* as derived titanosaurs in all most parsimonious trees. The topology of the strict consensus tree is similar to that obtained in previous studies using the same dataset^{2,6}, although some taxa, such as *Baurutitan* and *Trigonosaurus* show

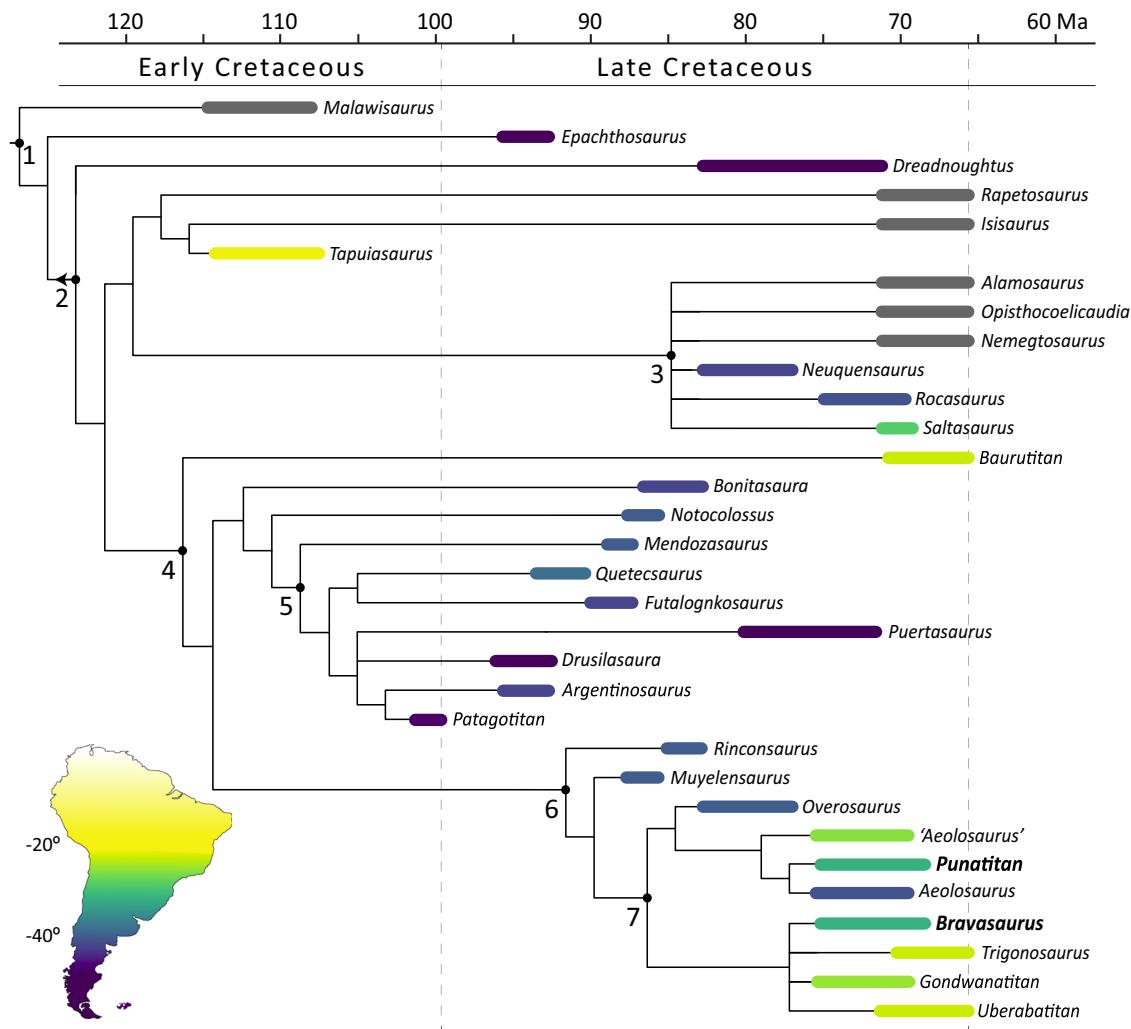


Fig. 5 Phylogenetic relationships of *Punatitan* and *Bravasaurus* within Lithostrotia. Phylogeny of derived titanosaurs, based on the data set of Carballido et al.⁶ (see “Methods” section and Supplementary Fig. 4). Time ranges for each terminal were obtained from published data. Colours in South American taxa are based on their palaeolatitudinal position. Both time ranges and palaeolatititude are given in Supplementary Table 4. 1. Lithostrotia, 2. Eutitanosauria, 3. Saltasauridae, 4. Colossosauria, 5. Lognkosauria, 6. Rinconsauria, and 7. Aeolosaurini.

noticeable changes in their position (Fig. 5; Supplementary Fig. 4). The former one is placed as the basalmost colossosaurian, and the latter is clustered together with *Uberabatitan*, *Gondwanatitan*, and *Bravasaurus*.

Both *Punatitan* and *Bravasaurus* are recovered within Colossosauria⁹. *Punatitan* shows three of the seven ambiguous synapomorphies that diagnose the newly erected clade⁹, and *Bravasaurus* five. Furthermore, the new Riojan species are placed within the clade Rinconsauria, along with several titanosaurs from SW Brazil and Patagonia (Fig. 5). *Punatitan* is nested with the Argentinean *Aeolosaurus*, by sharing the presence of distally expanded prezygapophyses in posteriormost anterior and middle caudal vertebrae. Other features of the caudal vertebrae, such as the dorsal edge of the anterior articular surface of the centrum ahead of the ventral margin, and the neural spines anteriorly oriented in the posteriormost anterior and middle caudal vertebrae, relate the latter taxa with the Brazilian ‘*Aeolosaurus*’ and *Overosaurus*, as successive sister taxa. *Bravasaurus* is included in a collapsed clade comprising the Brazilian *Trigonosaurus*, *Uberabatitan*, and *Gondwanatitan*. The clade is supported by a single synapomorphy: height/width ratio smaller than 0.7 in the posterior articular surface of cervical centra.

QSD nesting site. We documented three egg-bearing levels in the lower section of Ciénaga del Río Huaco Formation at QSD. The egg clutches and eggshells are included in an interval of floodplain deposits in at least three distinct but closely spaced horizons at 59.2, 62.8 and 63.9 m above the base of the unit (Supplementary Fig. 1). Fossil-bearing rocks are siltstones and sandy siltstones with horizontal lamination and graded and massive bedding that form thin tabular sheets, extending for tens to hundreds of metres. The fossiliferous layer is laterally traced over more than three kilometres, and the egg clutches and eggshells (CRILAR-Pv 620–621) are exposed regularly all along with it. Nineteen egg clutches were spotted, one with up to 15 sub-spherical eggs, arranged in two superposed rows.

The QSD eggs are similar to some Late Cretaceous titanosaurian eggs⁶⁹. Among the remarkable diversity of eggs worldwide, only Auca Mahuevo⁷⁰ (Argentina), Dholi Dungi⁷¹ (India), and Totești⁷² (Romania) preserve titanosaurian embryos. Therefore, these sites are the most reliable to correlate eggs with their producers. At QSD, the eggs are cracked, slightly compressed and flattened by the sedimentary load (Fig. 6a, b). We estimate an egg size of 130–140 mm, similar to the eggs from Auca Mahuevo⁷⁰ and Totești⁷², but slightly smaller than the ones from Dholi

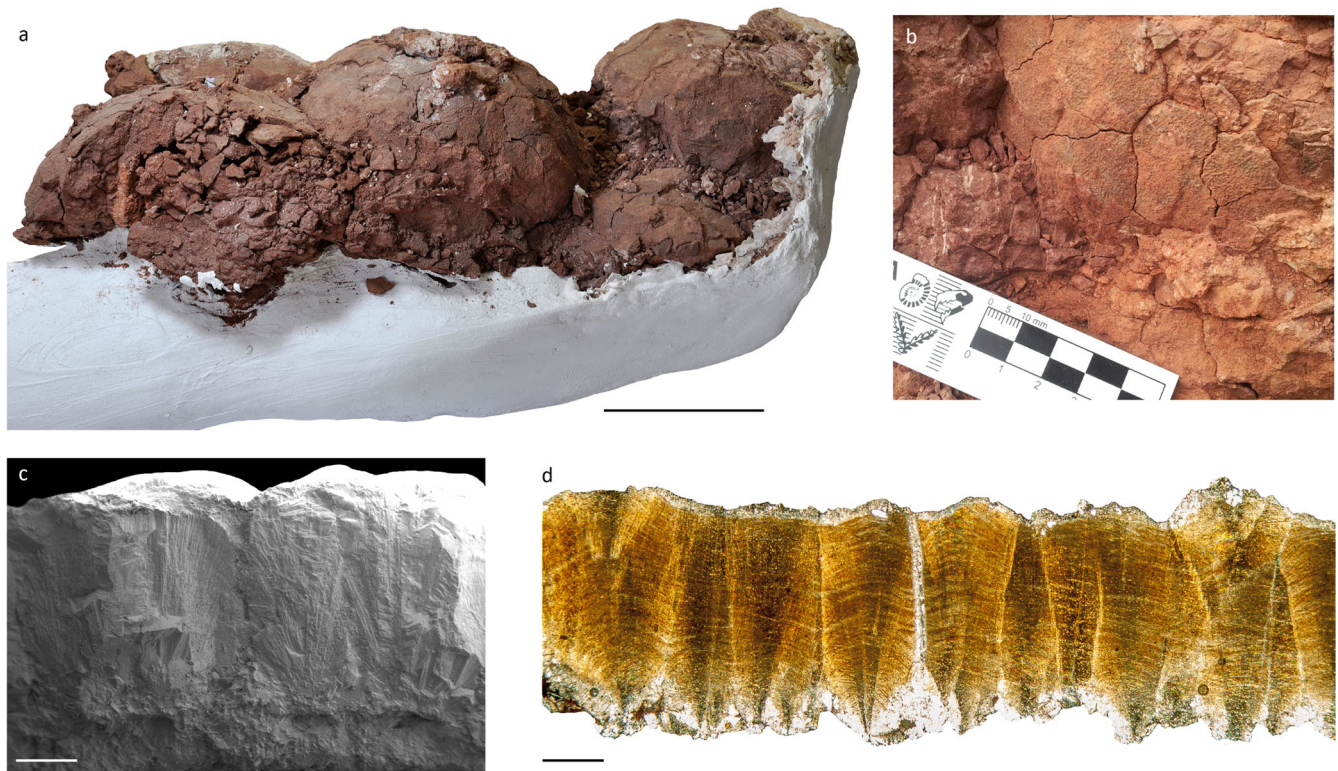


Fig. 6 Quebrada de Santo Domingo nesting site. **a** Part of a titanosaurian egg clutch, CRILAR-PV 620/001. **b** Partial egg and the surrounding matrix. **c, d** Eggshell micrographs under SEM **c** and TLM **d**. Note the straight pore canal with a funnel-shaped aperture in **c**. Scale bars: 100 mm in **a**, and 0.5 mm in **c, d**.

Dungri⁷¹ (160 mm). The eggshells are mono-layered, measuring 1.67 ± 0.31 mm ($n = 30$). The thickness is similar to the eggshells from layers 1–3 of Auca Mahuevo. The eggshells from Totești and layer 4 of Auca Mahuevo are slightly thicker, measuring 1.7–1.8 mm, whereas in Dholi Dungri they reach 2.26–2.36 mm. The QSD shells are composed of densely packed shell units of calcite crystals, which radiate from nucleation centres (Fig. 6c, d). They flare out at 50°, and their lateral margins become parallel at the inner third of the shell, like in the Auca Mahuevo specimens⁷⁰. Outwards, the units end out in rounded nodes of 0.3–0.4 mm in diameter, forming densely packed ornamentation that is typical of the titanosaurian clade^{69–72}. Multiple straight pore canals run through the eggshell, between the shell units. They have funnel-shaped external apertures that form round depressions between the surficial nodes. Among titanosaurian eggshells, those from Dholi Dungri and Auca Mahuevo (layers 1–3) also have straight pore canals, whereas, in those from Totești and the layer 4 of Auca Mahuevo, the pore canals ramify in a Y-shaped pattern.

As in Auca Mahuevo and other Cretaceous nesting sites, the QSD specimens are preserved in a floodplain palaeoenvironment. The occurrence of compact accumulations of whole eggs is consistent with the hypothesis of incubation within the substrate, as currently do the megapode birds from Australasia⁶⁹. Along with the egg clutches, hundreds of shells also appear scattered within the egg-bearing levels. Such an arrangement could be a consequence of the local transport of exposed shells during floods, but also the product of local removal during subsequent nesting episodes. Soft sediment deformation and dislocation are frequent, and could also have contributed to their dispersion. These features suggest that each of the three egg-bearing levels could constitute a time-averaged assemblage.

Discussion

As far as we know, *Punatitan* and *Bravasaurus* represent the first confirmed occurrence of colossosaurian titanosaurians⁹ in NW Argentina. For 40 years, *Saltasaurus* remained as the only well-represented sauropod for this region. *Saltasaurus* is closely related with the Patagonian *Rocasaurus* and *Neuquensaurus*, as well as *Yamanasaurus*¹⁹, from Ecuador. There is a consensus regarding the close relationship of these taxa, which constitute the Saltasaurinae, a clade of small-sized titanosaurians from the Late Cretaceous that is also supported by our phylogenetic result. The phylogenetic data also suggest that saltosaurines may not have a close relationship with other Late Cretaceous titanosaurians from South America (Fig. 5). Fragmentary findings in NW Argentina^{20,23,73} and Chile⁷⁴ suggested the occurrence of non-saltosaurine titanosaurians between Patagonia and Bauru, but the hitherto known evidence was insufficient to conjecture about their phylogenetic affinities. The new phylogenetic analysis recovers *Punatitan* within a clade of typically “aeolosaurine” taxa, such as *Aeolosaurus* and *Overosaurus*, whereas *Bravasaurus* is nested in a collapsed clade with Brazilian species. The Patagonian and Brazilian *Aeolosaurus* species show a close relationship as previously supported¹¹, but recent phylogenetic analyses, including the one here presented, suggest the Brazilian species may represent a distinctive genus, other than *Aeolosaurus*^{12,13}. Both Riojan species expand the diversity of the clade Rinconsauria, and its geographical distribution.

Based on a combination of direct observations and body mass estimation, *Bravasaurus* was a small-sized titanosaurian, though not as small as the dwarf *Magyarosaurus* or *Lirainosaurus*. Although it had probably reached its maximum size, it is much smaller than *Punatitan* (Fig. 1c, d). The largest titanosaurians ever known are placed within colossosaurians^{2,9} (e.g., *Argentinosaurus*, *Patagotitan*), but others are relatively smaller, such as

Rinconsaurus, *Overosaurus*, *Trigonosaurus*, *Baurutitan*, and *Gondwanatitan*. In this context, the available evidence suggests that *Bravasaurus* (~3 tons) is the smallest colossosaurian yet recorded, followed by the taxa mentioned above. In contrast to *Magyarosaurus*⁶⁸, *Bravasaurus* appears to have inhabited inland territories. By the latest Late Cretaceous, there is an evident reduction in size in saltasaurids and rinconsaurians across South America, which may be related to fluctuations in climate⁷⁵ and vegetation⁷⁶ (e.g., grassland), as a result of more temperate conditions and influence of remnant epicontinental seas during the dynamic aperture of the Atlantic.

The new findings from La Rioja reduce the paleobiogeographic gap of Late Cretaceous colossosaurians in South America, which were previously restricted to Patagonia and SW Brazil. Colossosauria is divided into the gigantic Lognkosauria (e.g., *Patagotitan*, *Futalognkosaurus*), plus some related forms, and the Rinconsauria. So far, the former clade is mostly limited to Patagonia (although there are few putative non-rinconsaurians in Brazil¹⁴), whereas Rinconsauria may contain a few Brazilian forms^{2,6,9,77}. Besides, some taxa recovered within Rinconsauria are often included within Aeolosaurini, a group of titanosaurs with unstable interspecific phylogenetic relationships¹². Our results suggest that Rinconsauria is much more diverse and widely distributed than previously thought^{2,3,6,9,37}. The oldest representatives of this clade would be in northern Patagonia, for the earliest Late Cretaceous. By the Campanian–Maastrichtian, the Rinconsauria increased their diversity and spread geographically northward, through La Rioja, to SW Brazil.

Comparison of the QSD eggs with confirmed occurrences of titanosaurian eggs, such as Auca Mahuevo⁷⁰ and Totești⁷², allow their identification. The spherical shape of the eggs, the monostratified shells and the nodular external ornamentation indicate that the QSD eggs belong to titanosaurian sauropods. More specific features (e.g., egg size, shell thickness, and straight vertical pore canals), associate the QSD specimens with the Auca Mahuevo eggs (layers 1–3). La Rioja Province is already known for its titanosaurian nesting sites in the Los Llanos region, several hundred kilometres southeast of QSD^{78,79}. There, two localities preserve Late Cretaceous nesting sites that show distinct palaeoenvironmental conditions. The eggs from these sites markedly differ in their shell thicknesses but share the same egg diameter, around 170 mm, larger than the 140 mm eggs from QSD. In South America, the only eggs to match that size are those from Auca Mahuevo and Río Negro⁸⁰, in Patagonia, as well as an isolated record from Bauru⁸¹. Eggs similar in diameter were attributed to dwarf Cretaceous titanosaurs from Totești⁷². The QSD eggs are relatively small, so either *Bravasaurus* or *Punatitan* may have been the producers. Further specimens are required to evaluate each scenario.

Both the oological and sedimentological data suggest a distinct nesting strategy from other sites of La Rioja. Unlike the sites in Los Llanos, the titanosaurian eggs of QSD appear in successive floodplain deposits, as occurs in Auca Mahuevo and other nesting sites worldwide⁶⁹. Each of the egg-bearing levels contains multiple egg accumulations that were not necessarily laid contemporaneously. The several episodes interspersed in the sedimentary sequence allow us to infer nesting site philopatry, a behaviour that seems to have been frequent among Cretaceous titanosaurs^{69,72,78,82,83}. This evidence and egg morphological features advocate a nesting strategy similar to that displayed at Auca Mahuevo. The QSD site provides further evidence on the plasticity of Late Cretaceous titanosaurian sauropods regarding their nesting strategies. Although it is still necessary to better understand the nesting conditions in other regions, such as Brazil, it seems increasingly evident that the adaptation to different

nesting strategies could have been crucial in the diversification and dispersal of titanosaurs across South America.

Methods

Specimens. All material described in this study is housed at the Paleovertebrate Collection of CRILAR (La Rioja, Argentina).

Taxa and systematic definitions. For the sake of simplicity, we used generic names when they are monotypic. The only exception corresponds to *Aeolosaurus*. The data set already included ‘*Aeolosaurus*’ *maximus*, a taxon which has been recognised as a member of Aeolosaurini⁸⁴, although it does not exhibit the diagnostic features of the genus (see Martinelli et al.¹² for further discussion) and is not grouped with the Patagonian species in some analyses^{13,14}. Consequently, we refer to it as ‘*Aeolosaurus*’. We followed the systematic definitions provided by Carballido et al.² and González Riga et al.⁹.

Eggshell micro-characterisation. We selected several eggshell fragments from QSD for microscopic imaging. Thin sections were carried out in the Petrology Lab at CRILAR, La Rioja, using the standard protocol for petrographic sectioning. We cut and mounted six eggshell fragments for their observation under a scanning electron microscope, following the protocol described in a previous study⁸⁵. We used a LEO 1450VP equipment in the Laboratorio de Microscopía Electrónica y Microanálisis (Universidad Nacional de San Luis, San Luis, Argentina).

Body mass. We estimated the body mass of *Bravasaurus* using a scaling equation adjusted for phylogenetic correlation/covariance⁶⁷. The equation

$$\log \text{BM} = 2.754 \cdot \log C_{H+F} - 1.097$$

where BM is body mass, and C_{H+F} is the sum of circumferences of the humerus and femur. It has been used to estimate the body mass of gigantic (e.g., *Patagotitan*²), as well as medium-sized titanosaurs (e.g., *Rapetosaurus*⁸⁶).

Phylogenetic analysis. We tested the phylogenetic position of *Bravasaurus* and *Punatitan* amongst 30 derived titanosaurian terminals using a modified version of the data matrix of Carballido et al.⁶. This matrix has been used to assess the phylogenetic position of derived titanosaurs and related taxa (e.g., *Sarmientosaurus*⁴, *Patagotitan*²).

Data on several South American titanosaurs was added in order to expand the representation of their diversity. We added scorings for *Gondwanatitan* and *Uberabatitan* to increase the information on Brazilian taxa. We also included *Aeolosaurus rionegrinus*³⁰ and the saltasaurine *Rocasaurus*, from Patagonia to the data set.

We added five characters (four from previous studies and one new) and modified few scorings (Supplementary Tables 4, 5; Supplementary Data 1). This resulted in a data set of 96 taxa and 421 characters (Phylogenetic Analysis in Supplementary Information, and Supplementary Data 2). As in previous studies⁶, 24 characters were considered as ordered (14, 61, 100, 102, 109, 115, 127, 132, 135, 136, 167, 180, 196, 257, 260, 277, 278, 279, 280, 300, 304, 347, 353, 355).

Statistics and reproducibility. We performed a parsimony analysis of the modified data matrix using TNT v.1.18⁷. We did a heuristic search with 1000 replicates of Wagner trees and two rounds of tree bisection-reconnection branch swapping. Branch support was quantified using decay indices (Bremer support values). They were calculated with TNT v.1.18⁷, and are given in the Supplementary Fig. 4. A TNT file containing raw data for the parsimony analysis is available in the Supplementary Data 2.

Nomenclatural acts. This published work and the nomenclatural acts it contains have been registered in ZooBank, the proposed online registration system for the International Code of Zoological Nomenclature (ICZN). The ZooBank LSIDs (Life Science Identifiers) can be resolved and the associated information viewed through any standard web browser by appending the LSID to the prefix “<http://zoobank.org/>”. The LSIDs for this publication are: urn:lsid:zoobank.org:pub:CDA87D24-50DA-415A-9FAF-54FB7CF26D73; urn:lsid:zoobank.org:act:18840DCF-33EF-465D-8F69-0B38BB601BF7; urn:lsid:zoobank.org:act:658B5D64-1432-46BC-B543-DF1155EC71E; urn:lsid:zoobank.org:act:336215DA-56AB-4B69-8059-C1FFA564D58A; urn:lsid:zoobank.org:act:84B7ECE6-60B4-4324-B983-CD86C8952E8A.

Reporting summary. Further information on research design and fieldwork is available in the Nature Research Reporting Summary linked to this article.

Data availability

Additional information, including the dataset analysed in this study, is available in the Supplementary Information, and Supplementary Data 1, 2 files. CRILAR-Pv 612-614 and

620–621 are deposited at the Paleovertebrate Collection of CRILAR (Anillaco, La Rioja), and are available upon request.

Received: 11 March 2020; Accepted: 29 September 2020;

Published online: 27 October 2020

References

- Salgado, L., Coria, R. A. & Calvo, J. O. Evolution of titanosaurid sauropods. I: phylogenetic analysis based on the postcranial evidence. *Ameghiniana* **34**, 3–32 (1997).
- Carballido, J. L. et al. A new giant titanosaur sheds light on body mass evolution among sauropod dinosaurs. *Proc. R. Soc. B* **284**, 20171219 (2017).
- González Riga, B. J., Mannion, P. D., Poropat, S. F., Ortiz David, L. D. & Coria, J. P. Osteology of the Late Cretaceous Argentinean sauropod dinosaur *Mendozasaurus neguyelap*: implications for basal titanosaur relationships. *Zool. J. Linn. Soc.* **184**, 136–181 (2018).
- Martínez, R. D. F. et al. A basal lithostrotian titanosaur (Dinosauria: Sauropoda) with a complete skull: implications for the evolution and paleobiology of Titanosauria. *PLoS ONE* **11**, e0151661 (2016).
- Gorscak, E. & O'Connor, P. M. Time-calibrated models support congruency between Cretaceous continental rifting and titanosaurian evolutionary history. *Biol. Lett.* **12**, 20151047 (2016).
- Carballido, J. L., Scheil, M., Knötschke, N. & Sander, P. M. The appendicular skeleton of the dwarf macronarian sauropod *Europasaurus holgeri* from the Late Jurassic of Germany and a re-evaluation of its systematic affinities. *J. Syst. Palaeontol.* **18**, 739–781 (2020).
- Otero, A. & Salgado, L. El registro de Sauropodomorpha (Dinosauria) de la Argentina. *Publ. Electrón. Asoc. Paleontol. Argent.* **15**, 69–89 (2015).
- Vieira, W. L. S. et al. Species richness and evidence of random patterns in assemblages of South American Titanosauria during the Late Cretaceous (Campanian–Maastrichtian). *PLoS ONE* **9**, e108307 (2014).
- González Riga, B. J. et al. An overview of the appendicular skeletal anatomy of South American titanosaurian sauropods, with definition of a newly recognized clade. *An. Acad. Bras. Ciênc.* **91**, e20180374 (2019).
- Casal, G., Martínez, R., Luna, M., Sciotto, J. C. & Lamanna, M. *Aeolosaurus colhuehuapensis* sp. nov. (Sauropoda, Titanosauria) de la Formación Bajo Barreal, Cretácico Superior de Argentina. *Rev. Bras. Paleontol.* **10**, 53–62 (2007).
- Santucci, R. M. & Arruda-Campos, A. C. de. A new sauropod (Macronaria, Titanosauria) from the Adamantina Formation, Bauru Group, Upper Cretaceous of Brazil and the phylogenetic relationships of Aeolosaurini. *Zootaxa* **33**, 1–33 (2011).
- Martinelli, A., Riff, D. & Lopes, R. Discussion about the occurrence of the genus *Aeolosaurus* Powell 1987 (Dinosauria, Titanosauria) in the Upper Cretaceous of Brazil. *Gaea* **7**, 34–40 (2011).
- Silva Junior, J. C. G., Marinho, T. S., Martinelli, A. G. & Langer, M. C. Osteology and systematics of *Uberabatitan ribeiroi* (Dinosauria; Sauropoda): a Late Cretaceous titanosaur from Minas Gerais, Brazil. *Zootaxa* **4577**, 401–438 (2019).
- Bandeira, K. L. N. et al. A new giant Titanosauria (Dinosauria: Sauropoda) from the Late Cretaceous Bauru Group, Brazil. *PLoS ONE* **11**, 1–25 (2016).
- Candeiro, C. R. A., Martinelli, A. G., Avilla, L. S. & Rich, T. H. Tetrapods from the Upper Cretaceous (Turonian–Maastrichtian) Bauru Group of Brazil: a reappraisal. *Cretac. Res.* **27**, 923–946 (2006).
- Pol, D. & Leardi, J. M. Diversity patterns of Notosuchia (Crocodyliformes, Mesoeucrocodylia) during the Cretaceous of Gondwana. *Publ. Electrón. Asoc. Paleontol. Argent.* **15**, 172–186 (2015).
- Fiorelli, L. E. et al. A new Late Cretaceous crocodyliform from the western margin of Gondwana (La Rioja Province, Argentina). *Cretac. Res.* **60**, 194–209 (2016).
- Scotese, C. R. & Wright, N. *PALEOMAP Paleodigital Elevation Models (PaleoDEMS) for the Phanerozoic (PALEOMAP Project)* <https://www.earthbyte.org/paleodem-resourcescotese-and-wright-2018> (2018).
- Apesteeguía, S., Soto Luzziaga, J. E., Gallina, P. A., Granda, J. T. & Guaman Jaramillo, G. A. The first dinosaur remains from the Cretaceous of Ecuador. *Cretac. Res.* **108**, 104345 (2020).
- Powell, J. E. Sobre una asociación de dinosaurios y otras evidencias de vertebrados del Cretácico Superior de la región de La Candelaria, Prov. de Salta, Argentina. *Ameghiniana* **16**, 191–204 (1979).
- D'Emic, M. D. & Wilson, J. A. New remains attributable to the holotype of the sauropod dinosaur *Neuquensaurus australis*, with implications for saltasaurine systematics. *Acta Palaeontol. Pol.* **56**, 61–73 (2011).
- Bittencourt, J. S. & Langer, M. C. Mesozoic dinosaurs from Brazil and their biogeographic implications. *Ann. Braz. Acad. Sci.* **83**, 23–60 (2011).
- Hechenleitner, E. M., Fiorelli, L. E., Martinelli, A. G. & Grellet-Tinner, G. Titanosaur dinosaurs from the Upper Cretaceous of La Rioja province, NW Argentina. *Cretac. Res.* **85**, 42–59 (2018).
- Coria, R. A., Filippi, L. S. & Chiappe, L. M. *Overosaurus paradasorum* gen. et sp. nov., a new sauropod dinosaur (Titanosauria: Lithostrotia) from the Late Cretaceous of Neuquén, Patagonia, Argentina. *Zootaxa* **3683**, 357–376 (2013).
- Powell, J. E. Osteología de *Saltasaurus loricatus* (Sauropoda-Titanosauridae) del Cretácico Superior del noroeste argentino. In *Los dinosaurios y su entorno biótico, Actas del Segundo Curso de Paleontología en Cuenca*, Vol. 4 (eds Sanz, J. L. & Buscalioni, Á. D.), 165–230 (Instituto Juan Valdes, Cuenca, 1992).
- Salgado, L., Apesteeguía, S. & Heredia, S. E. A new specimen of *Neuquensaurus australis*, a Late Cretaceous saltasaurine titanosaur from North Patagonia. *J. Vertebr. Paleontol.* **25**, 623–634 (2005).
- Otero, A. The appendicular skeleton of *Neuquensaurus*, a Late Cretaceous saltasaurine sauropod from Patagonia, Argentina. *Acta Palaeontol. Pol.* **55**, 399–426 (2010).
- Campos, D. A., Kellner, A. W. A., Bertini, R. J. & Santucci, R. M. On a titanosaurid (Dinosauria, Sauropoda) vertebral column from the Bauru Group, Late Cretaceous of Brazil. *Arq. Mus. Nac. Rio de J.* **63**, 565–596 (2005).
- Salgado, L. & Carvalho, I. D. S. *Uberabatitan ribeiroi*, a new titanosaur from the Marília Formation (Bauru Group, Upper Cretaceous), Minas Gerais, Brazil. *Palaeontology* **51**, 881–901 (2008).
- Powell, J. E. Revision of South American titanosaurid dinosaurs: palaeobiological, palaeobiogeographical and phylogenetic aspects. *Rec. Queen Vic. Mus.* **111**, 1–173 (2003).
- Gomani, E. M. Sauropod dinosaurs from the Early Cretaceous of Malawi, Africa. *Palaeontol. Electron.* **8**, 1–37 (2005).
- Calvo, J. O., Porfiri, J. D., González Riga, B. J. & Kellner, A. W. A. Anatomy of *Futalognkosaurus dukei* Calvo, Porfiri, González Riga & Kellner, 2007 (Dinosauria, Titanosauridae) from the Neuquén Group (Late Cretaceous), Patagonia, Argentina. *Arq. Mus. Nac. Rio de J.* **65**, 511–526 (2007).
- Lacovara, K. J. et al. A gigantic, exceptionally complete titanosaurian sauropod dinosaur from southern Patagonia, Argentina. *Sci. Rep.* **4**, 1–9 (2014).
- Díez Díaz, V., Pereda Suberbiola, X. & Sanz, J. L. The axial skeleton of the titanosaur *Lirainosaurus astibiae* (Dinosauria: Sauropoda) from the latest Cretaceous of Spain. *Cretac. Res.* **43**, 145–160 (2013).
- Mannion, P. D. & Otero, A. A reappraisal of the Late Cretaceous Argentinean sauropod dinosaur *Argyrosaurus superbus*, with a description of a new titanosaur genus. *J. Vertebr. Paleontol.* **32**, 614–638 (2012).
- Filippi, L. S. et al. A new sauropod titanosaur from the Plottier Formation (Upper Cretaceous) of Patagonia (Argentina). *Geol. Acta* **9**, 1–12 (2011).
- Calvo, J. O., González Riga, B. J. & Porfiri, J. D. A new titanosaur sauropod from the Late Cretaceous of Neuquén, Patagonia, Argentina. *Arq. Mus. Nac.* **65**, 485–504 (2007).
- Salgado, L. & Coria, R. A. *Barrosasaurus casamiquelai* gen. et sp. nov., a new titanosaur (Dinosauria, Sauropoda) from the Anacleto Formation (Late Cretaceous: early Campanian) of Sierra Barrosa (Neuquén, Argentina). *Zootaxa* **2222**, 1–16 (2009).
- Juarez-Valieri, R. & Ríos Díaz, S. D. Assignment of the vertebra CPP 494 to *Trigonosaurus pricei* Campos et al., 2005 (Sauropoda: Titanosauriformes) from the Late Cretaceous of Brazil, with comments on the laminar variation among lithostrotian titanosaurs. *Bol. Mus. Nac. Hist. Nat. Parag.* **17**, 20–28 (2013).
- Salgado, L. & Powell, J. E. Reassessment of the vertebral laminae in some South American titanosaurian sauropods. *J. Vertebr. Paleontol.* **30**, 1760–1772 (2010).
- Gallina, P. A. Notes on the axial skeleton of the titanosaur *Bonitasaura salgadoi* (Dinosauria-Sauropoda). *An. Acad. Brasil. Ciênc.* **83**, 235–245 (2011).
- Simón, E., Salgado, L. & Calvo, J. O. A new titanosaur sauropod from the Upper Cretaceous of Patagonia, Neuquén Province, Argentina. *Ameghiniana* **55**, 1–29 (2018).
- Curry Rogers, K. A. The postcranial osteology of *Rapetosaurus krausei* (Sauropoda: Titanosauria) from the Late Cretaceous of Madagascar. *J. Vertebr. Paleontol.* **29**, 1046–1086 (2009).
- Gallina, P. A. & Apesteeguía, S. Postcranial anatomy of *Bonitasaura salgadoi* (Sauropoda, Titanosauria) from the Late Cretaceous of Patagonia. *J. Vertebr. Paleontol.* **35**, e924957 (2015).
- Cerda, I. A., Casal, G. A., Martínez, R. D. & Ibiricu, L. M. Histological evidence for a supraspinous ligament in sauropod dinosaurs. *R. Soc. Open Sci.* **2**, 150369 (2015).
- Salgado, L. & Azpilicueta, C. Un nuevo saltasaurino (Sauropoda, Titanosauridae) de la provincia de Río Negro (Formación Allen, Cretácico Superior), Patagonia, Argentina. *Ameghiniana* **37**, 259–264 (2000).
- Kellner, A. W. A., Campos, D. A. & Trotta, M. N. F. Description of a titanosaurid caudal series from the Bauru Group, Late Cretaceous of Brazil. *Arq. Mus. Nac.* **63**, 529–564 (2005).
- Otero, A., Gallina, P. A., Canale, J. I. & Haluza, A. Sauropod haemal arches: morphotypes, new classification and phylogenetic aspects. *Hist. Biol.* **24**, 1–14 (2012).

49. Wilson, J. A. & Upchurch, P. A revision of *Titanosaurus* Lydekker (Dinosauria - Sauropoda), the first dinosaur genus with a 'Gondwanan' distribution. *J. Syst. Palaeontol.* **1**, 125–160 (2013).
50. Benson, R. B. J. et al. Rates of dinosaur body mass evolution indicate 170 Million years of sustained ecological innovation on the avian stem lineage. *PLoS Biol.* **12**, e1001853 (2014).
51. Whitlock, J. A. Was *Diplodocus* (Diplodocoidea, Sauropoda) capable of propalinal jaw motion? *J. Vertebr. Paleontol.* **37**, e1296457-3 (2017).
52. Wilson, J. A. Redescription of the Mongolian sauropod *Nemegtosaurus mongoliensis* Nowinski (Dinosauria: Saurischia) and comments on Late Cretaceous sauropod diversity. *J. Syst. Palaeontol.* **3**, 283–318 (2005).
53. Gallina, P. A. & Apesteguía, S. Cranial anatomy and phylogenetic position of the titanosaurian sauropod *Bonitasaura salgadoi*. *Acta Palaeontol. Pol.* **56**, 45–60 (2011).
54. Curry Rogers, K. & Forster, C. A. The skull of *Rapetosaurus krausei* (Sauropoda: Titanosauria) from the Late Cretaceous of Madagascar. *J. Vertebr. Paleontol.* **24**, 121–144 (2004).
55. Zaher, H. et al. A complete skull of an Early Cretaceous sauropod and the evolution of advanced titanosaurs. *PLoS ONE* **6**, e16663 (2011).
56. Irmis, R. B. Axial skeleton ontogeny in the Parasuchia (Archosauria: Pseudosuchia) and its implications for ontogenetic determination in archosaurs. *J. Vertebr. Paleontol.* **27**, 350–361 (2007).
57. Brochu, C. A. Closure of neurocentral sutures during crocodylian ontogeny: implications for maturity assessment in fossil archosaurs. *J. Vertebr. Paleontol.* **16**, 49–62 (1996).
58. Fronimos, J. A. & Wilson, J. A. Neurocentral suture complexity and stress distribution in the vertebral column of a sauropod dinosaur. *Ameghiniana* **54**, 36–49 (2017).
59. Calvo, J. O. & González Riga, B. J. *Rincosaurus caudamirus* gen. et sp. nov., a new titanosaurid (Dinosauria, Sauropoda) from the Late Cretaceous of Patagonia, Argentina. *Rev. Geol. Chile* **30**, 333–353 (2003).
60. Borsuk-Bialynicka, M. A new camarasaurid sauropod *Opisthocoelecaudia skarzynskii* gen. n., sp. n. from the Upper Cretaceous of Mongolia. *Paleontol. Pol.* **37**, 5–64 (1977).
61. Lehman, T. M. & Coulson, A. B. A juvenile specimen of the sauropod dinosaur *Alamosaurus sanjuanensis* from the Upper Cretaceous of Big Bend National Park, Texas. *J. Paleontol.* **76**, 156–172 (2002).
62. Poropat, S. F. et al. Reassessment of the non-titanosaurian somphospondylan *Wintonotitan watti* (Dinosauria: Sauropoda: Titanosauriformes) from the mid-Cretaceous Winton Formation, Queensland, Australia. *Pap. Palaeontol.* **1**, 59–106 (2015).
63. Poropat, S. F. et al. Revision of the sauropod dinosaur *Diamantinasaurus matildae* Hocknull et al. 2009 from the mid-Cretaceous of Australia: implications for Gondwanan titanosauriform dispersal. *Gondwana Res.* **27**, 995–1033 (2015).
64. Poropat, S. F. et al. New Australian sauropods shed light on Cretaceous dinosaur palaeobiogeography. *Sci. Rep.* **6**, 34467 (2016).
65. Martinelli, A. G. & Forasiepi, A. M. Late Cretaceous vertebrates from Bajo de Santa Rosa (Allen Formation), Río Negro province, Argentina, with the description of a new sauropod dinosaur (Titanosauridae). *Rev. Mus. Argent. Cienc. Nat.* **6**, 257–305 (2004).
66. Ibric, L. M., Martínez, R. D. & Casal, G. A. The pelvic and hindlimb myology of the basal titanosaur *Epachthosaurus sciuttoi* (Sauropoda: Titanosauria). *Hist. Biol.* **32**, 1–16 (2020).
67. Campione, N. E. & Evans, D. C. A universal scaling relationship between body mass and proximal limb bone dimensions in quadrupedal terrestrial tetrapods. *BMC Biol.* **10**, 60 (2012).
68. Stein, K. et al. Small body size and extreme cortical bone remodeling indicate phyletic dwarfism in *Magyarosaurus dacus* (Sauropoda: Titanosauria). *Proc. Natl Acad. Sci. USA* **107**, 9258–9263 (2010).
69. Hechenleitner, E. M., Grellet-Tinner, G. & Fiorelli, L. E. What do giant titanosaur dinosaurs and modern Australasian megapodes have in common? *PeerJ* **3**, e1341 (2015).
70. Grellet-Tinner, G., Chiappe, L. M. & Coria, R. A. Eggs of titanosaurid sauropods from the Upper Cretaceous of Auca Mahuevo (Argentina). *Can. J. Earth Sci.* **41**, 949–960 (2004).
71. Wilson, J. A., Mohabey, D. M., Peters, S. E. & Head, J. J. Predation upon hatchling dinosaurs by a new snake from the Late Cretaceous of India. *PLoS Biol.* **8**, e1000322 (2010).
72. Grellet-Tinner, G., Codrea, V., Folie, A., Higa, A. & Smith, T. First evidence of reproductive adaptation to 'island effect' of a dwarf Cretaceous Romanian titanosaur, with embryonic integument in ovo. *PLoS ONE* **7**, e32051 (2012).
73. Gallina, P. A. & Otero, A. Reassessment of *Laplatasaurus araukanicus* (Sauropoda: Titanosauria) from the Late Cretaceous of Patagonia, Argentina. *Ameghiniana* **52**, 487–501 (2015).
74. Kellner, A. W. A., Rubilar-Rogers, D., Vargas, A. & Suárez, M. A new titanosaur sauropod from the Atacama Desert. *Chile* **83**, 211–219 (2011).
75. Cao, W. et al. Palaeolatitudinal distribution of lithologic indicators of climate in a palaeogeographic framework. *Geol. Mag.* **156**, 331–354 (2019).
76. Strömberg, C. A. E. Evolution of grasses and grassland ecosystems. *Annu. Rev. Earth Planet. Sci.* **39**, 517–544 (2011).
77. Salgado, L., Gallina, P. A. & Paulina Carabajal, A. Redescription of *Bonitan reigi* (Sauropoda: Titanosauria), from the Campanian–Maastrichtian of the Río Negro Province (Argentina). *Hist. Biol.* **27**, 1–24 (2014).
78. Grellet-Tinner, G. & Fiorelli, L. E. A new Argentinian nesting site showing neosauropod dinosaur reproduction in a Cretaceous hydrothermal environment. *Nat. Commun.* **1**, 32 (2010).
79. Hechenleitner, E. M. et al. A new Upper Cretaceous titanosaur nesting site from La Rioja (NW Argentina), with implications for titanosaur nesting strategies. *Palaeontology* **59**, 433–446 (2016).
80. Salgado, L., Magalhães Ribeiro, C., Garcia, R. A. & Fernández, M. S. Late Cretaceous Megaloolithid eggs from Salitral de Santa Rosa (Río Negro, Patagonia, Argentina): inferences on the titanosaurian reproductive biology. *Ameghiniana* **46**, 605–620 (2009).
81. Grellet-Tinner, G. & Zaher, H. Taxonomic identification of the megaloolithid egg and eggshells from the Cretaceous Bauru Basin (Minas Gerais, Brazil): comparison with the Auca Mahuevo (Argentina) titanosaurid eggs. *Pap. Avulsos Zool.* **47**, 105–112 (2007).
82. Chiappe, L. M. et al. Sauropod dinosaur embryos from the Late Cretaceous of Patagonia. *Nature* **396**, 258–261 (1998).
83. Sander, P. M., Peitz, C., Jackson, F. D. & Chiappe, L. M. Upper Cretaceous titanosaur nesting sites and their implications for sauropod dinosaur reproductive biology. *Palaeontogr. Abt. A* **284**, 69–107 (2008).
84. Franco-Rosas, A. C., Salgado, L., Rosas, C. F. & de Souza Carvalho, I. Nuevos materiales de titanosaurios (Sauropoda) en el Cretácico Superior de Mato Grosso, Brasil. *Rev. Bras. Paleontol.* **7**, 329–336 (2004).
85. Grellet-Tinner, G., Chiappe, L., Norell, M. & Bottjer, D. Dinosaur eggs and nesting behaviors: a paleobiological investigation. *Palaeogeogr. Palaeoclimatol. Palaeoecol.* **232**, 294–321 (2006).
86. Curry Rogers, K., Whitney, M., D'Emic, M. & Bagley, B. Precocity in a tiny titanosaur from the Cretaceous of Madagascar. *Science* **352**, 450–453 (2016).
87. Goloboff, P. A., Farris, J. S. & Nixon, K. C. TNT, a free program for phylogenetic analysis. *Cladistics* **24**, 774–786 (2008).

Acknowledgements

We thank Secretaría de Cultura, Subsecretaría de Patrimonio, and Gobierno de La Rioja. We are grateful to Sergio de la Vega, Carlos Bustamante, Julia Desojo, Hernán Aciar, Leonel Acosta, Marcelo Miñana, Victoria Fernandez Blanco, Tomaz Melo, Jimena Trotteyn, Mariano Larrovere, Marcos Macchioli, Tatiana Sánchez, Gabriel Hechenleitner, Eugenio Sanchez, and Walter Bustamante for their help during fieldwork and preparation of the specimens. Special thanks to Grupo Roggio, and Alberto Acevedo, Germán Brizuela, Rubén Brizuela, and Carlos Verazai, for providing us with accommodation at their facilities during fieldworks (2016–2019). We thank Tim Coughlin, Rod Holcombe, and Andrea Arcucci for sharing information about QSD. Comparative data were collected in previous visits thanks to Pablo Ortiz (Instituto Miguel Lillo, Tucumán), Ignacio Cerda (Museo Carlos Ameghino, Río Negro), Diógenes de Almeida Campos and Rodrigo Machado (MCT), and Luiz Carlos Borges Ribeiro (CPPLIP-UFTM). We thank Jose Carballido for his help with the phylogenetic analysis. The Willi Henning Society for TNT software. Research supported by CONICET, The Jurassic Foundation (E.M.H.), and the Palaeontological Society PalSIRP (E.M.H.). Fieldwork permits (2015–2019): RES S.C. 135, 238, 109, 124.

Author contributions

E.M.H. coordinated the project (including fieldwork); E.M.H., A.G.M., L.E.F. were involved in study concept. E.M.H., L.L., A.G.M., and S.R. wrote the paper, and with J.R.A.T., L.E.F., and L.S. gathered the data. L.L., L.E.F., and S.R. made the figures. All authors discussed the results and commented on the manuscript.

Competing interests

The authors declare no competing interests.

Additional information

Supplementary information is available for this paper at <https://doi.org/10.1038/s42003-020-01338-w>.

Correspondence and requests for materials should be addressed to E.M.H.

Reprints and permission information is available at <http://www.nature.com/reprints>

Publisher's note Springer Nature remains neutral with regard to jurisdictional claims in published maps and institutional affiliations.



Open Access This article is licensed under a Creative Commons Attribution 4.0 International License, which permits use, sharing, adaptation, distribution and reproduction in any medium or format, as long as you give appropriate credit to the original author(s) and the source, provide a link to the Creative Commons license, and indicate if changes were made. The images or other third party material in this article are included in the article's Creative Commons license, unless indicated otherwise in a credit line to the material. If material is not included in the article's Creative Commons license and your intended use is not permitted by statutory regulation or exceeds the permitted use, you will need to obtain permission directly from the copyright holder. To view a copy of this license, visit <http://creativecommons.org/licenses/by/4.0/>.

© The Author(s) 2020

ELECTRONIC SUPPLEMENTARY INFORMATION

for

Two Late Cretaceous sauropods reveal titanosaurian dispersal across South America

E. Martín Hechenleitner*, Léa Leuzinger, Agustín G. Martinelli, Sebastián Rocher,
Lucas E. Fiorelli, Jeremías R.A. Taborda, Leonardo Salgado

*Corresponding author emails: martinh@conicet.gov.ar; emhechenleitner@gmail.com

This file includes:

Geological setting	2
Taphonomy	6
Measurements	9
Titanosauria in South America	12
Anatomical characters	14
Phylogenetic analysis	16
Latitudinal position of South American taxa	20
Character list	22
References	53

Geological setting

The Andean Precordillera of western Argentina (Supplementary Fig. 1a) preserves a protracted geological history of convergence and accretion that took place along the south-western margin of Gondwana since at least the early Palaeozoic (Ramos, 1988). The present relief of Precordillera results from crustal thickening that occurred mainly in Neogene times during the Andean orogeny (Jordan et al., 1983). Contractional deformation resulted in a fold-and-thrust belt that exposed Palaeozoic, Mesozoic and Cenozoic strata (Bracaccini, 1946).

Since the 1990s, paleontological discoveries have allowed sedimentary units in the northern Precordillera to be ascribed an Upper Cretaceous age. Main outcrop areas with published stratigraphic studies are Huaco (Fosdick et al., 2017; Limarino et al., 2000; Reat and Fosdick, 2018), Puesto La Flecha (Ciccioli et al., 2005), and Río La Troya (Tedesco et al., 2007) (Supplementary Fig. 1a). These strata consist of a 100-200 m thick red bed succession deposited in fluvial and lacustrine environments referred to collectively as the Ciénaga del Río Huaco Formation (Limarino et al., 2000). The previously known fossil record includes palynomorphs and freshwater ostracods (Chaía, 1990; Ciccioli et al., 2005; Limarino et al., 2000; Pérez et al., 1993). The microfossil assemblages allowed an Upper Cretaceous age (Maastrichtian) to be inferred for the upper part of the unit. Additionally, a radiometric age of 108.1 ± 4.4 Ma (Albian) by K-Ar method in a tuff was determined by Tedesco et al. (2007) in La Troya section (Supplementary Fig. 1a). More recently Fosdick et al. (2017) and Reat and Fosdick (2018) established a maximum depositional age of ~96-93 Ma (Cenomanian-Turonian) based on interpretation of detrital zircon U-Pb ages on samples from the lower part of the unit at the Huaco area. The combined biostratigraphic and geochronological data suggest a wide time range for the deposition of the Ciénaga del Río Huaco Formation within the Late Cretaceous and highlight the lack of more precise absolute ages to establish an accurate chronostratigraphic framework for the unit.

Outcrops of Ciénaga del Río Huaco Formation were recognized in subsequent studies at Quebrada Santo Domingo (QSD), a locality of the Andean Precordillera of La Rioja province (Supplementary Fig. 1a). For this area, Arcucci et al. (2005) and Hechenleitner et al. (2018) reported fragmentary caudal remains of a titanosaurian sauropod collected by the geologists Tim Coughlin and Rod Holcombe (Coughlin,

2000) and ascribed the fossil-bearing rocks to the Ciénaga del Río Huaco Formation. A stratigraphic description and map of the unit were recently offered by Limarino et al. (2016).

At QSD area, the Ciénaga del Río Huaco Formation consists of a sandy-silty succession with scarce conglomerates (Supplementary Fig. 1b). It disconformably overlies the Upper Triassic Santo Domingo Formation and supports, in apparent transition, the Eocene Puesto La Flecha Formation (Supplementary Fig. 1c). In our stratigraphic inspections, we note that sandstone sheets interleaved with siltstones and nodular gypsum of the upper part of Ciénaga del Río Huaco Formation are gradually replaced upwards by laminated siltstones and fine sandstones and higher up to fine to medium sandstones that characterize the lower Puesto La Flecha Formation. We do not discard that this transition could be stratigraphically representative of the Puesto La Flecha Formation as it was considered by Fosdick et al. (2017) and Reat and Fosdick (2018). In this scenario, *Punatitan* would belong to the basal portion of the Puesto La Flecha Formation. For the lower part of this unit Reat and Fosdick (2018) determined a ~65 Ma maximum depositional age. According to the interpretation of the authors, this transition can represent a low accommodation depocentre with lacustrine sedimentation during Palaeogene times containing numerous disconformities. To avoid confusion, we adopt the name of Ciénaga del Río Huaco Formation for the stratigraphic interval containing dinosaur remains. We place the limit between both units 250 m above the base of Ciénaga del Río Huaco Formation which is the thickness ascribed for this unit at Quebrada Santo Domingo (Limarino et al., 2016).

Here we divided the Ciénaga del Río Huaco Formation strata at QSD into lower, middle and upper sections.

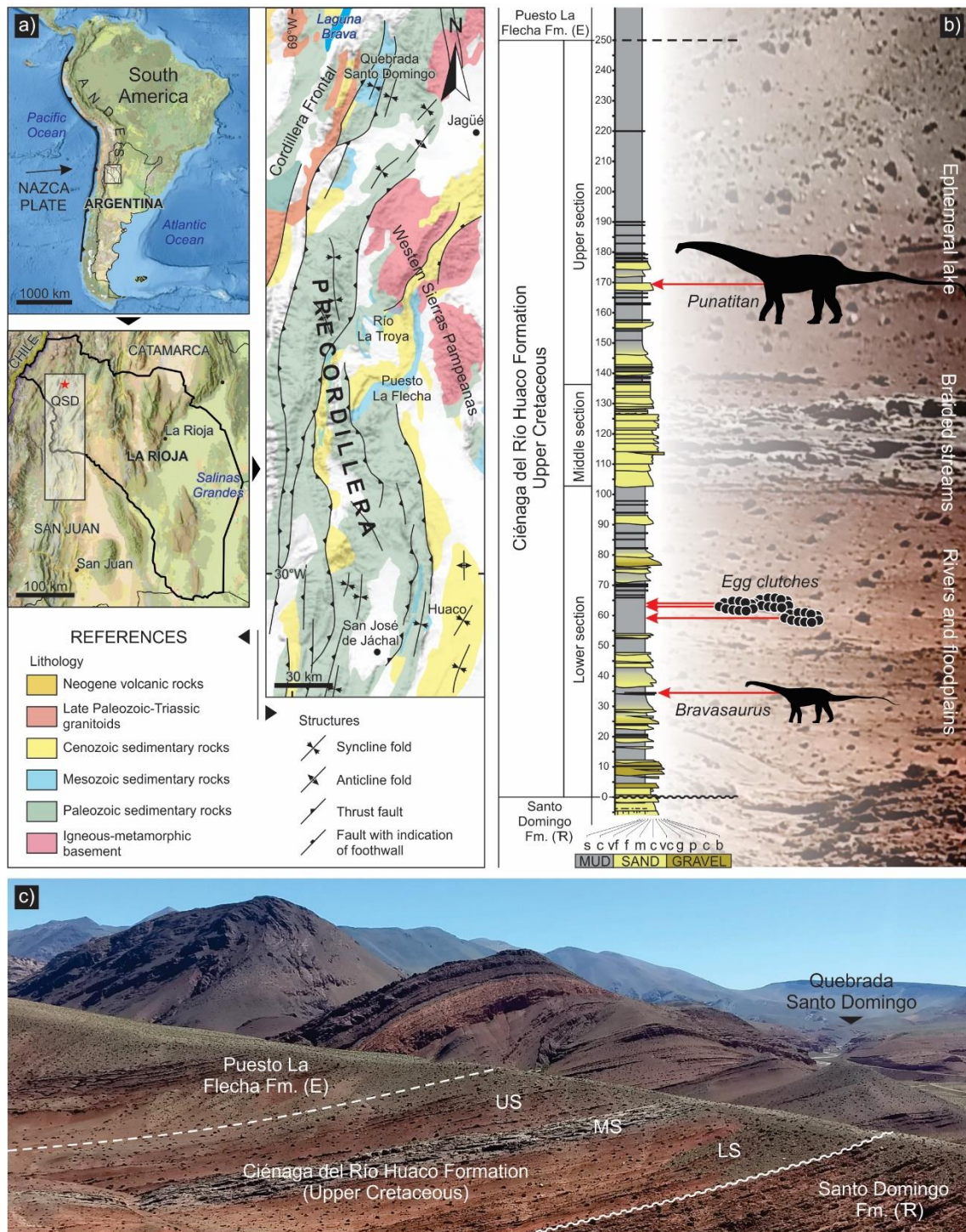
Lower section. The lower section is a 103 m thick interval of moderate reddish-brown colour formed by regular intercalations of sandstone bodies interleaved between siltstones (Supplementary Fig. 1b, c). Conglomeratic facies are infrequent and mostly present in the basal section in close association with sandy facies. They occur as the infill of narrow and relatively deep channels and are interpreted as bottom channel fills and gravelly bedforms. The sandstones commonly show well-developed internal structure characterized by trough and planar cross-bedding, although structureless sandstones also occur. Basal contacts are mostly defined by low angle erosive scours.

Sandstones represent various migrating bedforms deposited in lower, transitional and upper flow regimes. They are present mainly as channel fills and proximal and distal overbank deposits (levee and crevasse splay deposits). Siltstones occur in thick intervals that host thin intercalations of sandstone sheets. They show massive or horizontal lamination structure. These fine-grained rocks represent proximal overbank deposits accumulated in floodplains, from suspension load. In association with the overbank fines, some thin tabular layers of limestone occur. The presence of limestone is here interpreted as the resultant of chemically or biochemically induced precipitation of carbonates in small saline ephemeral lakes or ponds. Pedogenetic alterations were also recognized in some horizons of the overbank fine deposits mainly present in the form of root marks, as well as calcite and silica nodules. Facies and architectural elements described here suggest a paleoenvironment characterized by the development of fine-grained, mixed-load meandering rivers (Bridge, 2003; Miall, 1996).

Middle section. The middle section is a 24 m thick interval formed mostly by trough cross-bedded coarse sandstones that can be easily recognized by its conspicuous light greyish color (Supplementary Fig. 1b, c). The unit shows variations including moderate to poorly sorted, coarse, very coarse and some clast-supported pebble conglomerate lenses. They form 2-5 m thick channelized bodies with scoured bases, and sparse pebble basal lags that fine upward into well-developed, large-scale, trough-cross bedded, coarse- and medium-grained sandstones. The facies are interpreted as bottom channel fills and sandy bedforms. This interval represents deposits of a sand-bed, braided fluvial system with high energy transport (Allen, 1983; Miall, 1996).

Upper section. The upper section is a 116 m thick moderate red coloured silty-sandy interval (Supplementary Fig. 1b, c). The lower part consists of tabular beds of regularly to well-sorted medium- to fine-grained sandstones, usually graded, massive or planar cross-bedded, interleaved with massive and fine laminated siltstones and mudstones, including sparse nodular gypsum and thin beds of marls. The lower thick sandstones represent deposits of sheet-type flood surges. High evaporative rates produced chemical precipitation of evaporite minerals. Upsection, deposits are gradually replaced by finely laminated siltstone and mudstone with sparse intercalations of thin sheets of fine sandstones. Fine sediments settled during relatively prolonged periods in temporary water bodies, which were occasionally interrupted by the invasion of flood surges that resulted in spreading of fine sand blankets. The lower and upper parts of this section

represent respectively sand to mudflats of the margins and floor of an ephemeral lake system (Tunbridge, 1984).



Supplementary Fig. 1. Geographical and geological settings of the Ciénaga del Río Huaco Formation at QSD. **a** Relative location of the studied area in northern Precordillera, La Rioja province, NW Argentina. It shows the location of regions with stratigraphic studies: Huaco, Puesto La Flecha and Río La Troya. **b** Stratigraphic section with an indication of fossil-bearing levels. **c** Panoramic photograph of QSD area showing field relations of Ciénaga del Río Huaco Formation. The column is in metres. LS: lower section; MS: middle section; US: upper section.

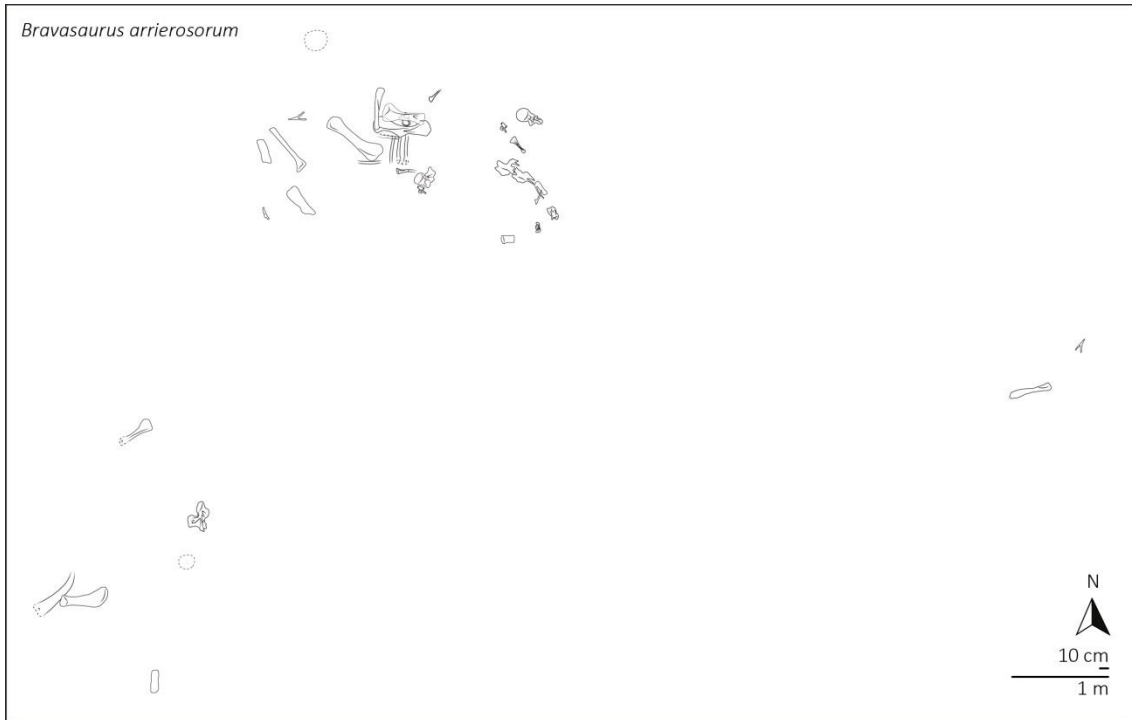
Taphonomy

Partial skeletons and egg clutches are found in different horizons of the Ciénaga del Río Huaco Formation at QSD. They differ in their depositional modes and preservation.

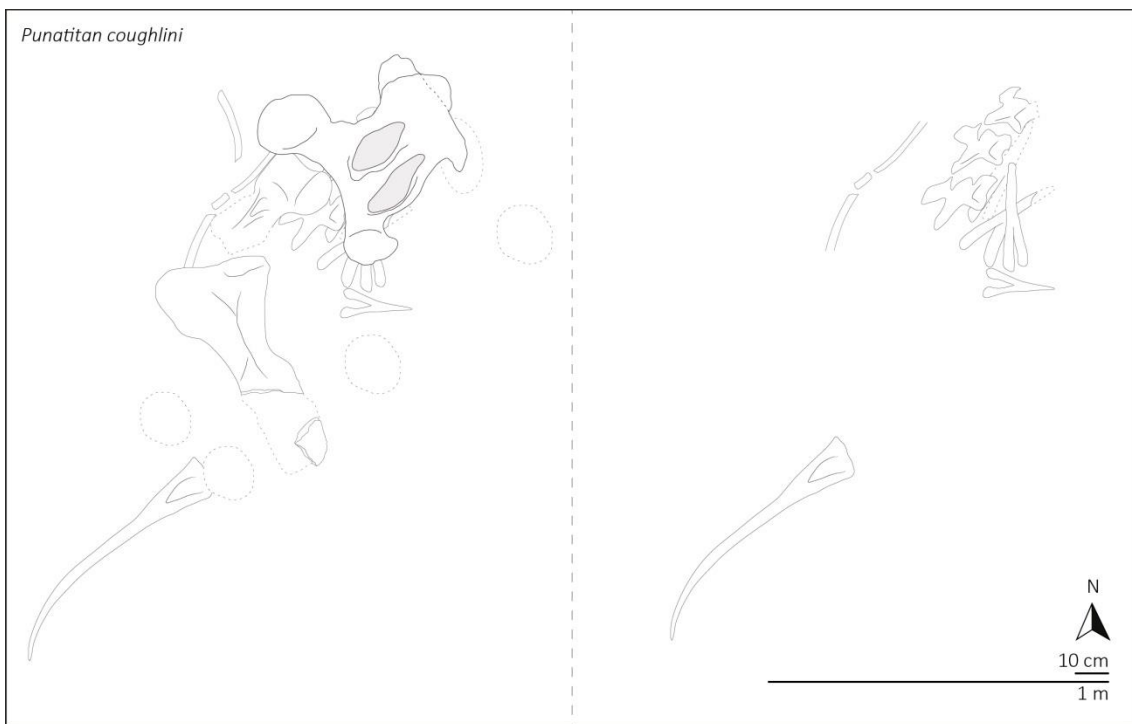
Bravasaurus. The remains of *Bravasaurus*, both the holotype and the paratype, consist of partial skeletons found at the lower section of the Ciénaga del Río Huaco Formation, approximately at the same horizon, 34 m above the base of the unit (Supplementary Fig. 1b), but separated laterally over a distance of 240 m. In both cases, they occur in 0.5 to 2 m thick beds of moderately to poorly sorted medium-grained sandstone, mostly structureless or with diffuse horizontal and cross-beddings. These features and association with floodplain deposits are interpreted as characteristic of proximal crevasse splay deposits (Burns et al., 2017). Bones were found semi-articulated with no evidence of abrasion and weathering. Long bones in this layer tend to have their long axes oriented NW-SE (Supplementary Fig. 2). These features suggest fortuitous preservation of dead bodies with a short exposure and only partial disarticulation. The remains had minimal transport and were quickly buried during events with a high rate of deposition such as channel overbanks that produce crevasse splays (Behrensmeyer and Hook, 1992).

Punatitan. The remains of *Punatitan* consist of a partial skeleton found at the upper section of the Ciénaga del Río Huaco Formation, 170 m above the base of the unit (Supplementary Fig. 1b). The deposit that contains the fossils is a 2.2 m thick graded bed of medium- to fine-grained sandstone. Its basal part shows a horizontal and planar cross-bedded arrangement, whereas the upper portion is structureless. It is interpreted as a sandy lobe deposit, part of the marginal sand flat of an ephemeral lake system (Hubert and Hyde, 1982). The remains are semi-articulated, closely spaced and partly stacked on each other with no evidence of abrasion. Long elements of the skeleton are disposed of with a preferred NE-SW orientation (Supplementary Fig. 3). The good preservation and sedimentological features suggest rapid deposition of sand and quick burial, preventing higher degrees of disaggregation and dispersion (Behrensmeyer and Hook, 1992). Favourable conditions are created during flash flood events that spread out in sheet flows, decelerating and promoting high deposition rates. The sheet-like progradational mode of deposition probably favoured minimal transport and staking of the remains.

Titanosaurian eggs. Eggshells and egg clutches were found in at least three distinct but closely spaced horizons in a 5 m thick interval located 59-64 m above the base of the Ciénaga del Río Huaco Formation (Supplementary Fig. 1b). This interval can be traced laterally for more than 3 km. The deposits consist of laminated siltstones and mudstones commonly in mixture with very fine sand-sized grains. Lamination is recognized by subtle centimetre-scale variations in grain size, between silt and clay, and by different proportions of fine sand. They represent both rapid and gradual deposition from a suspensive load of low-energy flow during flooding events in a floodplain setting. The bedding was caused by variations in flood energy during deposition and different flooding events. Particularly, eggs in clutches occur closely packed and show one- or two-row arrangement in cross-section. The latter occupy a vertical space within the strata of ~15-30 cm, which means that they are contained by various flooding events, each one typically a few centimetres thick. Since it is unlikely that spherical, low-density objects, stacked on a flatbed (the floodplain), may be able to stay grouped *in situ* during and between several flood events, titanosaurs must have adopted a burial nesting strategy (Fowler and Hall, 2011; Hechenleitner et al., 2015; Vila et al., 2010a, 2010b) that would have prevented the collapse and transport of eggs. The low-energy floodplain depositional setting and the proximity to water bodies would be preferred places for nesting.



Supplementary Fig. 2. Outcrop map of the *Bravasaurus* gen. nov. holotype quarry. Distances between skeletal elements and their respective orientations were restored to their original horizontal position, as the bearing strata dip c. 30°. Dotted lines represent undetermined bone fragments.



Supplementary Fig. 3. Outcrop map of the *Punatitan* gen. nov. holotype quarry. Distances between skeletal elements and their orientations are shown as observed in the field (not restored to horizontal). Dotted lines represent undetermined bone fragments.

Measurements

Measurements made on the holotype specimens of *Punatitan* and *Bravasaurus* are listed in Supplementary Table 1 and Supplementary Table 2, respectively.

Supplementary Table 1. Representative elements of *Punatitan* gen. nov. Measurements are in cm. Asterisks indicate dubious data because the exact limits of one or both landmarks are difficult to recognise.

Cervical vertebra

<i>CRILAR-Pv 614/</i>	<i>1</i>
Centrum height	8.5
Centrum width	21.5
Distance between prezygapophyses	6.5

Dorsal vertebrae

<i>CRILAR-Pv 614/</i>	<i>2</i>	<i>3</i>
Centrum length	20.7	-
Height of the posterior articular surface	16.5	-
Width of the posterior articular surface	15.4	-
Total height	45	-
Height of the neural spine (above the medial border of the postzygapophyses)	17.5	-

Caudal vertebrae

<i>CRILAR-Pv 614/</i>	<i>4</i>	<i>5</i>	<i>6</i>	<i>7</i>	<i>8</i>	<i>9</i>	<i>10</i>
Centrum length (excluding posterior articular surface)	-	9	8	8	8	8.5	8.5
Height of the posterior articular surface	13	12	11	8.5	7.5	7.5	7.5
Total height	-	-	23.5	24.5	22.5	18	16.5
Height of the neural spine (above the medial border of the postzygapophyses)	-	-	9	12.5	12	10	7

<i>CRILAR-Pv 614/</i>	<i>11</i>	<i>12</i>	<i>13</i>	<i>14</i>	<i>15</i>	<i>16</i>
Centrum length (excluding posterior articular surface)	9	8.5	8.5	8	8	-
Height of the posterior articular surface	7	7	6.5	6.5	6	-
Total height	13.5	13*	13.5	13.5*	-	-
Height of the neural spine (above the medial border of the postzygapophyses)	6.5	5.5*	-	-	-	-

Supplementary Table 2. Representative elements of *Bravasaurus* gen. nov.
Measurements are in cm. Asterisks indicate dubious data because the exact limits of one or both landmarks are difficult to recognise.

Cervical vertebrae

<i>CRILAR-Pv 612/</i>	<i>1</i>	<i>2</i>	<i>3</i>	<i>4</i>
Centrum length	15.5	16.5	19	21
Centrum height	3.5	4.5	4.7	5.5
Centrum width	4	4.5	4.7	5.5
Total height	10	?	12.5	13.5
Distance between prezygapophyses	5	?	?	?

Dorsal vertebrae

<i>CRILAR-Pv 612/</i>	<i>5</i>	<i>6</i>	<i>7</i>	<i>8</i>	<i>9</i>
Centrum length	-	13.5*	-	-	-
Height of the posterior articular surface	7.5	7.5	8.5	10.7	9
Width of the posterior articular surface	9.5	10	13	11.5	10.7
Total height	20.5*	22.5	24.5*	26.5	25.5
Height of the neural spine (above the medial border of the postzygapophyses)	6.5*	8.7	12*	11.5	11.5

Caudal vertebrae

<i>CRILAR-Pv 612/</i>	<i>10</i>	<i>11</i>	<i>12</i>
Centrum length	9	8.3	8
Height of the posterior articular surface	5*	-	3.5
Width of the posterior articular surface	7*	5	4
Total height	12.5*	-	7.5
Height of the neural spine (above the medial border of the postzygapophyses)	3.3*	-	2.2

Forelimb

<i>Humerus CRILAR-Pv 612/</i>	<i>13</i>
Length	53
Maximum proximal width	24
Maximum distal width	18.5
Minimum section perimeter	24.5

<i>Metacarpal CRILAR-Pv 612/</i>	<i>14</i>
Length	19

Maximum proximal width	8
Maximum distal width	5.2

Pelvic girdle

<i>Pubis CRILAR-Pv 612/</i>	<i>15</i>
Length	47.5

Hind limb

<i>Femur CRILAR-Pv 612/</i>	<i>16</i>
Length	68
Maximum proximal width	23
Maximum distal width	22*
Minimum section perimeter	31

<i>Fibulae CRILAR-Pv 612</i>	<i>17</i>	<i>18</i>
Length	-	48.7
Maximum proximal width	-	10
Maximum distal width	8.2	8.3
Minimum section perimeter	11.5	12

Titanosauria in South America

In the Cretaceous Period, the titanosaurian clade reached a worldwide distribution (Cerdeña et al., 2012; Faria et al., 2015; Gorscak and O'Connor, 2016). Particularly in South America, there are 51 valid species, of which nearly 75% were found in the Argentinean Patagonia (Supplementary Table 3).

Supplementary Table 3. Valid species of Cretaceous Titanosauria in South America, by regions.

NW Argentina + Chile	<i>Saltasaurus loricatus</i> <i>Atacamatitan chilensis</i> <i>Punatitan coughlini</i> gen. et sp. nov. <i>Bravasaurus arrierosorum</i> gen. et sp. nov.
Brazil	<i>Maxakalisaurus topai</i> <i>'Aeolosaurus' maximus</i> <i>Uberabatitan ribeiroi</i> <i>Austroposeidon magnificus</i> <i>Trigonosaurus pricei</i> <i>Tapuiasaurus macedoi</i> <i>Baurutitan britoi</i> <i>Gondwanatitan faustoi</i> <i>Brasilotitan nemophagus</i> <i>Adamantisaurus mezzalirai</i>
Patagonia	<i>Puertasaurus reuili</i> <i>Argyrosaurus superbus</i> <i>Aeolosaurus colhuehuapensis</i> <i>Epachthosaurus sciuttoii</i> <i>Drusilasaura deseadensis</i> <i>Dreadnoughtus schrani</i> <i>Elaltitan lilloi</i> <i>Sarmientosaurus musacchioi</i> <i>Nullotitan glaciarius</i> <i>Antarctosaurus wichmannianus</i> <i>Andesaurus delgadoi</i> <i>Aeolosaurus rionegrinus</i> <i>Argentinosaurus huinculensis</i> <i>Barrosasaurus casamiquelai</i> <i>Bonitasaura salgadoi</i> <i>Bonatitan reigi</i> <i>Futalognkosaurus dukei</i> <i>Malarguesaurus florenciae</i> <i>Mendozasaurus neguyelap</i> <i>Quetecsaurus rusconii</i>

Notocolossus gonzalezparejasi
Muyelensaurus pecheni
Rinconsaurus caudamirus
Narambuenatitan palomoi
Neuquensaurus australis
Overosaurus paradisorum
Panamericansaurus schroederi
Pellegrinisaurus powelli
Petrobrasaurus puestohernandezii
Pitekunsaurus macayai
Rocasaurus muniozi
Traukutitan eocaudata
Baalsaurus mansillai
Kaijutitan maui
Choconsaurus baileywillisi
Laplatasaurus araukanicus

Ecuador

Yamanasaurus lojaensis

Anatomical characters

Taxa added to the analysis. We added six taxa to the dataset provided by Carballido et al. (2020), including *Rocasaurus* (Salgado and Azpilicueta, 2000), *Aeolosaurus rionegrinus* (Powell, 2003), *Gondwanatitan* (Kellner and de Azevedo, 1999), *Uberabatitan* (Salgado and Carvalho, 2008; Silva et al., 2019), and *Punatitan* and *Bravasaurus*. Personal observations were also made on all these taxa.

Characters. We added just five characters to the original data matrix of 417 characters provided by Carballido et al. (2020). Two of them are from Salgado et al. (1997), one from Salgado et al. (2014), one from Santucci and Arruda-Campos (2011), and one is new. In addition, a few characters were slightly modified (Supplementary Table 4). Some scorings were also changed according to new observations and published data (Supplementary Data 1). We introduced 169 modifications to the dataset provided by Carballido et al. (2020), 80% of which were previously missing data. From 33 changes to the original scorings, 17 are due to modifications in the characters' definitions or their states (e.g., character 300). Among the other 16, three are changes to ambiguous states (e.g., *Overosaurus*, character 178), one to "not-applicable" and another to missing data. The remaining 11 modifications are listed in Supplementary Table 5.

Supplementary Table 4. Characters added or modified.

Character	Modifications
Ch. 141	One state added (state 2; see below).
Ch. 177	Modified definition (now it also considers the middle dorsal vertebrae).
Ch. 233	One state added (state 2; see below).
Ch. 250	One state added (state 3; see below)
Ch. 251	One state added (state 2; see below).
Ch. 254	One state added (state 2; see below).
Ch. 300	One state added (split state 1 into states 1 and 2; see below)
Ch. 418	Character added from Salgado et al., 1997.
Ch. 419	Character added from Salgado et al., 1997.
Ch. 420	Character added from Salgado et al., 2014.
Ch. 421	New Character.
Ch. 422	New Character.

Supplementary Table 5. Specific modifications.

<i>Epachthosaurus</i>	164	0→1	<i>Epachthosaurus</i> has prespinal laminae in its dorsal vertebrae.
<i>Overosaurus</i>	122	1→2	Modified based on Coria et al. (2013).
	223	1→0	Modified based on Coria et al. (2013). The transverse processes can be traced until caudal 16 o 17.
<i>Muyelensaurus</i>	159	1→3	Modified based on Calvo et al., 2007a
	175	0→1	The preserved anterior dorsal is not complete so that interpretations could be controversial (Calvo et al., 2007a). We interpret its condition as state 1.
<i>Rinconsaurus</i>	126	2→3	Modified based on Calvo and González Riga 2003. No evident pleurocoel is observed, but there is a deep fossa as observed in related forms.
<i>Trigonosaurus</i>	128	1→0	Epiphyses are not well developed as in saltosaurids (Campos et al., 2005).
	175	0→1	Modified after personal photos/observations of the specimens. Also, see Campos et al. (2005).
	196	1→0	Dorsal vertebrae 6-10 do not show aliform processes. A subtle expansion on one side of the neural spine in D5 might look like an aliform process, but it does not seem entirely consistent.
<i>Baurutitan</i>	237	2→1	The neural spine is slightly wider than long, but not as much as 1.5 times (Kellner et al., 2005).
	257	2→1	The neural spines are vertical (Kellner et al., 2005).

Phylogenetic analysis

We performed a maximum parsimony analysis of a modified version of the dataset of Carballido et al. (2020; see below) using TNT v. 1.1 (Goloboff et al., 2008). After doing a heuristic search with 1,000 replicates of Wagner trees and the first round of tree bisection-reconnection (TBR) branch swapping, we obtained 100 most parsimonious trees (MPTs). With another round of TBR the number of MPTs increased up to 150,000, once the memory overflowed. A strict consensus tree of 1480 steps (consistency index, 0.353; retention index, 0.724) is shown in Supplementary Fig. 4.

The present phylogenetic analysis recovers almost the same topology as previous studies (Canudo et al., 2018; Carballido et al., 2020, 2017; Supplementary Fig. 4). However, some inconsistencies about Late Cretaceous sauropods deserve a more detailed discussion. The main variations correspond to the affinities of *Andesaurus* with probably more basal taxa, the more basal position of *Malawisaurus*, outside Eutitanosauria, the colossosaurian affinities of *Baurutitan*, and the inclusion of *Gondwanatitan*, *Aeolosaurus rionegrinus*, *Uberabatitan*, *Trigonosaurus*, *Punatitan* and *Bravasaurus* as members of Rinconsauria and Aeolosaurini.

In the present analysis, *Andesaurus* is recovered as part of a large polytomy that includes brachiosaurids, euhelopodids and sister taxa of Lithostrotia, among others. A discrepancy regarding the position of *Andesaurus* could be linked to the presence of some taxa that have been previously recognized as unstable, such as *Padillasaurus*, *Malarguesaurus*, *Lusotitan* or *Rayososaurus* (Carballido et al., 2020, 2017). However, its affinities with other somphospondylans are beyond the scope of this paper.

Malawisaurus is recovered from the analysis as more basal than *Epachthosaurus* and, thus, outside Eutitanosauria. Such position contrasts with that obtained by Carballido et al. (2017) and Canudo et al. (2018). However, it is consistent with other analyses based on different data sets (González Riga et al., 2018; Salgado et al., 2014; Tykoski and Fiorillo, 2016).

The Brazilian titanosaurian *Baurutitan* has been included in a few phylogenetic analyses. Martínez et al. (2016) recovered its position within a major polytomy that consists of the saltasaurines *Saltasaurus*, *Rocasaurus* and *Neuquensaurus*, some basal titanosaurs, such as *Epachthosaurus*, and few other Brazilian forms, such as

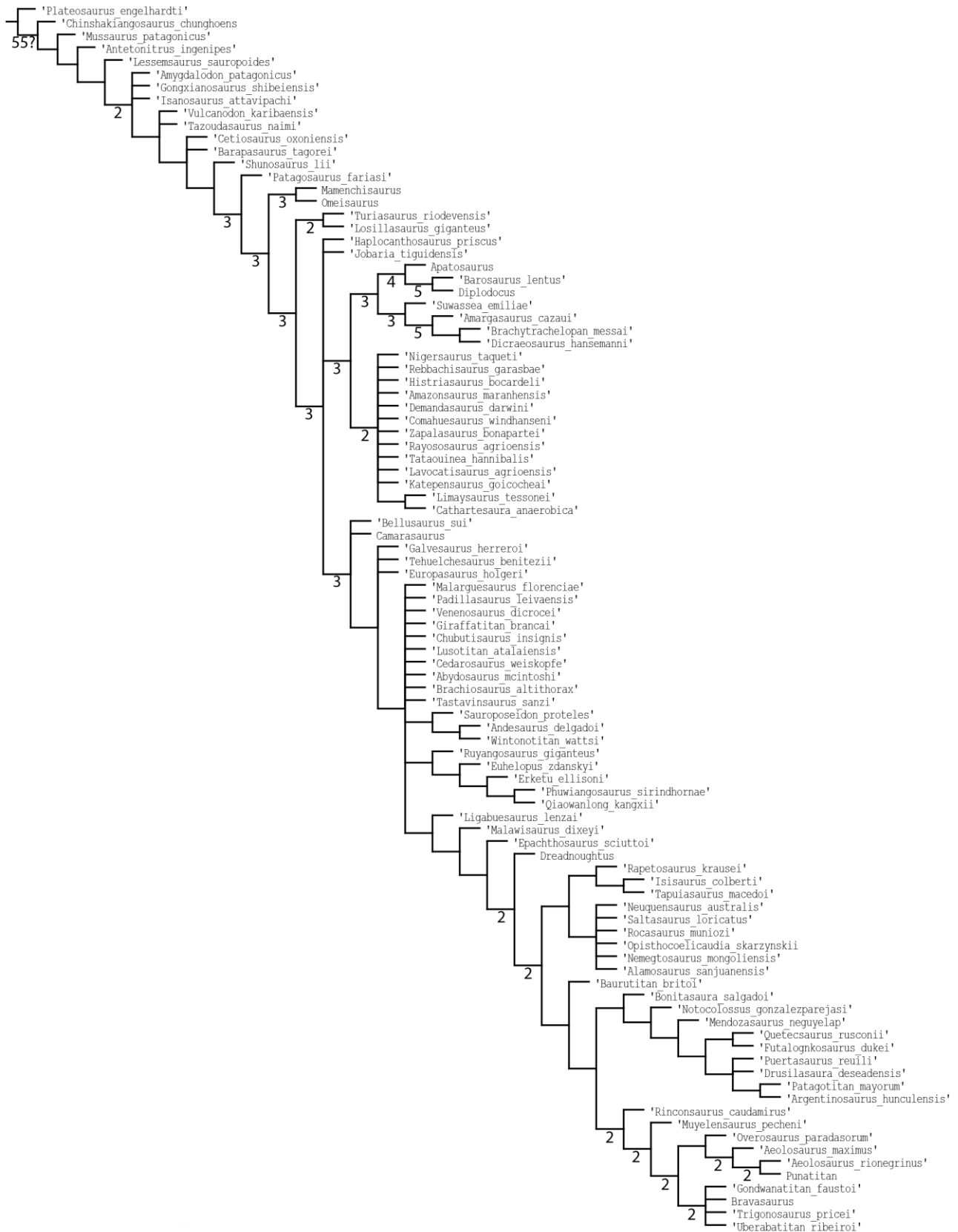
Tapuiasaurus, *Gondwanatitan* and *Trigonosaurus*, among others. Based on a modified version of the latter data set, Silva et al. (2019) recognised *Baurutitan* as a non-saltosaurine titanosaurian, more closely related to *Rapetosaurus*. It is worth mentioning that their analysis only includes one member of Colossosauria: *Bonitasaura*. The study conducted by Bandeira et al. (2016) posits *Baurutitan* outside Titanosauria, although this taxon has evident titanosaurian affinities, such as the presence of strongly procoelous caudal centra (a synapomorphy of Titanosauria). Using a different data matrix, Carballido et al. (2017), and subsequent analyses derived from it (Canudo et al., 2018; Carballido et al., 2020), recovered *Baurutitan* as the sister taxon of a major polytomy that includes South American saltosaurines and related forms (e.g. *Opisthocoelicaudia*, *Nemegtosaurus*, *Alamosaurus*) plus *Rapetosaurus* + *Isisaurus* + *Tapuiasaurus*. The polytomy is apparently resolved by pruning *Nemegtosaurus* (Carballido et al., 2017), although, here, the removal of this taxon does not resolve the polytomy (see below; Supplementary Fig. 4). *Baurutitan* is here recovered as the most basal member of Colossosauria.

Despite the incorporation of *Rocasaurus* into the analysis, the relations of the saltosaurine titanosaurians remain obscure. In our phylogenetic result, they are recovered separately from a clade formed by *Rapetosaurus* (Madagascar), *Isisaurus* (India) and *Tapuiasaurus* (South America). As stated above, the same topology was obtained in a previous study after pruning *Nemegtosaurus* from the strict consensus tree (Carballido et al., 2017).

The main change compared to previous studies is the grouping of several Late Cretaceous titanosaurians from Bauru, plus *Bravasaurus* and *Punatitan*, within Rinconsauria. The clade that includes *Bonitasaura* + (*Notocolossus* + Lognkosauria) remains invariable with respect to the results obtained by Carballido et al. (2020, 2017). In contrast, the clade Rinconsauria has undergone several modifications. This clade originally included *Rinconsaurus* and *Muyelensaurus* (Calvo et al., 2007a; Salgado et al., 2014). It was further supported by Tykoski and Fiorillo (2016) and González Riga et al. (2018), who also recognised similarities with *Aeolosaurus rionegrinus* and *Gondwanatitan*. However, the latter taxa were not included in the data matrix provided by Carballido et al. (2020, 2017). Instead, their analyses recover the Patagonian *Overosaurus* and the Brazilian '*Aeolosaurus*' as members of Rinconsauria. Although the present data provide strong information about the invalidity of the Brazilian

'*Aeolosaurus*' genus, it can still be considered an Aeolosaurini (Martinelli et al., 2011). The results of the present study group *Rinconsaurus* and *Muyelensaurus* as successive, sister taxa of the clade Aeolosaurini. This clade is divided into two smaller clades. The first one includes *Overosaurus* + ('*Aeolosaurus*' + (*Aeolosaurus* + *Punatitan*)), whereas the other corresponds to an unresolved polytomy between *Gondwanatitan*, *Trigonosaurus*, *Uberabatitan* and *Bravasaurus*.

The incorporation of *Trigonosaurus* within Rinconsauria and the position of *Bravasaurus* and *Punatitan* within two independent but closely related clades are worth mentioning. As well as *Uberabatitan*, *Trigonosaurus* has been included in a few data matrices (Bandeira et al., 2016; Carballido et al., 2017; Silva et al., 2019). Bandeira et al. (2016) did not find direct affinities between *Trigonosaurus* and other Brazilian taxa, such as *Uberabatitan* or '*Aeolosaurus*' *maximus*. Based on a data matrix modified from Martínez et al. (2016) Silva et al. (2019) recovered *Trigonosaurus* as a non-saltosaurine titanosaur, related with the saltosaurines plus *Epachthosaurus* and *Bonitasaura*. Using a different data set, Carballido et al. (2020, 2017) excluded *Trigonosaurus* from their reduced consensus tree after finding it unstable. Here, *Bravasaurus* and *Punatitan* (from La Rioja), *Overosaurus* and *Aeolosaurus* (from Patagonia), as well as *Trigonosaurus*, *Gondwanatitan*, '*Aeolosaurus*', and *Uberabatitan* (from SW Brazil) are recovered as members of Aeolosaurini (Franco-Rosas et al., 2004). *Bravasaurus* shares several features with *Uberabatitan* (Salgado and Carvalho, 2008; Silva et al., 2019). The cervical, dorsal and caudal vertebrae of both taxa also show many similarities with those of *Trigonosaurus*, which is reflected in their position (although unresolved) in the strict consensus tree (Supplementary Fig. 4). *Punatitan* exhibits most of the typical features that allow recognition of aeolosaurine titanosaurians, e.g., caudal vertebrae with anteriorly oriented neural arches. In fact, the current analysis suggests that *Punatitan* could have been more related to *Aeolosaurus rionegrinus* than the Brazilian '*Aeolosaurus*'. On the other hand, although *Bravasaurus*, *Uberabatitan* and *Trigonosaurus* do not have typically aeolosaurine caudals, they are recovered in a polytomy with *Gondwanatitan* and, thus, they are also members of the clade Aeolosaurini.



Supplementary Fig. 4. Strict consensus tree. From 150,000 most parsimonious trees, of 1480 steps. Bremer supports higher than one are shown on their respective branches.

Latitudinal position of South American taxa

Our phylogenetic analysis recovers 30 derived titanosaurs within Lithostrotia; 25 of them were found in different Cretaceous basins across South America. The latitudinal gradient is one of the most obvious patterns in biogeography (e.g., Pianka, 1966; Sax, 2001). We calculated the palaeogeographic coordinates for each South American taxon using the software GPlates (Müller et al., 2018; Seton et al., 2012) (Supplementary Table 6). We translated this data into a colour gradient, which we used in the phylogenetic tree in Fig. 4. The colour coding enhances the visualization of latitudinal differences between clades of derived titanosaurs. Then it is easy to observe, for example, that Lognkosauria is a strictly Patagonian clade. In contrast, the small clade of aeolosaurines that contains *Bravasaurus* seems to be restricted to lower latitudes, whereas the clade in which *Punatitan* is nested comprises a much larger latitudinal interval, between Patagonia and SW Brazil.

Supplementary Table 6. Latitude, palaeolatitude, location, and age of South American Lithostrotia included in the phylogenetic analysis.

Taxon	Latitu de (deg.)	Palaeo lat. (deg.)	Basin	Max. age (My)	Min. age (My)	Reference
<i>Tapuiasaurus</i>	-16.7	-21.1	Sanfranciscana	125.0	113.0	Zaher et al., 2011
<i>Uberabatitan</i>	-19.6	-22.8	Bauru	72.1	66.0	Salgado and Carvalho, 2008
<i>Trigonosaurus</i>	-19.7	-23.0	Bauru	72.1	66.0	(Campos et al., 2005)
<i>Baurutitan</i>	-19.7	-23.0	Bauru	72.1	66.0	Kellner et al., 2005
<i>Gondwanatitan</i>	-22.1	-25.4	Bauru	83.5	66.0	Kellner and de Azevedo, 1999
<i>Aeolosaurus'</i>	-23.0	-26.3	Bauru	83.5	66.0	Santucci and Arruda-Campos, 2011
<i>Saltasaurus</i>	-26.1	-28.8	Salta Group	70.6	66.0	Bonaparte and Powell, 1980
<i>Punatitan</i>	-28.6	-31.6	?	75.8	66.0	This work
<i>Bravasaurus</i>	-28.6	-31.6	?	75.8	66.0	This work
<i>Quetecsaurus</i>	-34.1	-38.5	Neuquén	93.5	89.3	González Riga and Ortiz David, 2014
<i>Mendozasaurus</i>	-37.1	-41.3	Neuquén	89.3	85.8	González Riga, 2003
<i>Notocolossus</i>	-37.1	-41.0	Neuquén	89.3	83.5	González Riga et al., 2016
<i>Muyelensaurus</i>	-37.4	-41.3	Neuquén	89.3	83.5	Calvo et al., 2007a
<i>Rinconsaurus</i>	-37.4	-41.2	Neuquén	86.3	83.6	Calvo and González Riga, 2003
<i>Overosaurus</i>	-37.6	-41.4	Neuquén	86.3	83.6	Coria et al., 2013
<i>Rocasaurus</i>	-39.3	-42.4	Neuquén	83.5	66.0	Salgado and Azpilicueta, 2000
<i>Aeolosaurus</i>	-38.8	-41.9	Neuquén	83.6	66.0	Powell, 2003
<i>Bonitasaura</i>	-39.6	-43.4	Neuquén	86.3	83.6	Apesteguía, 2004
<i>Futalognkosaurus</i>	-38.5	-42.9	Neuquén	93.5	85.8	Calvo et al., 2007b
<i>Neuquensaurus</i>	-39.0	-42.8	Neuquén	86.3	83.6	Powell, 1992

<i>Argentinosaurus</i>	-38.9	-43.5	Neuquén	99.6	89.8	Bonaparte and Coria, 1993
<i>Patagotitan</i>	-43.8	-48.8	Somuncurá- Cañadón Asfalto	105.3	99.6	Carballido et al., 2017
<i>Epachthosaurus</i>	-45.3	-49.8	Golfo San Jorge	99.6	89.3	Powell, 1990
<i>Drusilasaura</i>	-46.7	-51.2	Golfo San Jorge	99.6	89.3	Navarrete et al., 2011
<i>Puertasaurus</i>	-49.9	-52.9	Austral	83.6	66.0	Novas et al., 2005
<i>Dreadnoughtus</i>	-49.9	-52.9	Austral	83.6	66.0	Lacovara et al., 2014

Character list

Skull

1. Posterolateral processes of premaxilla and lateral processes of maxilla, shape: without midline contact (0); with midline contact forming marked narial depression, subnarial foramen not visible laterally (1). (Wilson, 2002: character 1).
2. Premaxillary anterior margin shape: without step (0); with marked step but short step (1); with marked and long step (2). (Modified from Wilson, 2002: character 2).
3. Premaxilla, ascending process shape in lateral view: convex (0); concave, with a large dorsal projection (1); sub-rectilinear and directed posterodorsally (2). (Whitlock, 2011: character 3).
4. Premaxilla, external surface: without anteroventrally orientated vascular grooves originating from an opening in the maxillary contact (0); vascular grooves present (1). (Whitlock, 2011: character 2).
5. Premaxilla-maxilla suture, shape: planar (0); twisted along its length, giving the contact a sinuous appearance in lateral view (1). (D'Emic, 2012: character 2).
6. Premaxilla, small finger-like, vertically oriented premaxillary process near anteromedial corner of external naris: (0) absent; (1) present. (D'Emic, 2012: character 3).
7. Maxillary border of external naris, length: short, making up much less than one-fourth narial perimeter (0); long, making up more than one-third narial perimeter (1). (Wilson, 2002: character 3).
8. Maxilla, foramen anterior to the preantorbital fenestra: absent (0); present (1). (Zaher et al., 2011).
9. Preantorbital fenestra: absent (0); present, being wide and laterally opened (1). (Modified from Wilson, 2002: character 4).
10. Subnarial foramen and anterior maxillary foramen, position: well distanced from one another (0); separated by narrow bony isthmus (1). (Wilson, 2002: character 5).
11. Antorbital fenestra: much shorter than orbital maximum diameter, less than 85% of orbit (0); subequal to orbital maximum diameter, greater than 85% orbit (1). (Modified from Wilson, 2002: character 6 following to Whitlock, 2011: character 13).
12. Antorbital fenestra, shape of dorsal margin: straight or convex (0); concave (1). (Whitlock, 2011: character 14).
13. Antorbital fossa: present (0); absent (1). (Wilson, 2002: character 7).

14. External nares position: terminal (0); retracted to level of orbit (1); retracted to a position between orbits (2). (Wilson, 2002: character 8).
15. External nares, maximum diameter: shorter (0); or longer than orbital maximum diameter (1). (Wilson, 2002: character 9).
16. Orbital ventral margin, anteroposterior length: broad, with subcircular orbital margin (0); reduced, with acute orbital margin (1). (Wilson, 2002: character 10).
17. Lacrimal, anterior process: present (0); absent (1). (Wilson, 2002: character 11).
18. Lacrimal, anteriorly projecting vertical plate of bone: absent (0); present (1). (D'Emic, 2012: character 4).
19. Jugal contribution to the ventral border of the skull: present and long (0); absent or very reduced (1). (Carballido et al., 2012: character 16).
20. Quadratojugal-maxilla contact: absent or small (0); broad (1). (Whitlock, 2011: character 10).
21. Jugal-ectopterygoid contact: present (0); absent (1). (Wilson, 2002: character 12).
22. Jugal, contribution to antorbital fenestra: absent (0); present, but very reduced (1); present and large, bordering approximately one-third its perimeter (2). (Modified from Wilson, 2002: character 13).
23. Quadratojugal, position of anterior terminus: posterior to middle of orbit (0); anterior margin of orbit or beyond (1). (Whitlock, 2011: character 30).
24. Quadratojugal, anterior process length: short, anterior process shorter than dorsal process (0); long, anterior process more than twice as long as dorsal process (1). (Wilson, 2002: character 32).
25. Quadratojugal, angle between anterior and dorsal processes: less than or equal to 90°, so that the quadrate shaft is directed dorsally (0); greater than 90°, approaching 130°, so that the quadrate shaft slants posterodorsally (1). (Whitlock, 2011: character 31).
26. Ventral edge of anterior surface of the quadratojugal: straight, not expanded ventrally (0); slightly expanded ventrally, forming a small bulge, which height is less than twice the ramus height (1); well expanded ventrally, forming a notorious bulge, which height is twice or more the minimum height of the ramus (2). (Modified from Upchurch et al., 2004: character 26).
27. Squamosal contribution to the supratemporal fenestra: present, the squamosal is well visible in dorsal view (0); reduced or absent (1). (Curry-Rogers, 2005: character 37).
28. Squamosal-quadratojugal contact: present (0); absent (1). (Wilson, 2002: character 31).

29. Squamosal, posteroventral margin: smooth (0); "with prominent, ventrally directed "prong"" (1). (Whitlock, 2011: character 37).
30. Prefrontal posterior process size: small, not projecting far posterior of frontal-nasal suture (0); elongate, approaching parietal (1). (Wilson, 2002: character 14).
31. Prefrontal, posterior process shape: flat (0); hooked (1). (Wilson, 2002: character 15).
32. Prefrontal, anterior process: absent (0); present (1). (Curry-Rogers, 2005: character 30).
33. Prefrontal-frontal contact width: large, equal or longer than the anteroposterior length of the prefrontal (0); narrow, less than half the anteroposterior length of the prefrontal (1). (Zaher et al., 2011: character 239).
34. Postorbital, ventral process shape: transversely narrow (0); broader transversely than anteroposteriorly (1). (Wilson, 2002: character 16).
35. Postorbital, posterior process: present (0); absent (1). (Wilson, 2002: character 17).
36. Postorbital, posterior margin articulating with the squamosal: with tapering posterior process (0); with a deep posterior process (1). (Zaher et al., 2011: character 245).
37. Frontal contribution to supratemporal fossa: present (0); absent (1). (Wilson, 2002: character 18).
38. Frontals, midline contact (symphysis): sutured (0); or fused in adult individuals (1). (Wilson, 2002: character 19).
39. Frontal, anteroposterior length: approximately twice (0); or less than minimum transverse breadth (1). (Wilson, 2002: character 20).
40. Frontal-nasal suture, shape: flat or slightly bowed anteriorly (0); V-shaped, pointing posteriorly (1). (Whitlock, 2011: character 21).
41. Frontals, dorsal surface: without paired grooves facing anterodorsally (0); grooves present, extend on to nasal (1). (Whitlock, 2011: character 22).
42. Frontal, contribution to dorsal margin of orbit: contribution to dorsal margin of orbit: less than 1.5 times the contribution of prefrontal (0); at least 1.5 times the contribution of prefrontal (1). (Whitlock, 2011: character 23).
43. Parietal occipital process, dorsoventral height: short, less than the diameter of the foramen magnum (0); deep, nearly twice the diameter of the foramen magnum (1). (Wilson, 2002: character 21).
44. Parietal, contribution to post-temporal fenestra: present (0); absent (1). (Wilson, 2002: character 22).

45. Parietal, distance separating supratemporal fenestrae: less than the long axis of supratemporal fenestra, 0.8 or less (0); almost the same as the long axis of supratemporal fenestra 0.8-1.2 (1); much larger than the long axis of supratemporal fenestra, more than 1.2 (2). (Modified from Wilson, 2002: character 24).
46. Postparietal foramen: absent (0); present (1). (Wilson, 2002: character 23).
47. Paroccipital process distal terminus: straight, slightly expanded surface (0); rounded, tongue-like process (1). (Whitlock, 2011: character 42).
48. Supratemporal fenestra: present (0); absent (1). (Wilson, 2002: character 25).
49. Supratemporal fenestra, long axis orientation: anteroposterior (0); transverse (1). (Wilson, 2002: character 26).
50. Supratemporal fenestra, maximum diameter: much longer than (0); or subequal to that of foramen magnum (1). (Wilson, 2002: character 27).
51. Supratemporal region, anteroposterior length: temporal bar longer (0); or shorter anteroposteriorly than transversely (1). (Wilson, 2002: character 28).
52. Supratemporal fossa, lateral exposure: not visible laterally, obscured by temporal bar (0); visible laterally, temporal bar shifted ventrally (1). (Wilson, 2002: character 29).
53. Supraoccipital, sagittal nuchal crest: broad, weakly developed (0); narrow, sharp and distinct (1). (Whitlock, 2011: character 45).
54. Laterotemporal fenestra, anterior extension: posterior to orbit (0); ventral to orbit (1). (Wilson, 2002: character 30).
55. Quadrate fossa: absent (0); present (1). (Wilson, 2002: character 33).
56. Quadrate fossa, depth: shallow (0); deeply invaginated (1). (Wilson, 2002: character 34).
57. Quadrate fossa, orientation: posterior (0); posterolateral (1). (Wilson, 2002: character 35).
58. Quadrate, articular surface shape: quadrangular in ventral view, oriented transversely (0); roughly triangular in shape or thin, crescent-shaped surface with anteriorly directed medial process (1). (Modified, based on Mannion et al., 2012 from Whitlock, 2011: character 32)
59. Quadrate, articular surface shape: quadrangular in ventral view, oriented transversely or roughly triangular in shape (0); thin, crescent-shaped surface with anteriorly directed medial process (1). (Modified, based on Mannion et al., 2012 from Whitlock, 2011: character 32).

60. Palatobasal contact, shape: pterygoid with small facet (0); dorsomedially orientated hook (1); or rocker-like surface for basipterygoid articulation (2). (Wilson, 2002: character 36).
61. Pterygoid, transverse flange (i.e. ectopterygoid process) position: posterior of orbit (0); between orbit and antorbital fenestra (1); anterior to antorbital fenestra (2). (Wilson, 2002: character37).
62. Pterygoid, quadrate flange size: large, palatobasal and quadrate articulations well separated (0); small, palatobasal and quadrate articulations approach (1). (Wilson, 2002: character 38)
63. Pterygoid, palatine ramus shape: straight, at level of dorsal margin of quadrate ramus (0); stepped, raised above level of quadrate ramus (1). (Wilson, 2002: character39).
64. Pterygoid, sutural contact with ectopterygoid: broad, along the medial or lateral surface (0); narrow, restricted to the anterior tip of the ectopterygoid (1). (Zaher et al., 2011: character 240)
65. Palatine, lateral ramus shape: plate-shaped (long maxillary contact) (0); rod-shaped (narrow maxillary contact) (1). (Wilson, 2002: character 40).
66. Epipterygoid: present (0); absent (1). (Wilson, 2002: character 41).
67. Vomer, anterior articulation: maxilla (0); premaxilla (1). (Wilson, 2002: character 42).
68. Supraoccipital, height: twice subequal to (0); or less than height of foramen magnum (1). (Wilson, 2002: character 43).
69. Paroccipital process, ventral non-articular process: absent (0); present (1). (Wilson, 2002: character 44).
70. Crista prootica, size: rudimentary (0); expanded laterally into dorsolateral process (1). (Wilson, 2002: character 45).
71. Basipterygoid processes, length: short, approximately twice (0); or elongate, at least four times basal diameter (1). (Wilson, 2002: character 46).
72. Basipterygoid processes, angle of divergence: approximately 45° (0); less than 30° (1). (Wilson, 2002: character 47).
73. Basal tubera, anteroposterior depth: approximately half dorsoventral height (0); sheet-like, 20% dorsoventral height (1). (Wilson, 2002: character 48).
74. Basal tubera, breadth: much broader than (0); or narrower than occipital condyle (1). (Wilson, 2002: character 49).

75. Basal tubera: distinct from basiptyergoid (0); reduced to slight swelling on ventral surface of basiptyergoid (1). (Whitlock, 2011: character 53).
76. Basal tubera, shape of posterior face: convex (0); slightly concave (1). (Whitlock, 2011: character 54)
77. Basisoccipital depression between foramen magnum and basal tubera: absent (0); present (1). (Wilson, 2002: character 50).
78. Basisphenoid/basiptyergoid recess: present (0); absent (1). (Wilson, 2002: character 51).
79. Basisphenoid/quadrato contact: absent (0); present (1). (Wilson, 2002).
80. Basisphenoid, sagittal ridge between basiptyergoid processes: absent (0); present (1). (Zaher et al., 2011: character 242).
81. Basiptyergoid processes, orientation: perpendicular to (0); or angled approximately 45° to skull roof (1). (Wilson, 2002: character 53).
82. Basiptyergoid, area between the basiptyergoid processes and parasphenoid rostrum: is a mildly concave subtriangular region (0); forms a deep slot-like cavity that passes posteriorly between the bases of the basiptyergoid processes (1). (Mannion et al., 2012: character 48).
83. Occipital region of skull, shape: anteroposteriorly deep, paroccipital processes oriented posterolaterally (0); flat, paroccipital processes oriented transversely (1). (Wilson, 2002: character 54).
84. Occipital condyle, lateral surface of the basisoccipital: flat or slightly convex (0); strongly concave (1). (Remes et al., 2009: character 50).
85. Dentary, depth of anterior end of ramus: slightly less than that of dentary at midlength (0); 150% minimum depth (1). (Wilson, 2002: character 55).
86. Dentary, anteroventral margin shape: gently rounded (0); sharply projecting triangular process (1). (Wilson, 2002: character 56).
87. Dentary symphysis, orientation: angled 15° or more anteriorly to (0); or perpendicular to axis of jaw ramus (1). (Wilson, 2002: character 57).
88. Dentary, cross-sectional shape of symphysis: oblong or rectangular (0); subtriangular, tapering sharply towards ventral extreme (1); subcircular (2). (Whitlock, 2011: character 60).
89. Dentary, tuberosity on labial surface near symphysis: absent (0); present (1). (Whitlock, 2011: character 57).

90. Dentary, posteroventral process shape: single (0); divided (1). (D'Emic, 2012: character 10).
91. Mandible, coronoid eminence: strongly expressed, clearly rising above plane of dentigerous portion (0); absent (1). (Whitlock, 2011: character 62).
92. External mandibular fenestra: present (0); absent (1). (Wilson, 2002: character 58).
93. Surangular depth: less than twice (0); or more than two and one-half times maximum depth of the angular (1). (Wilson, 2002: character 59).
94. Surangular ridge separating adductor and articular fossae: absent (0); present (1). (Wilson, 2002: character 60).
95. Adductor fossa, medial wall depth: shallow (0); deep, prearticular expanded dorsoventrally (1). (Wilson, 2002: character 61).
96. Splenial posterior process, position: overlapping angular (0); separating anterior portions of prearticular and angular (1). (Wilson, 2002: character 62).
97. Splenial posterodorsal process: present, approaching margin of adductor chamber (0); absent (1). (Wilson, 2002: character 63).
98. Coronoid, size: extending to dorsal margin of jaw (0); reduced, not extending dorsal to splenial (1); absent (2). (Wilson, 2002: character 64).
99. Tooth rows, shape of anterior portions: narrowly arched, anterior portion of tooth rows V-shaped (0); broadly arched, anterior portion of tooth rows U-shaped (1); rectangular, tooth bearing portion of jaw perpendicular to jaw rami (2). (Wilson, 2002: character 65).
100. Tooth rows, length: extending to orbit (0); restricted anterior to orbit (1); restricted anterior to antorbital fenestra (2); restricted anterior to subnarial foramen (3). (Modified from Wilson, 2002: character 66).
101. Maxillary teeth shape: straight along axis (0); twisted axially through an arc of 30-45°: absent (0); present (1). (D'Emic, 2012: character 15).
102. Dentary teeth, number: greater than 20 (0); 10-17 (1); 9 or fewer (2). (Modified from Wilson, 2002: character 73).
103. Replacement teeth per alveolus, number: two or fewer (0); more than four (1). (Wilson, 2002: character 74).
104. Lateral plate: absent (0); present (1). (Upchurch et al., 2004: character 9).
105. Teeth, orientation: perpendicular (0); or oriented anteriorly relative to jaw margin (1). (Wilson, 2002: character 75).

106. Tooth crowns, orientation: aligned along jaw axis, crowns do not overlap (0); aligned slightly anterolingually, tooth crowns overlap (1). (Wilson, 2002: character 69).
107. Tooth crowns, shape: narrow crowns (0); broad crowns (1). (Carballido et al., 2017).
108. Tooth crowns, cross-sectional shape at mid-crown: elliptical (0); D-shaped (1); subcylindrical (2); cylindrical (3). (Wilson, 2002: character 70).
109. SI values for tooth crowns: less than 3.0 (0); 3.0-4.0 (1); 4.0-5.0 (2); more than 5.0 (3). (Upchurch et al., 2004: characters 67-69).
110. Crown-to-crown occlusion: absent (0); present (1). (Wilson, 2002: character 67).
111. V-shaped wear facets: present (0); absent (1). (Modified from Wilson, 2002: character 68).
112. Development of the marginal wear facets: well developed (0); slightly developed as marginal facets (1). (Carballido et al., 2017)
113. One high angle wear facet and a second low angle wear facet: absent (0); present (1). (Carballido et al., 2017)
114. Single planar wear facet in labial or lingual surface of the teeth: absent (0); present (1). (Carballido et al., 2017)
115. Marginal tooth denticles: present (0); absent on posterior edge (1); absent on both anterior and posterior edges (2). (Wilson, 2002: character 72).
116. Enamel surface texture: smooth (0); wrinkled (1). (Wilson, 2002: character 71).
117. Thickness of enamel asymmetric labiolingually: absent (0); present (1). (Whitlock, 2011: character 74).
118. Teeth, longitudinal grooves on lingual aspect: absent (0); present (1). (Wilson, 2002: character 76).

Cervical vertebrae

119. Cervical vertebrae, number: 10 or fewer (0); 12 (1); 13-14 (2); 15 (3); 16 or more (4). (Modified from Wilson, 2002: character 80 and Upchurch et al., 2004: characters 96-100).
120. Atlas, intercentrum occipital facet shape: rectangular in lateral view, length of dorsal aspect subequal to that of ventral aspect (0); expanded anteroventrally in lateral view, anteroposterior length of dorsal aspect shorter than that of ventral aspect (1). (Wilson, 2002: character 79).

121. Axis, centrum shape: over two and a half times as long as tall (0); less than twice as long as tall (1). (D'Emic, 2012: character 20).
122. Cervical vertebrae, parapophyses, shape and orientation: short and weakly developed, projected laterally or slightly ventrally (0); middle development, ventrally such that the cervical ribs are displaced ventrally around half the height of the centrum (1); well developed, broad and ventrally projected such that cervical ribs are displaced ventrally more than the height of the centrum (2). (Modified from D'Emic, 2012: character 29).
123. Cervical centra, articulations: amphicoelous (0); opisthocoelous (1). (Salgado et al., 1997: character 1; Wilson, 2002: character 82; Upchurch, 1998: character 81 and Upchurch et al., 2004: character 103).
124. Cervical centra, ventral surface: is flat or slightly convex transversely (0); transversely concave (1). (Upchurch, 1998: character 84 and Upchurch et al., 2004: character 107).
125. Cervical centra, midline keels on ventral surface: prominent and plate-like (0); reduced to low ridges or absent (1). (Upchurch, 1998: character 83 and Upchurch et al., 2004: character 106).
126. Cervical centra, pleurocoels: absent (0); present with well-defined anterior, dorsal, and ventral edges, but not the posterior one (1); present, with well-defined edges (2); absent, but with deep lateral fossa which bears small pneumatopores that communicate to the interior pneumatic cavities (3). (Carballido et al., 2012)
127. Cervical centra, pleurocoels: singles without division (0); with a well-defined anterior excavation and a posterior smooth fossa (1); divided by a bone septum, resulting in an anterior and a posterior lateral excavation (2); divided in three or more lateral excavations, resulting in a complex morphology (3); with a well-defined anterior excavation and a posterior smooth fossa (Harris, 2006; Modified from Salgado et al., 1997; Wilson, 2002).
128. Cervical vertebrae, well developed epipophyses: absent (0); present (1). (Carballido et al., 2017)
129. Cervical vertebrae, epipophyses shape: stout, pillar-like expansions above postzygapophyses (0); posteriorly projecting prongs (1). (D'Emic, 2012: character 24).
130. Prezygapophyses, anterior process situated ventrolaterally to the articular surface: absent (0); present (1). (Remes et al., 2009: character 79).
131. Cervical vertebrae with an accessory lamina, which runs from the PODL (or slightly anteriorly) up to the SPOL: absent (0); present (1). (Modified from D'Emic, 2012: character 25).

132. Cervical vertebrae, height divided width (measured in its posterior articular surface): higher than 1.1 (0), around 1 (1); between 0.9 and 0.7 (2); smaller than 0.7 (3). (Modified from Wilson, 2002: character 84; Upchurch, 1998: character 85 and Upchurch et al., 2004: character 108).
133. Cervical centra, small notch in the dorsal margin of the posterior articular surface: absent (0); present (1). (Carballido et al., 2012).
134. Cervical vertebrae, neural arch lamination: well developed, with well-marked laminae and fossae (0); rudimentary, with diapophyseal laminae absent or very slightly marked (1). (Wilson, 2002: character 81).
135. Cervical vertebrae with an accessory lamina, which runs from the postzygodiapophyseal lamina (PODL) up to the spinoprezygapophyseal lamina (SPRL): absent (0); present (1). (Modified from Sereno et al., 2007: characters 50, 51; Whitlock, 2011: characters 78, 96).
136. Cervical centra, internal pneumaticity: absent (0); present with singles and wide cavities (1); present, with several small and complex internal cavities (2). (Modified from Carballido et al., 2011).
137. Anterior cervical vertebrae, prespinal lamina: absent (0); present (1). (Carballido et al., 2012).
138. Anterior cervical vertebrae, neural spine shape: single (0); bifid (1). (Wilson, 2002: character 72; Upchurch et al., 2004: character 118).
139. Middle and posterior cervical vertebrae, prespinal lamina: absent (0); present (1). (Carballido et al., 2012).
140. Middle cervical vertebrae, lateral fossae on the prezygapophysis process: absent (0); present (1). (Harris, 2006).
141. Middle, cervical vertebrae, height of the neural arch: less than the height of the posterior articular surface (0); higher than the height of the posterior articular surface, with spine lower than distance between postzygapophysis and the dorsal margin of the centrum (1); higher, with spine lower than distance between postzygapophysis and the dorsal margin of the centrum (2). (Wilson, 2002: character 87; similar Upchurch et al., 2004: 111 and 112). Modified here. In *Bravasaurus* and *Trigonosaurus*, among other derived titanosaurs, the neural arch is taller than the posterior articular surface, but the segment above the postzygapophyses is relatively low compared to other titanosaurs.
142. Middle cervical centrum, anteroposterior length divided the height of the posterior articular surface: less than 4 (0); more than 4 (1). (Wilson, 2002: character 74; and Upchurch et al., 2004: character 102).

143. Middle and posterior cervical vertebrae, morphology of the centroprezygapophyseal lamina: single (0); dorsally divided, resulting in a lateral and medial lamina, being the medial lamina linked with the intraprezygapophyseal lamina and not with the prezygapophysis (1); divided, resulting in the presence of a “true” divided centroprezygapophyseal lamina, which is dorsally connected to the prezygapophysis (2). (Carballido et al., 2012).
144. Middle and posterior cervical vertebrae, morphology of the centropostzygapophyseal lamina (CPOL): single (0); divided, with the medial part contacting the intrapostzygapophyseal lamina (1) (Carballido et al., 2012).
145. Middle and posterior cervical vertebrae, articular surface of zygapophyses: flat (0); transversally convex (1). (Upchurch et al., 2004).
146. Middle and posterior cervical vertebrae, prominent triangular flange on posterior edge of the diapophyseal process (in the PCDL): absent (0); present (1). (Remes et al., 2009: character 78).
147. Middle cervical vertebrae, prezygapophyses position: do not extend beyond the anterior margin of the centrum (0); extends beyond the anterior margin of the centrum (1). (Salgado et al., 1997, character 37).
148. Middle and posterior cervical vertebrae, parapophysis shape: subcircular (0); anteroposteriorly elongate (1). (D’Emic, 2012: character 28).
149. Posterior cervical vertebrae, lateral profile of the neural spine: displays steeply sloping cranial and caudal faces (0); displays steeply sloping cranial face and noticeably less steep caudal margin (1). (Upchurch et al., 2004: character 119).
150. Posterior cervical vertebrae, neural spine shape: not expanded distally (0); expanded but not as much as the width of the centrum (1); laterally expanded, being equal or wider than the vertebral centrum (1). (Modified from González Riga et al., 2009).
151. Posterior cervical vertebrae, lateral expansion: SPRLs does not contact the lateral margins of the neural spine (0); SPRLs are contacting the lateral margins of the neural spine (1). (Modified from González Riga and Ortiz David, 2014: characters 26-27).
152. Posterior cervical and anterior dorsal vertebrae, neural spine shape: single (0); bifid (1). (Wilson, 2002: character 90, Upchurch et al., 2004: character 118).
153. Posterior cervical vertebrae, proportions – ratio total height /centrum length: less than 1.5 (0); more than 1.5 (1). (González Riga et al., 2009: character 32).
154. Posterior cervical and anterior dorsal bifid neural spines, median tubercle: absent (0); present (1). (Carballido et al., 2012: character 133)

Dorsal vertebrae

155. Number of dorsal vertebrae: 14 or more (0); 13 (1); 12 (2); 10 (3). (Modified from Wilson, 2002: character 91; Upchurch et al., 2004: characters 122- 125).
156. Dorsal centra, pleurocoels: absent (0); present (1). (Wilson, 2002: character 78; Upchurch et al., 2004: character 128).
157. Dorsal vertebrae, transverse processes: are directed laterally or slightly upwards (0); are directed strongly dorsolaterally (1). (Upchurch et al., 2004: character 138).
158. Dorsal vertebrae, distal end of the transverse process: curves smoothly into the dorsal surface of the process (0); is set off from the dorsal surface, the latter having a distinct dorsally facing flattened area (1). (Upchurch et al., 2004: character 140).
159. Anterior dorsal vertebrae, non-bifid neural spine in anterior or posterior view: possess subparallel lateral margins (0); possess lateral margins which slightly diverge dorsally (1); possess lateral margins which strongly diverge dorsally (2). (Modified 52 from Wilson, 2002: character 107; Upchurch et al., 2004: character 155).
160. Middle to posterior dorsal vertebrae, non-bifid neural spine in anterior or posterior view: possess subparallel lateral margins (0); possess lateral margins which slightly diverge dorsally (1); possess lateral margins which strongly diverge dorsally (2). (Modified from Wilson, 2002: character 107; Upchurch et al., 2004: character 155).
161. Dorsal centra, pneumatic structures: absent, dorsal centra with solid internal structure (0); present, dorsal centra with simple and big air-spaces (camerate) (1); present, dorsal centra with small and complex air-spaces (polycamerate) (2); present, dorsal centra with small and complex air spaces (semicamellate/camellate) (3). (Modified from Carballido et al., 2011).
162. Anterior and middle dorsal neural spines, spinoprezygapophyseal lamina (SPRL): absent (0); present (1). (Modified from Upchurch et al., 2007: character 131).
163. Posterior dorsal neural spines, spinoprezygapophyseal lamina (SPRL): absent (0); present (1). (Modified from Upchurch et al., 2007: character 132).
164. Dorsal vertebrae, single not bifid neural spines, single prespinal lamina (PRSL): absent (0); present (1). (Modified from Salgado et al., 1997: character14).
165. Dorsal vertebrae, single not bifid neural spines, single prespinal lamina (PRSL): rough and wide, present in the dorsalmost part of the neural spine (0); rough and wide, extended through almost all the neural spine (1); smooth and narrow (2). (Carballido et al., 2012).
166. Dorsal vertebrae with single neural spines, middle single fossa projected through the midline of the neural spine: present (0); absent (1). (Carballido et al., 2012).

167. Dorsal vertebrae with single neural spines, middle single fossa, projected through the midline of the neural spine: relatively wide median simple fossa (0); a thin median simple fossa (1); extremely reduced median simple fossa (2). (Carballido et al., 2012).
168. Anterior dorsal centra, articular face shape: amphicoelous (0); opisthocoelous (1). (Wilson, 2002: character 94; Upchurch et al., 2004: character 104).
169. Anterior and middle dorsal centra, pleurocoels: have rounded caudal margins (0); have tapering, acute caudal margins (1). (Salgado et al., 1997; Upchurch, 1998: character 06; Upchurch et al., 2004: character 127).
170. Middle dorsal neural arches in lateral view, anterior edge of the neural spine: project anteriorly to the diapophysis (0); converge with the diapophysis (1); project posteriorly to the diapophysis (2). (Carballido et al., 2012).
171. Anterior and middle dorsal vertebrae, zygapophyseal articulation angle: horizontal or slightly posteroventrally oriented (0); posteroventrally oriented (around 30°) (1); strongly posteroventrally oriented (more than 40°) (2). (Carballido et al., 2012).
172. Anterior dorsal vertebrae, neural spine orientation: vertical, or slightly inclined (less than 20°) (0); posterodorsally, more than 20° (1); anteriorly directed (2). (Wilson, 2002: character 102; Upchurch et al., 2004: characters 153-154)
173. Anterior dorsal vertebrae neural spine, triangular aliform processes: absent (0); present but do not project far laterally (not as far as caudal zygapophyses) (1); present and project far laterally (as far as caudal zygapophyses) (2). (Modified from Wilson, 2002: character 102 and Upchurch et al., 2004: characters 153-154).
174. Anterior dorsal vertebrae, neural spine minimums width / length: 0.5 or greater (stout and short neural spine) (0); lower than 0.5 (thin and tall neural spines). (Carballido et al., 2017: character 174).
175. Anterior dorsal vertebrae, neural spine length (from TPRL to top): less than the height of the centrum (0); slightly higher than the centrum (1); twice or more the height of the centrum (2). (Carballido et al., 2017: character 175).
176. Anterior dorsal vertebrae, dorsal edge of the neural spine: flat (0); arrow-shaped (1); convex (2). (Carballido et al., 2017: character 176).
177. Middle to posterior dorsal vertebrae, dorsal edge of the neural spine: flat (0); arrow-shaped (1); convex (2). (Modified from Carballido et al., 2017: character 177). Modified here to include middle dorsal vertebrae.
178. Middle to posterior dorsal centra, ventral surface: convex transversely (0); flattened (1); is slightly concave, sometimes with one or two crests (2). (Upchurch et al., 2004).

179. Middle dorsal vertebrae, hyposphene-hypantrum system: present (0); absent (1). (Modified from Salgado et al., 1997: character 25; Wilson, 2002: character 106; Upchurch et al., 2004: character 145).
180. Posterior dorsal vertebrae, hyposphene-hypantrum system: present and well developed, usually with a rhomboid shape (0); present and weakly developed, mainly as a laminar articulation (1); absent or only present in posteriormost dorsal vertebrae (2). (Carballido et al., 2012).
181. Middle and posterior dorsal vertebrae, transverse processes length: short (0); long (projecting along 1.5 the articular surface width) (1). (Carballido et al., 2012).
182. Mid and posterior dorsal vertebrae with a single lamina (the single TPOL) supporting the hyposphene or postzygapophysis from below: absent (0); present (1). (Modified from Upchurch et al., 2004: character 146).
183. Middle and posterior dorsal vertebrae, neural canal in anterior view: entirely surrounded by the neural arch (0); enclosed in a deep fossa, enclosed laterally by pedicels (1). (Upchurch et al., 2004: character 136).
184. Middle and posterior dorsal vertebrae, neural spine height: approximately twice the centrum length (0); for times the centrum length (1). (Upchurch et al., 2004).
185. Middle and posterior dorsal neural spines orientation: vertical (0); slightly inclined, with an angle of around 70 degrees (1); strongly inclined, with an angle not larger than 40 degrees (2). (Modified from Wilson, 2002: character 104).
186. Middle and posterior dorsal vertebrae, central keel: absent (0); present (1). (D'Emic, 2012: character 49).
187. Dorsal vertebrae, height of the neural arch divided the height of the centrum: less than 0.8 (0); more than 0.8 (1). (Pol et al., 2011).
188. Middle to posterior dorsal vertebrae, pleurocoel dorsal margin: rounded (0); angular (1). (Rauhut et al., 2015: character 346).
189. Middle to posterior dorsal vertebrae, pleurocoel dorsal margin: well below the dorsal margin of the centrum (0); at the level of the dorsal margin of the centrum or higher (1). (Rauhut et al., 2015: character 347).
190. Middle to posterior dorsal vertebrae, small fossa anterior or anteroventral to the pleurocoel: absent (0); present (1). (Rauhut et al., 2015: character 348).
191. Middle and posterior dorsal neural arches, centropostzygapophyseal lamina (CPOL), shape: simple (0); divided (1). (Wilson, 2002: character 95).
192. Middle and posterior dorsal neural arches, anterior centroparapophyseal lamina (ACPL): absent (0); present (1). (Wilson, 2002: character 96; Upchurch et al., 2004: character 133).

193. Middle and posterior dorsal neural arches, prezygoparapophyseal lamina (PRPL): absent (0); present (1). (Wilson, 2002: character 97).
194. Middle and posterior dorsal neural arches, posterior centroparapophyseal lamina (PCPL): absent (0); present (1). (Wilson, 2002: character 98, Upchurch et al., 2004: character 137).
195. Middle and posterior dorsal centrum in transverse section (height: width ratio): subcircular (ratio, similar to 1 or a bit higher) (0); slightly dorsoventrally compressed (ratios between 0.8 and 1) (1); strongly compressed (ratios below 0.8) (2). (Modified from Upchurch et al., 2004).
196. Middle and posterior dorsal vertebrae neural spine, triangular aliform processes: absent (0); present but do not project far laterally (not as far as caudal zygapophyses) (1); present and project far laterally (as far as caudal zygapophyses) (2). (Modified from Wilson, 2002: character 102 and Upchurch et al., 2004: characters 153-154).
197. Middle and posterior dorsal vertebrae, spinodiapophyseal lamina (SPDL): absent (0); present (1). (Upchurch et al., 2004: character 157).
198. Middle and posterior dorsal vertebrae, accessory spinodiapophyseal lamina (SPDL): absent (0); present (1). (Upchurch et al., 2004: character 151).
199. Dorsal vertebrae, spinodiapophyseal webbing: lamina follows curvature of neural spine in anterior view (0); lamina "festooned" from spine, dorsal margin does not closely follow shape of neural spine and diapophysis (1). (Whitlock, 2011: character 104).
200. Anterior dorsal vertebrae, spinopostzygapophyseal lamina (SPOL): absent (0); present (1). (Upchurch et al., 2007: character 133).
201. Middle and posterior dorsal neural spines, lateral spinopostzygapophyseal lamina (LSPOL): absent (0); present (1). (Wilson, 2002: 100; Upchurch et al., 2004: character 159).
202. Middle and posterior dorsal neural arches, spinodiapophyseal lamina (SPDL) and spinopostzygapophyseal lamina (LSPOL) contact: absent (0); present (1). (Wilson, 2002: character 101).
203. Middle and posterior dorsal vertebrae, spinodiapophyseal (SPDL) and spinopostzygapophyseal lamina (LSPOL) contact: ventral, well separated from the triangular aliform process (0); dorsal, forms part of the triangular aliform process (1). (Carballido et al., 2012).
204. Middle and posterior dorsal vertebrae, height of neural arch below the postzygapophyses (pedicel): less than height of centrum (0); subequal to or greater than height of centrum (1). (Whitlock, 2011: character 109).

205. Posterior dorsal vertebrae, medial spinopostzygapophyseal lamina (mSPOL): absent (0); present and forms part of the median posterior lamina (1). (Carballido et al., 2012).
206. Posterior dorsal vertebrae, transverse processes: lie posterior, or posterodorsal, to the parapophysis (0); lie vertically above the parapophysis (1). (Upchurch et al., 2004: character 139).
207. Posterior dorsal centra, articular face shape: amphicoelous (0); slightly opisthocoelous (1); opisthocoelous (2). (Modified from Wilson, 2002: character 105).
208. Posterior dorsal vertebrae, neural spine: narrower transversely than anteroposteriorly (0); broader transversely than anteroposteriorly (1). (Wilson, 2002: character 92).
209. Posterior dorsal vertebra, posterior centrodiapophyseal lamina (PCDL): has an unexpanded ventral tip (0); expands and may bifurcate toward its ventral tip (1). (Salgado et al., 1997).

Ribs

210. Cervical ribs, distal shafts of longest cervical ribs: are elongate and form overlapping bundles (0); are short and do not project beyond the caudal end of the centrum to which they are attached (1). (Wilson, 2002: character 140).
211. Cervical ribs, angle between the capitulum and tuberculum: greater than 90°, so that the rib shaft lies close to the ventral edge of the centrum (0); less than 90°, so that the rib shaft lies below the ventral margin of the centrum (1). (Wilson, 2002: character 139).
212. Dorsal ribs, proximal pneumatopores: absent (0); present (1). (Wilson, 2002: character 141)
213. Anterior dorsal ribs, cross-sectional shape: subcircular (0); plank-like, anteroposterior breadth more than three times mediolateral breadth (1). (Wilson, 2002).

Sacrum

214. Sacral vertebrae, number: 3 or fewer (0); 4 (1); 5 (2); 6 (3). (Wilson, 2002: character 108).
215. Sacrum, sacricostal yoke: absent (0); present (1). (Wilson, 2002: character 109).
216. Sacral vertebrae contributing to acetabulum: numbers 1-3 (0); numbers 2-4 (1). (Wilson, 2002: character 110).

217. Sacral neural spines length: approximately twice length of centrum (0); approximately four times length of centrum (1). (Wilson, 2002: character 111).
218. Sacral ribs, dorsoventral length: low, not projecting beyond dorsal margin of ilium (0); high extending beyond dorsal margin of ilium (1). (Wilson, 2002: character 112).
219. Pleurocoels in the lateral surfaces of sacral centra: absent (0); present (1). (Upchurch et al., 2004: character 165).

Caudal vertebrae

220. Caudal vertebrae, number: 35 or fewer (0); 40 to 55 (1); increased to 70-80 (2). (Wilson, 2002: character 114).
221. Caudal bone texture: solid (0); spongy (camellate), with large internal cells (1). (Wilson, 2002: character 113).
222. Anterior caudals, pneumatized neural arch: absent (0); present (1).
223. Caudal transverse processes: persist through caudal 20 or more posteriorly (0); disappear by caudal 15 (1); disappear by caudal 10 (2). (Wilson, 2002: character 115).
224. First caudal centrum anterior articular surface: flat (0); concave (1); convex (2). (Carballido et al., 2017).
225. First caudal centrum, posterior articular surface: flat (0); concave (1); convex (2). (Carballido et al., 2017).
226. First caudal neural arch, coel on lateral aspect of neural spine: absent (0); present (1). (Wilson, 2002: character 117).
227. Anterior caudal vertebrae (mainly the first and second): ventral bulge on transverse process: absent (0); present (1). (D'Emic, 2012: character 52).
228. Anterior and middle caudal vertebrae, blind fossae in lateral centrum: absent (0); present (1). (D'Emic, 2012: character 56).
229. Posteriormost anterior and middle caudal vertebrae, transverse processes orientation: perpendicular (0); swept backwards, reaching the posterior margin of the centrum (1). (D'Emic, 2012: character 59).
230. Anterior caudal vertebrae, transverse processes: ventral surface directed laterally or slightly ventrally (0); directed dorsally (1). (Whitlock, 2011: character 125).
231. Anterior caudal centra (excluding the first), articular face shape: amphiplatyan or amphicoelous (0); procoelous/distoplatyan (1); slightly procoelous (2); procoelous (3); posterior surface markedly more concave than the anterior one (4). (Modified from González Riga et al., 2009).

232. Anterior caudal centra, pleurocoels: absent (0); present (1). (Wilson, 2002: character 119).
233. Anterior caudal vertebrae, ventral surfaces: convex transversely (0); concave transversely (1); flat or slightly concave (2). (Modified from Upchurch et al., 2004: character 182). Modified so as to distinguish the concave surface of the caudal vertebrae of some titanosaurs like *Punatitan* and *Aeolosaurus* from others with flat or practically flat (but not convex) surfaces like *Uberabatitan* and *Baurutitan*.
234. Anterior and middle caudal vertebrae, ventrolateral ridges: absent (0); present (1). (Upchurch et al., 2004: character 183).
235. Anterior and middle caudal vertebrae, triangular lateral process on the neural spine: absent (0); present (1). (Whitlock, 2011: character 123).
236. Anterior caudal transverse processes shape: triangular, tapering distally (0); "winglike", not tapering distally (1). (Wilson, 2002: character 128).
237. Anterior caudal neural spines, transverse breadth: approximately 50% of (0); or greater than anteroposterior length (1). (Wilson, 2002: character 126).
238. Anterior caudal transverse processes, proximal depth: shallow, on centrum only (0); deep, extending from centrum to neural arch (1). (Wilson, 2002: character 127).
239. Anterior caudal transverse processes, diapophyseal laminae (ACDL, PCDL, PRDL, PODL): absent (0); present (1). (Wilson, 2002: character 129).
240. Anterior caudal transverse processes, anterior centrodiapophyseal lamina (ACDL), shape: single (0); divided (1). (Wilson, 2002: character 130).
241. Anterior caudal vertebrae, hyosphene ridge: absent (0); present (1). (Upchurch et al., 2004: character 187).
242. Anterior caudal centra, length: approximately the same (0); or doubling over the first 20 vertebrae (1). (Wilson, 2002: character 120).
243. Anterior caudal neural arches, spinoprezygapophyseal lamina (SPRL): absent, or present as small short ridges that rapidly fade out into the anterolateral margin of the spine (0); present, extending onto lateral aspect of neural spine (1); present, well developed and extending onto the anterior or anterolateral edges of the neural spine (2) (Modified from Wilson, 2002: character 121). A third state was incorporated in order to include the morphology observed in some taxa in which the SPRL is well developed, but is not extending into the lateral aspect of the neural spine, as is the case of *Patagotitan*.
244. Anterior caudal neural arches, spinodiapophyseal lamina (SPDL): absent (0); present (1). In titanosaurs the SPDL, when present, is extending from the

- dyapophyseal section of the transverse process (the dorsalmost part of it) up to the neural spine. (Carballido et al., 2017).
245. Anterior caudal neural arches, spinoprezygapophyseal lamina (SPRL)-spinopostzygapophyseal lamina (SPOL) contact: absent (0); present, forming a prominent lamina on lateral aspect of neural spine (1). (Wilson, 2002: character 122).
 246. Anterior caudal neural arches, prespinal lamina (PRSL): absent (0); present (1). (Wilson, 2002: character 123). (Carballido et al., 2017).
 247. Anterior caudal vertebrae, ventral and medially placed SPRL, usually described as bifurcated PRSL: absent (0); present (1). (Carballido et al., 2017).
 248. Anterior caudal prespinal lamina (PRSL), triangular shaped product of a dorsal expansion of it: absent (0); present (1). (Carballido et al., 2017).
 249. Anterior caudal vertebrae, pair thin laminae that are bounding the prespinal laminae and that diverge dorsally: absent (0); present (1). (Carballido et al., 2017).
 250. Middle caudal centra, shape: cylindrical (0); with flat ventral margin (1); quadrangular, flat ventrally and laterally (2); trapezoidal (laterally compressed forming a shallow fossa) (3). (Modified from Wilson, 2002: character 131 and Carballido et al., 2020: character 250). We added a state that differentiates a centrum with a square profile, as in some more primitive sauropods (e.g. *Diplodocus*), from the centrum with a trapezoidal profile, in which the lateral faces are inclined medioventrally, and the ventral surface of the centrum is relatively narrower. The latter condition is frequent among rincosaurians.
 251. Anterior and middle caudal centra, ventral surface: without groove or hollow (0); with groove (1); with hollow divided by a longitudinal septum (2) (Modified from Wilson, 2002: character 132). We added a state to consider the diversity of ventral surfaces in the anterior and middle caudal centra of derived titanosaurs.
 252. Middle caudal centra, articular face shape: amphiplatyan or amphicoelous (0); procoelous/distoplatyan (1); slightly procoelous (2); procoelous (3). (González Riga et al., 2009).
 253. Posteriormost anterior and middle caudal vertebrae, location of the neural arches: over the midpoint of the centrum with approximately subequal amounts of the centrum exposed at either end (0); on the anterior half of the centrum (1). (Upchurch et al., 2004: character 185).
 254. Anterior caudal vertebrae, anterior face of the centrum strongly inclined anteriorly: straight (vertical) (0); slightly inclined anteroventrally (1); strongly inclined anteroventrally (2). (Modified from Santucci and Arruda Campos, 2011: character 256). Among rincosaurians the anteroventral inclination of the anterior face of the caudal centra is frequent. However, in *Uberabatitan* and *Trigonosaurus* the

inclination is subtle, whereas in *Aeolosaurus* and *Punatitan*, the anterior surfaces are strongly inclined. The new state allows better separating these differences.

255. Middle caudal vertebrae, with the anterior face strongly inclined anteriorly: absent (0); present (1). (Carballido et al., 2017).
256. Middle caudal vertebrae, height of the pedicels below the prezygapophysis: low with curved anterior edge of the pedicel (0); high with vertical anterior edge of the pedicel (1). (Carballido et al., 2012).
257. Middle caudal vertebrae, orientation of the neural spines: anteriorly (0); vertical (1); slightly directed posteriorly (2); strongly directed posteriorly (3). (Modified from Wilson, 2002: character 133).
258. Posterior caudal vertebrae, neural spine strongly displaced posteriorly: absent (0); present (1). (Carballido et al., 2012).
259. Middle caudal vertebrae, ratio of centrum length to centrum height: less than 2, usually 1.5 or less (0); 2 or higher (1). (Upchurch et al., 2004: character 179).
260. Anterior-posterior caudal vertebrae (those with still well-developed neural spine), neural spine orientation: vertical (0); slightly directed posteriorly (1); strongly directed posteriorly (2). (Carballido et al., 2012).
261. Posterior caudal centra, articular face shape: amphiplatic (0); procoelous (1); opisthocoelous (2). (Modified from González Riga et al., 2009).
262. Posterior caudal centra, shape: cylindrical (0); dorsoventrally flattened, breadth at least twice height (1). (Wilson, 2002: character 135).
263. Posterior caudal vertebrae, ratio of length to height: less than 5, usually 3 or less (0); 5 or higher (1). (Upchurch et al., 2004: character 180).
264. Distalmost caudal centra, articular face shape: platycoelous (0); biconvex (1). (Wilson, 2002: character 136).
265. Distalmost biconvex caudal centra, number: 10 or fewer (0); more than 30 (1). (Wilson, 2002: character 137).
266. Distalmost biconvex caudal centra, length-to height ratio: less than 4 (0); greater than 5 (1). (Wilson, 2002: character 138).
267. Forked chevrons with anterior and posterior projections: absent (0); present (1). (Wilson, 2002: character 143).
268. Forked chevrons, distribution: distal tail only (0); throughout middle and posterior caudal vertebrae (1). (Wilson, 2002: character 144).

269. Chevrons, crus bridging dorsal margin of haemal canal: present (0); absent (1). (Wilson, 2002: character 145).
270. Chevron haemal canal, depth: short, approximately 25% (0); or long, approximately 50% chevron length (1). (Wilson, 2002: character 146).
271. Chevrons: persisting throughout at least 80% of tail (0); disappearing by caudal 30 (1). (Wilson, 2002: character 147).
272. Posterior chevrons, distal contact: fused (0); unfused (open) (1). (Wilson, 2002: character 148).

Scapular girdle

273. Posture: bipedal (0); columnar, obligatory quadrupedal posture (1). (Wilson, 2002: character 149).
274. Scapular acromion process, size: Narrow (0); broad, width more than 150% minimum width of blade (1). (Wilson, 2002: character 150).
275. Scapular blade, orientation respect to coracoid articulation: perpendicular (0); forming a 45° angle (1). (Wilson, 2002: character 151).
276. Scapular blade, distal expansion: absent (0); present (1). This character was introduced for recognizing those sauropods which scapular blade is not markedly expanded distally. The third state is recognized in several sauropods, such as *Patagotitan*, *Alamosaurus*, *Rinconsaurus*. (Carballido et al., 2017).
277. Scapular blade, shape: acromial edge not expanded (both edges are running parallel to each other) (0); rounded expansion on acromial side (1); racquet-shaped (2); marked distal expansion due to the posterodorsal orientation of the dorsal edge (3). (Wilson, 2002: character 152; as modified by Carballido et al., 2017: character 277).
278. Scapula, acromion process dorsal margin: concave or straight (0); with V-shaped concavity (1); with U-shaped concavity (2). (Sereno, 2007: character 88).
279. Scapula, highest point of the dorsal margin of the blade: lower than the dorsal margin of the proximal end (0); at the same height than the dorsal margin of the proximal end (1); higher than the dorsal margin of the proximal end (2). (Carballido et al., 2012, from Mannion, 2009).
280. Scapula, development of the acromion process: undeveloped (0); well developed (1). (Carballido et al., 2012).
281. Scapular length/minimum blade breadth: 5.5 or less (0); 5.5 or more (1). (Carballido et al., 2012).
282. Scapula, ventral margin with a well-developed ventromedial process: absent (0); present (1). (Carballido et al., 2011).

283. Scapular, acromial process position: lies nearly glenoid level (0); lies nearly midpoint scapular body (1). (Carballido et al., 2012).
284. Scapular acromion length: less than 1/2 scapular length (0); at least 1/2 scapular length (1). (Mannion et al., 2012: character 168).
285. Glenoid scapular orientation: relatively flat or laterally facing (0); strongly bevelled medially (1). (Wilson, 2002: character 153).
286. Scapular blade, cross-sectional shape at base: flat or rectangular (0); D-shaped (1). (Wilson, 2002: character 154).
287. Coracoid, proximodistal length: less than the length of scapular articulation (0); approximately twice the length of scapular articulation (1). (Wilson, 2002: character 155).
288. Coracoid, anteroventral margin shape: rounded (0); rectangular (1). (Wilson, 2002: character 156).
289. Dorsal margin of the coracoid in lateral view: reaches or surpasses the level of the dorsal margin of the scapular expansion (0); lies below the level of the scapular proximal expansion and separated from the latter by a V-shaped notch (1). (Upchurch et al., 2004: character 207).
290. Coracoid, infraglenoid deep groove: absent (0); present (1). (D'Emic, 2012: character 76)
291. Coracoid, infraglenoid lip: absent (0); present (1). (Wilson, 2002: character 157).
292. Sternal plate, shape: posterolateral margin curved (0); posterolateral margin expanded as a corner (1). (D'Emic, 2012: character 76).
293. Sternal plate, shape: oval (0); crescentic (1). (Wilson, 2002: character 158).
294. Prominent posterolateral expansion of the sternal plate producing a kidney-shaped profile in dorsal view: absent (0); present (1). (Upchurch et al., 2004: character 211).
295. Prominent parasagittal oriented ridge on the dorsal surface of the sternal plate: absent (0); present (1). (Upchurch et al., 2004: character 212).
296. Ridge on the ventral surface of the sternal plate: absent (0); present (1). (Upchurch et al., 2004: character 213).
297. Ratio of maximum length of sternal plate to the humerus length: less than 0.75, usually less than 0.65 (0); greater than 0.75 (1). (Upchurch et al., 2004: character 209)

Forelimb

298. Humerus, strong posterolateral bulge around the level of the deltopectoral crest: absent (0); present (1). (D’Emic, 2012: character 80).
299. Humerus, radial and ulnar condyles shape: radial condyle divided on anterior face by a notch (0); undivided (1). (D’Emic, 2012: character 83).
300. Humerus-to-femur ratio: less than 0.60 (0); 0.60 to 0.69 (1); 0.70 to 0.90 (2); greater than 0.90 (3) (Modified from Upchurch et al., 2004: character 216 and Carballido et al., 2017: character 300). We split character state 1 in two, because there are noticeable differences between the humerus/femur proportions in the saltasaurines (0.60 to 0.69) and colossosaurian titanosaurs (0.70 to 0.90).
301. Humeral deltopectoral attachment, development: prominent (0); reduced to a low crest or ridge (1). (Wilson, 2002: character160).
302. Humeral deltopectoral crest, shape: relatively narrow throughout length (0); markedly expanded distally (1). (Wilson, 2002: character161).
303. Humeral midshaft cross-section, shape: circular (0); elliptical (1). (Mannion et al, 2012: character 170).
304. Humerus, RI (*sensu* Wilson and Upchurch, 2003): gracile (less than 0.27) (0); medium (0.28-0.32) (1); robust (more than 0.33) (2). (Carballido et al., 2012).
305. Humeral distal condyles, articular surface shape: restricted to distal portion of humerus (0); exposed on anterior portion of humeral shaft (1). (Wilson, 2002: character 163).
306. Humeral distal condyle, shape: divided (0); flat (1). (Wilson, 2002: character 164).
307. Humeral, lateral margin: medially deflected (0); almost straight until the half length or even more (1); almost straight until the proximal third of the total length of the humerus (2). (Carballido et al., 2012).
308. Humeral proximolateral corner, shape: rounded, the dorsal surface is well convex (0); pronounced / square, the dorsal surface low, almost flat (1). (Wilson, 2002: character 159).
309. Ulnar proximal condyle, shape: subtriangular (0); triradiate, with deep radial fossa (1). (Wilson, 2002: character 165).
310. Ulnar proximal condylar processes, relative lengths: subequal (0); unequal, anterior arm longer (1). (Wilson, 2002: character 166).
311. Ulnar olecranon process, development: prominent, projecting above proximal articulation (0); rudimentary, level with proximal articulation (1). (Wilson, 2002: character 167).

312. Ulna, length-to-proximal breadth ratio: gracile (0); stout (1). (Wilson, 2002: character 168).
313. Radial distal condyle, shape: round (0); subrectangular, flattened posteriorly and articulating in front of ulna (1). (Wilson, 2002: character 169).
314. Radius, distal breadth: slightly larger than midshaft breadth (0); approximately twice midshaft breadth (1). (Wilson, 2002: character 170).
315. Radius, distal condyle orientation: perpendicular to long axis of shaft (0); bevelled approximately 20° proximolaterally relative to long axis of shaft (1). (Wilson, 2002: character 171).
316. Carpal bones, number: 3 or more (0); 2 or fewer (1). (Wilson, 2002: character 173).
317. Carpal bones, shape: round (0); block-shaped, with flattened proximal and distal surfaces (1). (Wilson, 2002: character 174).
318. Metacarpus, shape: spreading (0); bound, with sub-parallel shafts and articular surfaces that extend half their length (1). (Wilson, 2002: character 175).
319. Metacarpals, shape of proximal surface in articulation: gently curving, forming a 90° arc (0); U-shaped, subtending a 270° arc (1). (Wilson, 2002: character 176).
320. Longest metacarpal-to-radius ratio: close to 0.3 (0); 0.45 or more (1). (Wilson, 2002: character 177).
321. Metacarpal I, length: shorter than metacarpal IV (0); longer than metacarpal IV (1). (Wilson, 2002: character 178).
322. Metacarpal I, distal condyle shape: divided (0); undivided (1). (Wilson, 2002: character 179).
323. Metacarpal I distal condyle, transverse axis orientation: bevelled approximately 20° respect to axis of shaft (0); proximodistally or perpendicular with respect to axis of shaft (1). (Wilson, 2002: character 180).
324. Manual digits II and III, phalangeal number: 2-3-4-3-2 or more (0); reduced, 2-2-2-2-2 or less (1); absent or unossified (2). (Wilson, 2002: character 181).
325. Manual phalanx I.1, shape: rectangular (0); wedge-shaped (1). (Wilson, 2002: character 182).
326. Manual non-ungual phalanges, shape: longer proximodistally than broad transversely (0); broader transversely than long proximodistally (1). (Wilson, 2002: character 183).

Pelvic girdle

327. Pelvis, anterior breadth: narrow, ilia longer anteroposteriorly than distance separating preacetabular processes (0); broad, distance between preacetabular processes exceeds anteroposterior length of ilia (1). (Wilson, 200: character 184).
328. Ilium, ischial peduncle size: large, prominent (0); low, rounded (1). (Wilson, 2002: character 185).
329. Ilium, dorsal margin shape: flat (0); semicircular (1). (Wilson, 2002: character 186).
330. Ilium, preacetabular ventral margin shape: straight (0), concave (1); with a convex ventral bump (2). (D'Emic, 2012: character 99)
331. Ilium, preacetabular process shape: pointed, arching ventrally (0); semicircular, with posteroventral excursion of cartilage cap (1). (Wilson, 2002: character 188).
332. Ilium, preacetabular process orientation: anterolateral to body axis (0); perpendicular to body axis (1). (Wilson, 2002: character 189).
333. Highest point on the dorsal margin of the ilium: lies caudal to the base of the pubic process (0); lies cranial to the base of the pubic process (1). (Upchurch et al., 2004: character 245).
334. Pubis length respect to ischium: pubis slightly smaller or subequal to ischium (0); pubis larger (120% +) than ischium (1). (Carballido et al., 2012).
335. Pubis, ambiens process development: small, confluent with anterior margin of pubis prominent, (0); projects anteriorly from anterior margin of pubis (1). (Wilson, 2002: character 189).
336. Pubic apron, shape: flat (straight symphysis) (0); canted anteromedially (gentle S-shaped symphysis) (1). (Wilson, 2002: character 190).
337. Puboischial contact, length: approximately one third total length of pubis (0); one half total length of pubis (1). (Wilson, 2002: character 191).
338. Ischium, acetabular articular surface: maintains approximately the same transverse width throughout its length (0); is transversely narrower in its central portion and strongly expanded as it approaches the iliac and pubic articulations (1). (Mannion et al., 2012: character 180).
339. Ischium, iliac peduncle with constriction or "neck": absent (0); present (1). (Whitlock, 2011: character 173).
340. Ischium, elongate muscle scar on proximal end: absent (0); present (1). (Whitlock, 2011: character 174).
341. Ischial blade, shape: emarginate distal to pubic peduncle (0); no emargination distal to pubic peduncle (1). (Wilson, 2002: character 193).

342. Ischia pubic articulation: less or equal to the anteroposterior length of pubic pedicel (0); greater than the anteroposterior length of pubic pedicel (1). (Salgado et al., 1997).
343. Ischia, anteroposterior pubic pedicel width divided the total length of the ischium: less than 0.5 (0); 0.5 or larger (1). (Carballido et al., 2012).
344. Ischial distal shaft, shape: triangular, depth of ischial shaft increases medially (0); blade-like, medial and lateral depths subequal (1). (Upchurch et al., 2004: character 194).
345. Ischial distal shafts, cross-sectional shape: V-shaped, forming an angle of nearly 50° with each other (0); flat, nearly coplanar (1). (Wilson, 2002: character 195).
346. Ischia, distal end: is only slightly expanded (0); is strongly expanded dorsoventrally (1). (Upchurch, 1998: character 183).
347. Ischium, angle formed between the shaft and the acetabular line: forming an almost right angle (80-110°) (0) or; a close angle (less than 70°) (1). (Carballido et al., 2012).
348. Ischial tuberosity: absent (0); present (1). The tuberosity, noted by Otero (2010) for the ischium of *Neuquensaurus* (Otero, 2010: Fig. 8) and is present in other taxa, such as *Patagotitan*, *Bonitasaura*, *Futalognkosaurus*, and *Alamosaurus*. (Carballido et al., 2017).

Hind limb

349. Femur, longitudinal ridge on the anterior face: absent (0); present (1). (D'Emic, 2012: character 107).
350. Femur, fibular condyle: well developed, having a similar height than the tibial one (0); much shorter than the tibial condyle (1). The fibular condyle of *Patagotitan* and *Bonitasaura* is reduced in its posterior projection respect to that of most other sauropods, which fibular and tibial condyles are almost equally posteriorly projected. (Carballido et al., 2017).
351. Femur, epicondyle development: well developed (0); reduced, almost absent (1). In *Patagotitan* the epicondyle is extremely developed and notorious in posterior and distal view, as a minor step laterally projected. In contrast in some titanosaurs the epicondyle is almost imperceptible, as is the case of *Dreadnoughtus*, *Opisthocoelicaudia*, *Neuquensaurus* and *Saltasaurus*. (Carballido et al., 2017).
352. Femur, fourth trochanter position: almost at the half of the femur (0); in the proximal third of the femur (1). The fourth trochanter of *Patagotitan* is positioned around the proximal third of the total femur length, similar to the position observed in *Futalognkosaurus*, *Bonitasaura*, and some other non-Lognkosauria as *Rapetosaurus*, *Saltasaurus* and *Neuquensaurus*. In contrast the fourth trochanter of

most sauropods is around the half of the total femur length, being even lower in *Opisthocoelicaudia*. (Carballido et al., 2017).

353. Femur, fourth trochanter development: prominent (0); reduced to crest or ridge (1); extremely reduced (2). (Modified from Wilson, 2002: character 196, following to Whitlock, 2011: character 186).
354. Femur, lesser trochanter: present (0); absent (1). (Wilson, 2002: character 197).
355. Femur midshaft, transverse diameter: subequal to anteroposterior diameter (0); 125- 150% anteroposterior diameter (1); at least 185% anteroposterior diameter (2). (Wilson, 2002: character 198).
356. Femur, lateral bulge (marked by the lateral expansion and a dorsomedial orientation of the laterodorsal margin of the femur, which starts below the femur head ventral margin): absent (0); present (1). (Salgado et al., 1997).
357. Femur, pronounced ridge on posterior surface between greater trochanter and head: absent (0); present (1). (Whitlock, 2011: character 181).
358. Femur head position: perpendicular to the shaft, rises at the same level as the greater trochanter (0); dorsally directed, rises well above the level of the greater trochanter (1). (Modified from Upchurch et al., 2004: character 263).
359. Femur, distal condyles relative transverse breadth: subequal (0); tibial much broader than fibular (1). (Wilson, 2002: character 2000).
360. Femur, distal condyles orientation: perpendicular or slightly bevelled dorsolaterally (0); or bevelled dorsomedially approximately 10° relative to femoral shaft (1). (Wilson, 2002: character 201).
361. Femur, distal condyles articular surface shape: restricted to distal portion of femur (0); expanded onto anterior portion of femoral shaft (1). (Wilson, 2002: character 202).
362. Situation of the femoral fourth trochanter: on the caudal surface of the shaft, near the midline (0); on the caudomedial margin of the shaft (1). (Upchurch et al., 2004: character 268).
363. Tibial proximal condyle, shape: narrow, long axis anteroposterior (0); expanded transversely, condyle subcircular (1). (Wilson, 2002: character 203).
364. Tibial cnemial crest, orientation: projecting anteriorly (0); or laterally (1). (Wilson, 2002: character 204).
365. Tibia, distal breadth: approximately 125% (0); more than twice midshaft breadth (1). (Wilson, 2002: character 205).

366. Tibial distal posteroventral process, size: broad transversely, covering posterior fossa of astragalus (0); shortened transversely, posterior fossa of astragalus visible posteriorly (1). (Wilson, 2002: character 206).
367. Fibula, proximal tibial scar, development: not well-marked (0); well-marked and deepening anteriorly (1). (Wilson, 2002: character 207).
368. Fibula, lateral trochanter: absent (0); present (1). (Wilson, 2002: character 208).
369. Fibular distal condyle, size: subequal to shaft (0); expanded transversely, more than twice midshaft breadth (1). (Wilson, 2002: character 209).
370. Fibular, proximal end, anterior crest: absent or poorly-developed (0); well-developed creating an interlocking proximal crus (1). (D'Emic, 2012: character 111).
371. Fibula, shaft shape: straight, or slightly sigmoidal (0); sigmoid, such that the proximal and distal faces are angled relative to midshaft (1). (D'Emic, 2012: character 113).
372. Astragalus, shape: at least 1.5 times wider than anteroposteriorly long (0); anteroposterior and transverse dimensions subequal (1). (D'Emic, 2012: character 115).
373. Astragalus, shape: rectangular (0); wedge shaped, with reduced anteromedial corner (1). (Wilson, 2002: character 210).
374. Astragalus, fibular facet: faces laterally (0); faces posterolaterally, anterior margin visible in posterior view (1). (Whitlock, 2011: character 186).
375. Astragalus, foramina at base of ascending process: present (0); absent (1). (Wilson, 2002: character 211).
376. Astragalus, ascending process length: limited to anterior two-thirds of astragalus (0); extending to posterior margin of astragalus (1). (Wilson, 2002: character 212).
377. Astragalus, posterior fossa shape: undivided (0); divided by vertical crest (1). (Wilson, 2002: character 213).
378. Astragalus, transverse length: 50% more than (0); or subequal to proximodistal height (1). (Wilson, 2002: character 214).
379. Calcaneum: present (0); absent or unossified (1). (Wilson, 2002: character 215).
380. Distal tarsals 3 and 4: present (0); absent or unossified (1). (Wilson, 2002: character 216).
381. Metatarsus, posture: bound (0); spreading (1). (Wilson, 2002: character 217).

382. Metatarsal I proximal condyle, transverse axis orientation: perpendicular to (0); angled ventromedially approximately 15° to axis of shaft (1). (Wilson, 2002: character 218).
383. Metatarsal I distal condyle, transverse axis orientation: perpendicular to (0); angled dorsomedially to axis of shaft (1). (Wilson, 2002: character 219).
384. Metatarsal III length divided by metatarsal I length: less than 1.3 (0); more than 1.3 (1). (González Riga et al., 2016: character 331).
385. Longest metatarsal: metatarsal III (0); metatarsal IV (1). (González Riga et al., 2016: character 334).
386. Metatarsal I distal condyle, posterolateral projection: absent (0); present (1). (Wilson, 2002: character 220).
387. Metatarsal I, minimum shaft width: less than that of metatarsals II-IV (0); or greater than that of metatarsals II-IV (1). (Wilson, 2002: character 221).
388. Metatarsal I and V proximal condyle, size: smaller than (0); or subequal to those of metatarsals II and IV (1). (Wilson, 2002: character 222).
389. Metatarsal III length: more than 30% (0); or less than 25% that of tibia (1). (Wilson, 2002: character 223).
390. Metatarsals III and IV, minimum transverse shaft diameters: subequal to (0); or less than 65% that of metatarsals I or II (1). (Wilson, 2002: character 224).
391. Metatarsal IV, proximomedial end, shape: flat or slightly concave (0); possesses a distinct embayment (1). (D'Emic, 2012: character 117).
392. Metatarsal IV, distal end, orientation: roughly perpendicular to long axis of bone (0); bevelled upwards medially (1). (D'Emic, 2012: character 118).
393. Metatarsal V, length: shorter than (0); or at least 70% length of metatarsal IV (1). (Wilson, 2002: character 225).
394. Pedal non-ungual phalanges, shape: longer proximodistally than broad transversely (0); broader transversely than long proximodistally (1). (Wilson, 2002: character 226).
395. Pedal digits II-IV, penultimate phalanges, development: subequal in size to more proximal phalanges (0); rudimentary or absent (1). (Wilson, 2002: character 227).
396. Pedal unguals, orientation: aligned with (0); or deflected lateral to digit axis (1). (Wilson, 2002: character 228).
397. Pedal digit I unguis, length relative to pedaldigit II unguis: subequal (0); 25% larger than that of digit II (1). (Wilson, 2002: character 229).

398. Pedal digit I ungual, length: shorter (0); or longer than metatarsal I (1). (Wilson, 2002: character 230).
399. Pedal ungual I, shape: broader transversely than dorsoventrally (0); sickle-shaped, much deeper dorsoventrally than broad transversely (1). (Wilson, 2002: character 231).
400. Pedal ungual II-III, shape: broader transversely than dorsoventrally (0); sickleshaped, much deeper dorsoventrally than broad transversely (1). (Wilson, 2002: character 232).
401. Pedal digit IV ungual, development: subequal in size to unguals of pedal digits II and III (0); rudimentary or absent (1). (Wilson, 2002: character 233).
402. Unguals of pedal digit II and III, proximal dimensions: as broad as deep (0); significantly broader than deep (1). (Allain and Aquesbi, 2008: character 253).
403. Number of phalanges in pedal digit II: 3 (0); 2 (1). (González Riga et al., 2016: character 348).
404. Number of phalanges in pedal digit III: 4 (0); 3 (1). (González Riga et al., 2016: character 349).
405. Number of phalanges in pedal digit IV: 3 or more (0); 2 (1); 1 (2). (González Riga et al., 2016: character 350)
406. Postorbital, excluded from the infratemporal fenestra due to the articulation of the jugal with the squamosal: absent (0), present (1). (Canudo et al., 2018).
407. Squamosal, ventral shape: thin (0); broad (1). (Canudo et al., 2018).
408. Preantorbital fenestra development: small, differentiated from the posterior maxillary foramen in its direction (see Wilson and Sereno, 1998) (0); laterally opened middle sized fenestra (1); laterally opened large fenestra (2). (Canudo et al., 2018).
409. Mid- and posterior dorsal neural arches, centroprezygapophyseal fossa depth: shallow or absent (0); deep, passing nearly all the way through the neural arch. (Wilson and Allain, 2015: character 101).
410. Mid- posterior dorsal vertebrae, parapophysis, position with respect to prezygapophyses: at the same level or below (0); well above (1). (Wilson and Allain, 2015: character 100).
411. Posterior dorsal neural arches, centroprezygapophyseal lamina (CPRL), shape: single (0); divided (1). (Wilson and Allain, 2015: character 107).
412. Posterior dorsal neural arches, spinoparapophyseal lamina (SPPL): absent (0); present (1). (Wilson and Allain, 2015: character 109).

413. Middle caudal vertebrae, prezygapophyses orientation: anterodorsally oriented (around 45 degrees) (0); anteriorly oriented (nearly horizontal) (1). (Canudo et al., 2018).
414. Scapular acromion, ventral process: absent (0), present (1). (Carballido et al., 2020).
415. Ilium, postacetabular posteroventral edge: open concave (0); U-shaped notch (1); horizontal and low V-shaped notch (2). (Carballido et al., 2020).
416. Pubis, ischiadic articular surface: continuous without marked angle change (0); marked step formed by a proximal posterior directed surface and a more distal posterodorsally oriented surface (1). (Carballido et al., 2020).
417. Pubis, proximal symphysis: merges with the pubic shaft (0); forms a marked ventromedially directed process (1). (Carballido et al., 2020).

Characters added

418. Posteriormost anterior and middle caudal centra, proportions: as high as wide (high) (0), wider than high (depressed) (1). (Modified from Salgado et al., 1997: character 34).
419. Middle caudal vertebrae, anterodorsal end of the neural spine located posteriorly with respect to anterior border of the postzygapophyses: absent (0); present (1) (Salgado et al., 1997: character 10).
420. Middle caudal vertebrae, length proportions of prezygapophyses with respect to the centrum length: shorter than 40% (0); between 40 and 50% (1); longer than 50% (2). (Modified from Salgado et al., 2014: character 54).
421. Posteriormost anterior and middle caudal vertebrae, prezygapophyses distally expanded dorsoventrally: absent (0); present (1). (Santucci and Arruda-Campos, 2011).
422. Quadrate, articular condyle: undivided (0); anteriorly divided (1); posteriorly divided (2); entirely divided by a sulcus, in a medial and lateral condyle (3). New.

References

- Allain, R., Aquesbi, N., 2008. Anatomy and phylogenetic relationships of *Tazoudasaurus naimi* (Dinosauria, Sauropoda) from the late Early Jurassic of Morocco. *Geodiversitas* 30, 345–424.
- Allen, J.R.L., 1983. Studies in fluvial sedimentation: bars, bar-complexes and sandstone sheets (low sinuosity braided streams) in the Brownstones (L. Devonian), Welsh Borders. *Sedimentary Geology* 33, 237–293.
- Apesteguía, S., 2004. *Bonitasaura salgadoi* gen. et sp. nov.: a beaked sauropod from the Late Cretaceous of Patagonia. *Naturwissenschaften* 91(10), 493–497.
- Arcucci, A.B., Marsicano, C.A., Coria, R.A., 2005. Una nueva localidad fosilífera en el Cretácico de la Precordillera de La Rioja. *Ameghiniana* 42, 60R.
- Bandeira, K.L.N., Simbras, F.M., Machado, E.B., De Almeida Campos, D., Oliveira, G.R., Kellner, A.W.A., 2016. A new giant Titanosauria (Dinosauria: Sauropoda) from the Late Cretaceous Bauru Group, Brazil. *PLoS ONE* 11, 1–25. doi:10.1371/journal.pone.0163373
- Behrensmeyer, A.K., Hook, R.W., 1992. Paleoenvironmental contexts and taphonomic modes, in: Behrensmeyer, A., Damuth, J., Di Michele, W., Potts, R., Sues, H.-D., Wings, S. (Eds.), *Terrestrial Ecosystems through Time: Evolutionary Paleocology of Terrestrial Plants and Animals*. University of Chicago Press, Chicago, pp. 15–93.
- Bonaparte, J.F., Coria, R.A., 1993. Un nuevo y gigantesco saurópodo titanosaurio de la Formación Río Limay (Albiano-Cenomaniano) de la Provincia del Neuquén, Argentina. *Ameghiniana* 30, 271–282.
- Bonaparte, J.F., Powell, J.E., 1980. A continental assemblage of tetrapods from the Upper Cretaceous beds of El Brete, northwest Argentina (Sauropoda-Coelurosauria-Carnosauria-Aves), *Table ronde internationale du Ecosystèmes Continentaux du Mésozoïque*.
- Bracaccini, O., 1946. Contribución al conocimiento geológico de la Precordillera Sanjuanina-Mendocina. *Boletín de Informaciones Petroleras* 1 258, 81–105.
- Bridge, J.S., 2003. *Rivers and floodplains: forms, processes and sedimentary record*. Wiley-Blackwell.
- Burns, C.E., Mountney, N.P., Hodgson, D.M., Colombera, L., 2017. Anatomy and dimensions of fluvial crevasse-splay deposits: Examples from the Cretaceous Castlegate Sandstone and Neslen Formation, Utah, U.S.A. *Sedimentary Geology* 351, 21–35. doi:10.1016/j.sedgeo.2017.02.003
- Calvo, J.O., González Riga, B.J., 2003. *Rinconsaurus caudamirus* gen. et sp. nov., a new titanosaurid (Dinosauria, Sauropoda) from the Late Cretaceous of Patagonia, Argentina. *Revista Geológica de Chile* 30, 333–353.
- Calvo, J.O., González Riga, B.J., Porfiri, J.D., 2007a. A new titanosaur sauropod from the Late Cretaceous of Neuquén, Patagonia, Argentina. *Arquivos do Museu*

Nacional 65, 485–504.

- Calvo, J.O., Porfiri, J.D., González-Riga, B.J., Kellner, A.W. a, 2007b. A new Cretaceous terrestrial ecosystem from Gondwana with the description of a new sauropod dinosaur. *Anais da Academia Brasileira de Ciências* 79, 529–41.
- Campos, D.A., Kellner, A.W.A., Bertini, R.J., Santucci, R.M., 2005. On a titanosaurid (Dinosauria, Sauropoda) vertebral column from the Bauru Group, Late Cretaceous of Brazil. *Arquivos do Museu Nacional, Rio do Janeiro* 63, 565–596.
- Canudo, J.I., Carballido, J.L., Garrido, A., Salgado, L., 2018. A new rebbachisaurid sauropod from the Aptian-Albian, Lower Cretaceous Rayoso Formation, Neuquén, Argentina. *Acta Palaeontologica Polonica* 63, 679–691.
doi:10.4202/app.00524.2018
- Carballido, J.L., Pol, D., Cerda, I., Salgado, L., 2011. The osteology of *Chubutisaurus insignis* del Corro, 1975 (Dinosauria: Neosauropoda) from the ‘middle’ Cretaceous of central Patagonia, Argentina. *Journal of Vertebrate Paleontology* 31, 93–110.
doi:10.1080/02724634.2011.539651
- Carballido, J.L., Pol, D., Otero, A., Cerda, I.A., Salgado, L., Garrido, A.C., Ramezani, J., Cúneo, N.R., Krause, J.M., 2017. A new giant titanosaur sheds light on body mass evolution among sauropod dinosaurs. *Proceedings of the Royal Society B: Biological Sciences* 284, 20171219. doi:10.1098/rspb.2017.1219
- Carballido, J.L., Salgado, L., Pol, D., Canudo, J.I., Garrido, A., 2012. A new basal rebbachisaurid (Sauropoda, Diplodocoidea) from the Early Cretaceous of the Neuquén Basin; evolution and biogeography of the group. *Historical Biology* 24, 631–654. doi:10.1080/08912963.2012.672416
- Carballido, J.L., Scheil, M., Knötschke, N., Sander, P.M., 2020. The appendicular skeleton of the dwarf macronarian sauropod *Europasaurus holgeri* from the Late Jurassic of Germany and a re-evaluation of its systematic affinities. *Journal of Systematic Palaeontology* 18, 739–781. doi:10.1080/14772019.2019.1683770
- Cerda, I.A., Paulina Carabajal, A., Salgado, L., Coria, R.A., Reguero, M.A., Tambussi, C.P., Moly, J.J., 2012. The first record of a sauropod dinosaur from Antarctica. *Naturwissenschaften* 99, 83–7. doi:10.1007/s00114-011-0869-x
- Chaía, T., 1990. Registro del Cenoniano lacustre en la provincia de San Juan, in: 1° Congreso Uruguayo de Geología, Resúmenes Ampliados. Montevideo, pp. 33–36.
- Ciccioli, P.L., Ballent, S., Tedesco, A.M., Barreda, V., Limarino, C.O., 2005. Hallazgo de depósitos Cretácicos en la Precordillera de La Rioja (Formación Ciénaga del Río Huaco). *Revista de la Asociación Geológica Argentina* 60, 122–131.
- Coria, R.A., Filippi, L.S., Chiappe, L.M., 2013. *Overosaurus paradasorum* gen. et sp. nov., a new sauropod dinosaur (Titanosauria: Lithostrotia) from the Late Cretaceous of Neuquén, Patagonia, Argentina. *Zootaxa* 3683, 357–376.
- Coughlin, T.J., 2000. Linked Orogen-Oblique Fault Zones in the Central Andes: the basis of a new model for Andean orogenesis and metallogenesis. University of Queensland, Brisbane.

- Curry-Rogers, K.A., 2005. Titanosauria: a phylogenetic overview, in: Curry-Rogers, K.A., Wilson, J.A. (Eds.), *The Sauropods: Evolution and Paleobiology*. University of California Press, pp. 50–103.
- D’Emic, M.D., 2012. The early evolution of titanosauriform sauropod dinosaurs. *Zoological Journal of the Linnean Society* 166, 624–671. doi:10.1111/j.1096-3642.2012.00853.x
- Faria, C.C. de J., González Riga, B., Candeiro, C.R. dos A., Marinho, T. da S., Ortiz David, L., Simbras, F.M., Castanho, R.B., Muniz, F.P., Gomes da Costa Pereira, P.V.L., 2015. Cretaceous sauropod diversity and taxonomic succession in South America. *Journal of South American Earth Sciences* 61, 154–163. doi:10.1016/j.jsames.2014.11.008
- Fosdick, J.C., Reat, E.J., Carrapa, B., Ortiz, G., Alvarado, P.M., 2017. Retroarc basin reorganization and aridification during Paleogene uplift of the southern central Andes. *Tectonics* 36, 493–514. doi:10.1002/2016TC004400
- Fowler, D.W., Hall, L.E., 2011. Scratch-digging sauropods, revisited. *Historical Biology* 23, 27–40. doi:10.1080/08912963.2010.504852
- Franco-Rosas, A.C., Salgado, L., Rosas, C.F., de Souza Carvalho, I., 2004. Nuevos materiales de titanosaurios (Sauropoda) en el Cretácico Superior de Mato Grosso, Brasil. *Revista Brasileira de Paleontologia* 7, 329–336. doi:10.4072/rbp.2004.3.04
- Goloboff, P.A., Farris, J.S., Nixon, K.C., 2008. TNT, a free program for phylogenetic analysis. *Cladistics* 24, 774–786.
- González Riga, B.J., 2003. A new titanosaur (Dinosauria, Sauropoda) from the Upper Cretaceous of Mendoza Province, Argentina. *Ameghiniana* 40, 155–172.
- González Riga, B.J., Lamanna, M.C., Ortiz David, L.D., Calvo, J.O., Coria, J.P., 2016. A gigantic new dinosaur from Argentina and the evolution of the sauropod hind foot. *Scientific Reports* 6, 19165. doi:10.1038/srep19165
- González Riga, B.J., Mannion, P.D., Poropat, S.F., Ortiz David, L.D., Coria, J.P., 2018. Osteology of the Late Cretaceous Argentinean sauropod dinosaur *Mendozasaurus neguyelap*: Implications for basal titanosaur relationships. *Zoological Journal of the Linnean Society* 184, 136–181. doi:10.1093/zoolinnea/zlx103
- González Riga, B.J., Ortiz David, L., 2014. A new titanosaur (Dinosauria, Sauropoda) from the Upper Cretaceous (Cerro Lisandro Formation) of Mendoza province, Argentina. *Ameghiniana* 51, 3–25. doi:10.5710/AMEGH.26.12.1013.1889
- González Riga, B.J., Previtera, E., Pirrone, C.A., 2009. *Malarguesaurus florenciae* gen. et sp. nov., a new titanosauriform (Dinosauria, Sauropoda) from the Upper Cretaceous of Mendoza, Argentina. *Cretaceous Research* 30, 135–148. doi:10.1016/j.cretres.2008.06.006
- Gorscak, E., O’Connor, P.M., 2016. Time-calibrated models support congruency between Cretaceous continental rifting and titanosaurian evolutionary history. *Biology Letters* 12, 20151047. doi:10.1098/rsbl.2015.1047
- Harris, J.D., 2006. Cranial osteology of *Suuwassea emiliae* (Sauropoda: Diplodocoidea:

- Flagellicaudata) from the Upper Jurassic Morrison Formation of Montana, USA. *Journal of Vertebrate Paleontology* 26, 88–102. doi:10.1671/0272-4634(2006)26[88:COOSES]2.0.CO;2
- Hechenleitner, E.M., Fiorelli, L.E., Martinelli, A.G., Grellet-Tinner, G., 2018. Titanosaur dinosaurs from the Upper Cretaceous of La Rioja province, NW Argentina. *Cretaceous Research* 85, 42–59. doi:10.1016/j.cretres.2018.01.006
- Hechenleitner, E.M., Grellet-Tinner, G., Fiorelli, L.E., 2015. What do giant titanosaur dinosaurs and modern Australasian megapodes have in common? *PeerJ* 3, e1341. doi:10.7717/peerj.1341
- Hubert, J.F., Hyde, M.G., 1982. Sheet-flow deposits of graded beds and mudstones on an alluvial sandflat-playa system: Upper Triassic Blomidon redbeds, St Mary's Bay, Nova Scotia. *Sedimentology* 29, 457–474. doi:10.1111/j.1365-3091.1982.tb01730.x
- Jordan, T.E., Isacks, B.L., Allmendinger, R.W., Brewer, J.A., Ramos, V.A., Ando, C.J., 1983. Andean tectonics related to geometry of subducted Nazca plate. *Geological Society of America Bulletin* 94, 341. doi:10.1130/0016-7606(1983)94<341:ATRTGO>2.0.CO;2
- Kellner, A.W.A., de Azevedo, S.A.K., 1999. A new sauropod dinosaur (Titanosauria) from the Late Cretaceous of Brazil, in: Tomida, Y., Rich, T.H., Vickers-Rich, P. (Eds.), *Proceedings of the Second Gondwanan Dinosaur Symposium*. National Science Museum Monographs, No. IS, Tokio, pp. 111–142.
- Lacovara, K.J., Lamanna, M.C., Ibiricu, L.M., Poole, J.C., Schroeter, E.R., Ullmann, P. V., Voegelé, K.K., Boles, Z.M., Carter, A.M., Fowler, E.K., Egerton, V.M., Moyer, A.E., Coughenour, C.L., Schein, J.P., Harris, J.D., Martínez, R.D., Novas, F.E., 2014. A gigantic, exceptionally complete titanosaurian sauropod dinosaur from southern Patagonia, Argentina. *Scientific Reports* 4, 1–9. doi:10.1038/srep06196
- Limarino, C.O., Ciccioli, P.L., Krapovickas, V., Benedito, L.D., 2016. Estratigrafía de las sucesiones mesozoicas, paleógenas y neógenas de las quebradas Santo Domingo y el Peñón (Precordillera Septentrional riojana). *Revista de la Asociación Geológica Argentina* 73, 301–318.
- Limarino, C.O., Net, L., Gutiérrez, P., Barreda, V., Caselli, A., Ballent, S., 2000. Definición litoestratigráfica de la Formación Ciénaga del Río Huaco (Cretácico Superior), Precordillera central, San Juan, Argentina. *Revista de la Asociación Geológica Argentina* 55, 83–99.
- Mannion, P.D., Upchurch, P., Mateus, O., Barnes, R.N., Jones, M.E.H., 2012. New information on the anatomy and systematic position of *Dinheirosaurus lourinhanensis* (Sauropoda: Diplodocoidea) from the Late Jurassic of Portugal, with a review of European diplodocoids. *Journal of Systematic Palaeontology* 10, 521–551. doi:10.1080/14772019.2011.595432
- Martinelli, A., Riff, D., Lopes, R., 2011. Discussion about the occurrence of the genus *Aeolosaurus* Powell 1987 (Dinosauria, Titanosauria) in the Upper Cretaceous of Brazil. *Gaea* 7, 34–40. doi:10.4013/gaea.2011.71.03

- Martínez, R.D.F., Lamanna, M.C., Novas, F.E., Ridgely, R.C., Casal, G.A., Martínez, J.E., Vita, J.R., Witmer, L.M., 2016. A basal lithostrotian titanosaur (Dinosauria: Sauropoda) with a complete skull: implications for the evolution and paleobiology of Titanosauria. *Plos One* 11, e0151661. doi:10.1371/journal.pone.0151661
- Miall, A.D., 1996. *The geology of fluvial deposits*. Springer, Berlin.
- Müller, R.D., Cannon, J., Qin, X., Watson, R.J., Gurnis, M., Williams, S., Pfaffelmoser, T., Seton, M., Russell, S.H.J., Zahirovic, S., 2018. GPlates: Building a Virtual Earth Through Deep Time. *Geochemistry, Geophysics, Geosystems* 19, 2243–2261. doi:10.1029/2018GC007584
- Navarrete, C., Casal, G., Martínez, R., 2011. *Drusilasaura deseadensis* gen. et sp. nov., un nuevo titanosaurio (Dinosauria-Sauropoda), de la Formación Bajo Barreal, Cretácico Superior del Norte de Santa Cruz, Argentina. *Revista Brasileira De Paleontologia* 14, 1–14. doi:10.4072/rbp.2011.1.01
- Novas, F.E., Salgado, L., Calvo, J.O., Agnolin, F.L., 2005. Giant titanosaur (Dinosauria, Sauropoda) from the Late Cretaceous of Patagonia. *Revista del Museo Argentino de Ciencias Naturales* 7, 37–41.
- Pérez, M., Fernández Seveso, F., Álvarez, L.A., Brison, I.E., 1993. Análisis ambiental y estratigráfico del Paleozoico Superior en el área anticlinal de Huaco, San Juan, Argentina, in: 10° Congreso Internacional de La Stratigraphie et Géologie Du Carbonifère et Permien, *Comptes Rendus, Actas* 2. pp. 297–318.
- Pianka, E.R., 1966. Latitudinal gradients in species diversity: a review of concepts. *American Naturalist* 100, 33–46.
- Pol, D., Garrido, A., Cerda, I.A., 2011. A new sauropodomorph dinosaur from the Early Jurassic of Patagonia and the origin and evolution of the sauropod-type sacrum. *PloS ONE* 6, e14572. doi:10.1371/journal.pone.0014572
- Powell, J.E., 1990. *Epachthosaurus sciuttoi* (gen. et sp. nov.) un dinosaurio sauropodo del Cretácico de Patagonia (Provincia de Chubut, Argentina), in: V Congreso Argentino de Paleontología y Bioestratigrafía. pp. 123–128.
- Powell, J.E., 2003. Revision of South American titanosaurid dinosaurs: palaeobiological, palaeobiogeographical and phylogenetic aspects. *Records of the Queen Victoria Museum* 111, 1–173.
- Ramos, V.A., 1988. The tectonics of the Central Andes; 30 to 33 S latitude. *Special Paper of the Geological Society of America* 218, 31–54. doi:10.1130/SPE218-p31
- Rauhut, O.W.M., Carballido, J.L., Pol, D., 2015. A diplodocid sauropod dinosaur from the Late Jurassic Canadon Calcereo Formation of Chubut, Argentina. *Journal of Vertebrate Paleontology* 35. doi:10.1080/02724634.2015.982798
- Reat, E.J., Fosdick, J.C., 2018. Basin evolution during Cretaceous-Oligocene changes in sediment routing in the Eastern Precordillera, Argentina. *Journal of South American Earth Sciences* 84, 422–443. doi:10.1016/j.jsames.2018.02.010
- Remes, K., Ortega, F., Fierro, I., Joger, U., Kosma, R., Ferrer, J.M.M., Ide, O.A., Maga, A., 2009. A new basal sauropod dinosaur from the middle Jurassic of Niger and the

- early evolution of Sauropoda. PLoS ONE 4, e6924.
doi:10.1371/journal.pone.0006924
- Salgado, L., Azpilicueta, C., 2000. Un nuevo saltosaurino (Sauropoda, Titanosauridae) de la provincia de Río Negro (Formación Allen, Cretácico Superior), Patagonia, Argentina. *Ameghiniana* 37, 259–264.
- Salgado, L., Carvalho, I.D.S., 2008. *Uberabatitan ribeiroi*, a new titanosaur from the Marília Formation (Bauru Group, Upper Cretaceous), Minas Gerais, Brazil. *Palaeontology* 51, 881–901. doi:10.1111/j.1475-4983.2008.00781.x
- Salgado, L., Coria, R.A., Calvo, J.O., 1997. Evolution of titanosaurid sauropods. I: Phylogenetic analysis based on the postcranial evidence. *Ameghiniana* 34, 3–32.
- Salgado, L., Gallina, P.A., Paulina Carabajal, A., 2014. Redescription of *Bonatitan reigi* (Sauropoda: Titanosauria), from the Campanian–Maastrichtian of the Río Negro Province (Argentina). *Historical Biology* 27, 1–24.
doi:10.1080/08912963.2014.894038
- Santucci, R.M., Arruda-Campos, A.C. de, 2011. A new sauropod (Macronaria, Titanosauria) from the Adamantina Formation, Bauru Group, Upper Cretaceous of Brazil and the phylogenetic relationships of Aeolosaurini. *Zootaxa* 33, 1–33.
- Sax, D.F., 2001. Latitudinal gradients and geographic ranges of exotic species: implications for biogeography. *Journal of Biogeography* 28, 139–150.
- Sereno, P.C., 2007. The phylogenetic relationships of early dinosaurs: a comparative report. *Historical Biology* 19, 145–155. doi:10.1080/08912960601167435
- Seton, M., Müller, R.D., Zahirovic, S., Gaina, C., Torsvik, T., Shephard, G., Talsma, A., Gurnis, M., Turner, M., Maus, S., Chandler, M., 2012. Global continental and ocean basin reconstructions since 200Ma. *Earth-Science Reviews* 113, 212–270.
doi:10.1016/j.earscirev.2012.03.002
- Silva, J.C.G., Marinho, T.S., Martinelli, A.G., Langer, M.C., 2019. Osteology and systematics of *Uberabatitan ribeiroi* (Dinosauria; Sauropoda): A Late Cretaceous titanosaur from Minas Gerais, Brazil. *Zootaxa* 4577, 401–438.
doi:10.11646/zootaxa.4577.3.1
- Tedesco, A.M., Limarino, C.O., Ciccioli, P.L., 2007. Primera edad radimétrica de los depósitos cretácicos de la precordillera central. *Revista de la Asociación Geológica Argentina* 62, 471–474.
- Tunbridge, I.P., 1984. Facies model for a sandy ephemeral stream and clay playa complex; the Middle Devonian Trentishoe Formation of North Devon, UK. *Sedimentology* 31, 697–715.
- Tykoski, R.S., Fiorillo, A.R., 2016. An articulated cervical series of *Alamosaurus sanjuanensis* Gilmore, 1922 (Dinosauria, Sauropoda) from Texas: new perspective on the relationships of North America's last giant sauropod. *Journal of Systematic Palaeontology* 2019, 1–26. doi:10.1080/14772019.2016.1183150
- Upchurch, P., 1998. The phylogenetic relationships of sauropod dinosaurs. *Zoological Journal of the Linnean Society* 124, 43–103.

- Upchurch, P., Barrett, P.M., Dodson, P., 2004. Sauropoda, in: *The Dinosauria*. pp. 259–324.
- Upchurch, P., Barrett, P.M., Galton, P.M., 2007. A phylogenetic analysis of basal sauropodomorph relationships: implications for the origin of sauropod dinosaurs. *Special Papers in Palaeontology* 57–90.
- Vila, B., Galobart, À., Oms, O., Poza, B., Bravo, A.M., 2010a. Assessing the nesting strategies of Late Cretaceous titanosaurs: 3-D clutch geometry from a new megaloolithid egg site. *Lethaia* 43, 197–208. doi:10.1111/j.1502-3931.2009.00183.x
- Vila, B., Jackson, F.D., Fortuny, J., Sellés, A.G., Galobart, A., 2010b. 3-D modelling of megaloolithid clutches: insights about nest construction and dinosaur behaviour. *PLoS ONE* 5, e10362. doi:10.1371/journal.pone.0010362
- Whitlock, J.A., 2011. A phylogenetic analysis of Diplodocoidea (Saurischia: Sauropoda). *Zoological Journal of the Linnean Society* 161, 872–915. doi:10.1111/j.1096-3642.2010.00665.x
- Wilson, J.A., 2002. Sauropod dinosaur phylogeny: critique and cladistic analysis. *Zoological Journal of the Linnean Society* 136, 217–276.
- Wilson, J.A., Allain, R., 2015. Osteology of *Rebbachisaurus garasbae* Lavocat, 1954, a diplodocoid (Dinosauria, Sauropoda) from the early Late Cretaceous-aged Kem Kem beds of southeastern Morocco. *Journal of Vertebrate Paleontology* 35, 37–41. doi:10.1080/02724634.2014.1000701
- Zaher, H., Pol, D., Carvalho, A.B., Nascimento, P.M., Riccomini, C., Larson, P., Juarez-Valieri, R., Pires-Domingues, R., da Silva, N.J., Campos, D.D.A., 2011. A complete skull of an Early Cretaceous sauropod and the evolution of advanced titanosaurs. *PLoS ONE* 6, e16663. doi:10.1371/journal.pone.0016663